Adhesins – Do they play a role in the *Epichloë festucae* association with perennial rye grass?

A thesis presented in partial fulfillment of the requirements for the degree of

Master of Science

In

Genetics

at Massey University, Palmerston North

New Zealand

Philippa Child

2014

Abstract

Adhesins have been extensively studied and characterised in prokaryotes and yeast. It has been shown that these proteins are important in development, symbiosis and pathogenicity. However, less is known about the role adhesins play in filamentous fungi. Adhesin genes have been identified and functionally characterised in *Metarhizium robertsii* and recently studied in *Beauveria bassiana.* The insect pathogen *M. robertsii* has two adhesin genes, *Mad1* and *Mad2*, which were shown to be important in insect adherence or plant adherence respectively. *Epichloë festucae* has two adhesins, *adsA* and *adsB*, homologous to *Mad1* and *Mad2* respectively. Bioinfomatic analysis of *E. festucae* adhesins showed that in Fl1 *adsA* and *adsB* are separated by 25 genes. Analysis of *adsB* illustrated that the second adhesin gene is restricted to the Hypocreomycetidae. Phylogenetic analysis confirmed that *adsB* and *adsA* group separately in filamentous fungi.

In this study, deletion mutants of *E. festucae adsA* and *adsB* were used to determine if one or both adhesins played a role in establishment of the hyphal network in culture and in symbiotic association with *L. perenne*. Deletion of *adsA* did not alter the growth of the hyphae in culture or *in planta*. Although, the growth of the *adsB* mutant in culture was not affected the growth *in planta* was different to that seen in wild-type associations. Mild whole plant stunting and colonisation of the large vascular bundles indicates that *adsB* plays a role in the early development of the symbiotic association. In contrast to *M. robertsii* where only *Mad2* confers adherence of yeast to onion epidermal tissue, both *E. festucae adsA* and *adsB* confer adherence. The attachment of yeast cells expressing *adsA,* suggests that *adsA* does play a role in the symbiotic association. Physical attachment of the hyphae to host cells was not abolished when either *adsA* or *adsB* were deleted in *E. festucae,* suggesting gene redundancy in regards to physical attachment to the host tissue. This work provides insight into the role adhesins play in the symbiotic association of *E. festucae* and *L. perenne*.

Acknowledgements

Firstly, I would like to thank my supervisor Professor Barry Scott. Thank you for welcoming me into your lab and providing great advice and opportunities throughout my project. Secondly, thank you to my co-supervisor Dr. Carla Eaton for initially starting the project and for technical assistance. Thirdly, thank you to Associate Professor Kathryn Stowell, your support throughout the final years of my Bachelors and during my Masters has been greatly appreciated – it was a bumpy road but I got there!

Thank you to all past and present members of the ScottBase Lab. Arvina, thank you for being so organised with the day-to-day running of the lab and sterile pipette tips when I had run out! To Emma, Conni, Gemma, Tetsyua and Will, thank you for all your advice on experimental techniques and discussing my ideas. To everyone else in the lab/computer office, Kim, Dan, Alex, Yonathan and Nazanin, thanks for being awesome!

To Dave Wheeler and Poppy Miller, thank you so much for helping with phylogenetic analysis and statistics. Also, to Mike Christensen, your knowledge has contributed so much to my project and I am truly grateful. To the team at the MMIC, Matthew, Jordan and Niki, thank you for all your technical advice and patience with all of my questions.

To my friends I have made throughout my time at Massey University thank you for your friendship and support throughout our studies. Specifically, Jordan and Bex for always telling me that I can get there – your support has been unbelievable.

Finally, thank you to my family. Mum and Dad thank you so much for all your emotional and financial support throughout my studies. I know I have been difficult to live with! But, I have achieved what I wanted to when I first enrolled at university!

Table of Contents

List of Figures

List of tables

List of abbreviations

aa	Amino acid
Amp	Ampicillin
Amp^R	Ampicillin resistance
An	*Aspergillus niger*
bp	Base pairs
BLAST	Basic local alignment search tool
Bb	*Beauveria bassiana*
CFW	Calcofluor white
C	Plant cuticle
Cm	*Cordyceps militaris*
°C	Degrees Celsius
DNA	Deoxyribonucleic acid
dNTP	Deoxyribonucleic triphosphate
DIC	Differential interference contrast
DMSO	Dimethyl sulfoxide
ECS	Extracellular space
EGFP	Enhanced green fluorescent protein
EDTA	Ethlyene diamine tetra-acetic acid
FS	Flanking sequence
FGI	Fungal genome initiative
Fg	*Fusarium gramineaurm*
Fo	*Fusarium oxysporium*
Gen	Geneticin
Gen^R	Geneticin resistance
gDNA	Genomic DNA
GPI	Glycosylphosphatidylinositol
g	Gram
h	Hours
H	Hyphae

hph	Hygromycin phosphotransferase
Hyg^R	Hygromycin Resistance
ICS	Intercellular space
INVSc1	Invitrogen non-adherent variant *Saccharomyces cerevisiae*
kb	Kilobase
kV	Kilovolts
KO	Knock-out
Leu	Leucine
L	Litre
LB	Luria-Bertani
Mo	*Magnaportha oryzae*
mRNA	Messenger ribonucleic acid
Mr	*Metarhizium robertsii*
µg	Microgram
µL	Microlitre
µM	Micromolar
mg	Milligram
mL	Millilitre
mM	Millimolar
min	Minute
M	Molar
Nox	NADPH oxidase
ng	Nanogram
nm	Nanometre
NCBI	National Centre for Biotechnology
Nh	*Nectria haematococca*
BLASTn	Nucleotide database search using a nucleotide query
Nc	*Neurospora crassa*
NADH	Nicotinamide adenine dinucleotise
NADPH	Nicotinamide adenine dinucleotise phosphate
NA	Numerical aperture
ORF	Open reading frame

P	Phloem
Pa	*Podospora anserina*
PC	Plant cell
PEG	Polyethylene glycol
PCR	Polymerase chain reaction
PD	Potato dextrose
PDA	Potato dextrose agar
PDS	Post diauxic shift element
polyA	Polyadenylation site
pro	C6-Zn transcription factor
BLASTp	Protein database search using a protein query
RG	Regeneration
rpm	Revolutions per minute
RNA	Ribonucleic acid
S	Sclerenchyma
s	Seconds
Sc	*Saccharomyces cerevisiae*
sak	Stress activated kinase
SD-Ura-Leu	Synthetic define uracil and leucine dropout
SD-Ura	Synthetic defined uracil dropout
SP	Signal peptide
spp.	Species
STRE	Stress responsive element
TSS	Transcription start site
TEM	Transmission electron microscopy
Tr	*Trichoderma ressi*
Tv	*Trichoderma virens*
TE	Tris – EDTA
TBE	Tris/Borate/EDTA
UV	Ultraviolet
U	Unit
Ura	Uracil

Va	*Verticillium alfalfae*
V	Volts
VB	Vascular bundle
v/v	Volume/volume ratio
w/v	Weight/volume ratio
WGA	Wheat germ agglutinin
WT	Wild-type
X	Xylem
YE	Yeast extract
YRC	Yeast recombinational cloning
YPD	Yeast-extract peptone dextrose

1. Introduction

1 Introduction

1.1. Plant-fungal interactions

Plant-fungal interactions are of great importance in the development and enhancement of agriculture and ecological communities. The most extensively studied plant-fungal interaction is that of mycorrhiza. These symbiotic interactions are specifically associated with the root systems of plants (Parniske, 2008). Arbuscular mycorrhiza (AM) associations are the most widespread symbiotic interactions, approximately 70-90% of all terrestrial plant species. These associations provide enhanced nutrient uptake as well as other beneficial advantages (Parniske, 2008). The formation of an arbuscule (feeding structure) between the plant cell and fungal cells is crucial in the symbiotic interaction and vastly increases the resulting surface area of the root system (Parniske, 2008). The arbuscule is key in water and nutrient exchange, specifically phosphate uptake, between the fungus and the plant cells (Parniske, 2008). A long history of this interaction is documented and illustrates the importance of the interaction and the co-evolution of plant-fungal associations indicative of an evolutionary advantage.

Less is known about plant-fungal interactions within the aerial tissue. Endophytic fungi are commonly found within the aerial tissue of vascular plants, including grasses, ranging from mutualistic through neutral to antagonistic. These interactions improve nutrient uptake from the immediate environment of the plant and in turn the fungus utilises the carbohydrates found in the apoplastic fluid within the intercellular spaces (Schardl, 2001). The mutualistic association is asymptomatic and the fungus is transmitted through the host seeds. In contrast, with antagonistic relationships the host seed production is completely suppressed ('choke'). The fungal hyphae are generally found in the aerial tissue and grow in the inter or intracellular spaces (Saikkonen *et al.*, 1998). Fungal species within the Clavicipitaceae (Ascomycota) are a significant group of endophytes which colonise intercellular spaces of grasses of the Poaceae family (Schardl *et al.*, 2004).

1.1.1. Epichloë endophyte lifestyle

The interaction of Epichloë endophytes with temperate grasses of the Festuca and Lolium genera within the sub-family Pooideae (Leuchtmann *et al.*, 1994; Schardl *et al.*, 1994), are important examples of the plant fungal interactions. *Epichloë* species are generally mutualistic and live asymptomatically within the cool season (temperate) grasses. Their reproduction is linked with the development of the host plant (Scott & Schardl, 1993). *Epichloë spp.* may transmit vertically (asexual) by colonisation of the host seeds and horizontally (sexual) by transmission due to the formation of a stroma over the inflorescence, 'choke' (Figure 1.1). In contrast strictly asexual *Epichloë spp.* (formerly *Neotyphodium spp.*, Leuchtmann *et al.*, 2014) are only disseminated vertically through the host seed (Clay & Schardl, 2002). These interactions differ to that of mycorrhizae, as the symbiotic interactions exist in the aerial tissues of the grass and are not found to interact with the root systems. The symbiotic interaction is also shown to have existed for a long period of time resulting in the co-evolution of the grass and fungus (Schardl *et al.*, 2004).

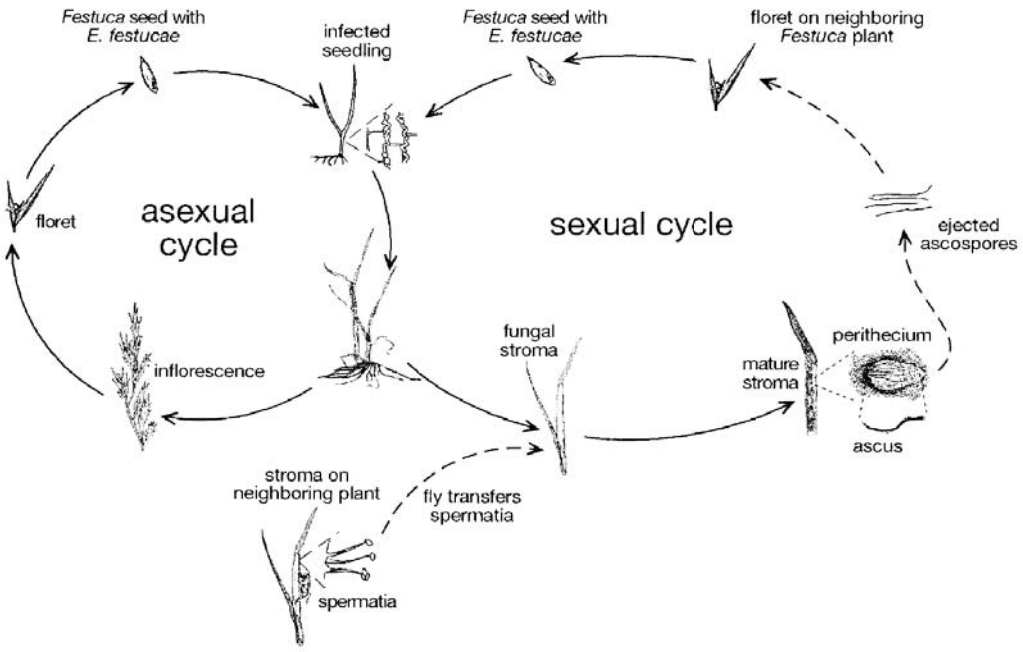

Figure 1.1 Lifecycle of Epichloë endophytes. The life cycle of *E. festucae* with alternative sexual and asexual life cycles. Reproduced from Clay and Schardl (2002).

Epichloë endophytes are present in the meristems and throughout the leaves of their host grasses (Leuchtmann *et al.*, 1994; Schardl *et al.*, 1994). These interactions increase the fitness of the host plant in a variety of ways (Schardl, 2001). In addition to an increase in nutrient uptake, the Epichloë endophytes produce bio-active alkaloids which act as feeding deterrents (Schardl, 2001). The growth of Epichloë endophytes *in planta* is highly regulated. Hyphae grow between mesophyll cells in the intercellular space parallel to the leaf axis and vascular bundles of the aerial tissues (Christensen *et al.*, 2002). These hyphae never breach the plant cell walls or develop feeding structures as in arbuscular mycorrhizae. Similar numbers of evenly distributed hyphae are seen in the layers of sheath tissue and the emerging leaf blade within the pseudostem (Christensen *et al.*, 2002). Hyphal growth continues in the developing leaves until leaf growth is complete (Schmid *et al.*, 2000). It appears likely that hyphae enter the leaf blade before cellular differentiation of the ligular zone. The thick layer of cells in the ligular zone acts as a physical barrier and thus, would result in minimal hyphal colonisation of the mature leaf blade (Christensen *et al.*, 2002). As the sheath tissue ages the large, circular, thin walled mesophyll cells begin to degenerate and the hyphae remain firmly attached and metabolically active (Figures 1.2 and 1.3).

Small vascular bundles differ from large vascular bundles by the lack of a sheath of thick-walled cells, which restrict the apoplastic movement of solutes and water (Figure 1.2) (Christensen *et al.*, 2002). Additionally, the large vascular bundles contain xylem cells that transport water. Small vascular bundles arise *de novo* as space becomes available in the developing tissue (Soper & Mitchell, 1956). The central large vascular bundle is present from the growth apex and differentiates from this point. The central large vascular bundle seen in the emerging leaf blade forms the main ridge of the mature blade (Figure 1.2). It is uncommon to find Epichloë endophytes colonising the vascular bundles of the host plant. However, in artificial associations large vascular bundle colonisation has been observed (Christensen *et al.*, 1997; Christensen *et al.*, 2001). Christensen *et al*. (2001) noted that colonisation of the vascular tissue may act as a disadvantage during plant establishment, resulting in the failure to produce seed. Natural selection may therefore eliminate strains that are able to colonise vascular tissue.

This provides evidence that the host plant strongly influences the growth of the endophytic hyphae.

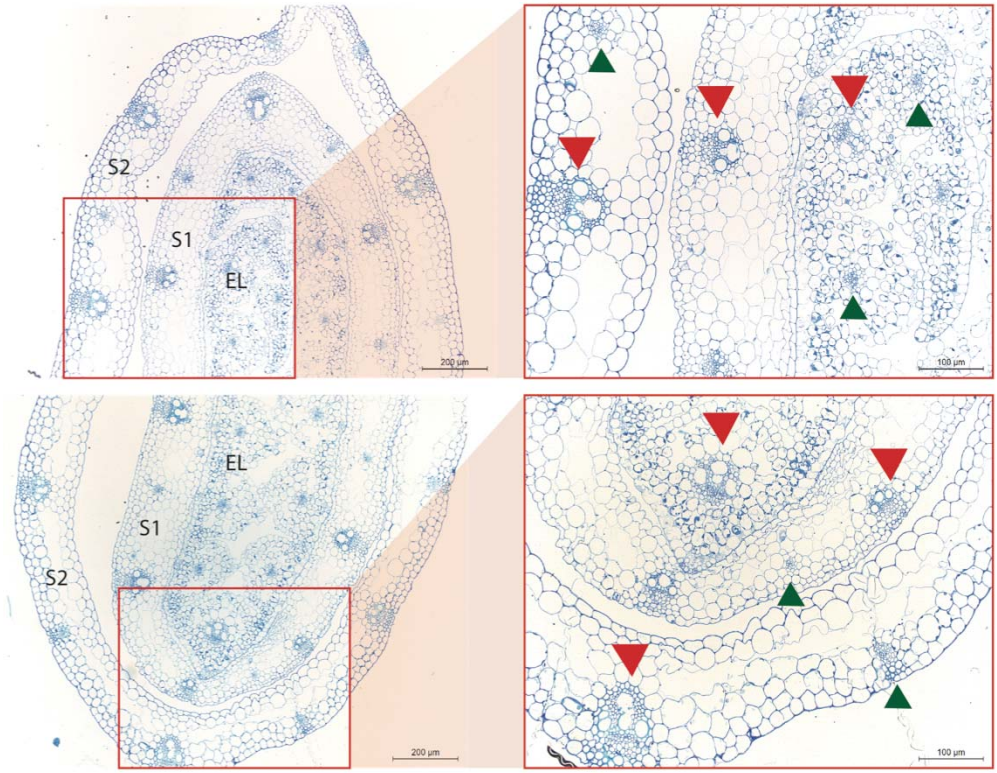

Figure 1.2 Light microscopy analysis of *E. festucae* Fl1 wild-type within *L. perenne*. Transverse sections of *L. perenne* pseudostem tissue infected with wild-type (WT) and stained with toluidine blue. Sample was taken from a plant 10 weeks post inoculation. S1 = Sheath layer 1 (inner), S2 = sheath layer 2 (outer), EL = emerging leaf. Red downward arrows = large vascular bundles, green upward arrows = small vascular bundles.

Transmission electron microscopy (TEM) carried out by Christensen *et al.* (2002) showed that hyphae in the expansion zone (pseudostem), where the plant cells are rapidly dividing, are electron dense, undifferentiated and firmly attached to the host cells. Mucilage surrounds hyphae that are in contact with host cells. Additionally the hyphal cell wall was fibrous (dark outer layer) and flattened at the point of contact with the host cell, yet no host cell response is commonly seen (Christensen *et al.*, 2002). Similar findings are illustrated in Figure 1.3.

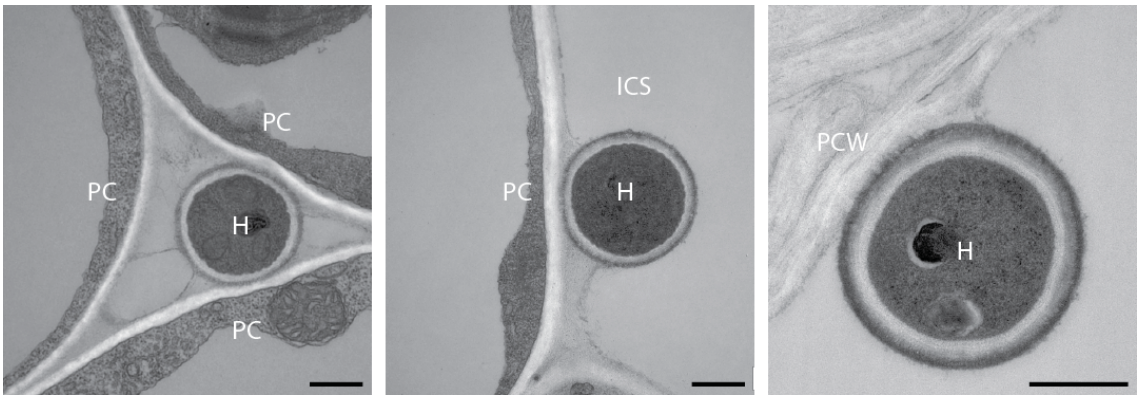

Figure 1.3 Transmission electron micrographs of *E. festucae* Fl1 wild-type within *L. perenne*. Transverse sections of pseudostem tissue containing hyphae of Fl1 wild-type. H = hyphae, PC = plant cell, PCW = plant cell wall, ICS = intercellular space. Bars = 500 nm.

Due to the physical attachment of fungal hyphae to the host plant cells the fungus has evolved a specialised growth mechanism to match the rapid growth rate of the host (Schardl *et al.*, 2004; Christensen *et al.*, 2008). As there is a significant difference in natural growth rate of the two organisms, the fungus undergoes intercalary extension in order to continue growing at the same rate and colonise the mature leaf blade (Christensen *et al.*, 2008). Intercalary extension is likely induced by the stretching of the fungal hyphae (physical stress), inducing cellular division along the hyphae undergoing the physical stress not only at the apical tip as in other fungal species (Christensen *et al.*, 2008). The age of the hyphae matches that of the host tissue that it is firmly attached to. In the mature differentiated leaf blade the hyphae are also differentiated (Christensen *et al.*, 2008) unlike, electron dense hyphae seen in the actively growing expansion zone (Figure 1.3). Due to the highly regulated growth of the fungus *in planta* it is important to understand the molecular mechanisms controlling the symbiotic interaction between Epichloë endophytes and the host plants.

The association of *Epichloë festucae* and *Lolium perenne* has been established as a model system for the study of the biology of symbiotic interactions with temperate grasses, including the biochemical processes involved in the production of bio-active alkaloids. This has been shown to be a stable representative symbiotic interaction (Christensen *et al.*, 2002; Scott *et al.*, 2007). *E. festucae* is a natural symbiont of *Festuca longifolia* and *Festuca rubra* (Christensen *et al.*, 2002), but

forms a stable association with *L. perenne*, exhibiting regulated symbiosis which is comparable to that of the natural fungal symbiont *Epichloë festucae var. lolii* (formerly *Neotyphodium lolii*, Leuchtmann *et al.*, 2014) (Christensen *et al.*, 2002; Scott *et al.*, 2007). *E. festucae* Fl1 is a preferred model system for experimental studies as it has a higher growth rate and is also more readily transformable than that of *E. festucae var. lolii* (Scott *et al.*, 2007). In light of this many experimental studies of *E. festucae in planta* have been carried out, to further understand the biology of the association. To date several genes have been identified to play a role in the symbiotic interaction, identified by their deletion resulting in a change from mutualistic to a pathogenic-like *in planta* phenotype.

1.2. Genetic approaches to understand symbiosis

Two main approaches have been used to gain an understanding of the symbiotic interaction at a molecular level. These are forward genetics, where random mutagenesis is carried out to generate mutants that change the interaction phenotype with *L. perenne* i.e. plasmid insertional mutations (Tanaka *et al.*, 2006). The mutants generated were analysed to determine what genes had been disrupted and their contribution to the resulting mutant phenotype. The second is that of reverse genetics, where specific genes that were selected as likely symbiotic regulators were knocked out and the phenotype examined to determine whether they have a role in the symbiosis.

Forward mutagenesis resulting in disruption of *noxA,* which encodes an NADPH oxidase, was the first gene reported resulting in a mutant phenotype of stunted growth of the host plant, premature senescence and death (Tanaka *et al.*, 2006). Additional phenotypic changes were identified in this mutant, such as the hyphae were hyper-branched in comparison to the wild-type (Tanaka *et al.*, 2006; Takemoto *et al.*, 2007). This hyper-branching resulted in prolific growth of the fungal hyphae throughout the aerial tissues. Due to this, an overall increase in the total fungal biomass also resulted (Tanaka *et al.*, 2006). Additionally extensive colonisation of the vascular bundles was observed, a phenotype not seen in wild-type associations. These phenotypic changes seen in Δ*noxA* demonstrates the loss

of synchronisation between the fungus and the plant. It has been identified that ROS signaling plays a significant role in the switch from controlled mutualistic growth to prolific pathogenic growth of the fungal hyphae *in planta* (Tanaka *et al.*, 2006).

Reverse genetics was carried out targeting *sakA* the stress-activated MAP kinase, as it is an important signaling gene. The resulting deletion mutant also exhibited significant phenotypic changes (Eaton *et al.*, 2010). Eaton *et al* (2010) noted that the Δ*sakA* mutant phenotype was not as severe as Δ*noxA*, resulting in varied host plant stunting, premature senescence, large vascular bundle colonisation and higher numbers of plant death. Additionally, Δ*sakA* mutants displayed elevated levels of ROS production (Eaton *et al.*, 2010). To gain a further understanding of additional genes that are important in the switch to pathogenicity high throughout RNA sequencing (RNAseq) was carried out using RNA from wild-type *in planta* and Δ*sakA in planta*.

1.2.1. High throughput RNA sequencing

A total of 1202 fungal genes, ~11% of the genome, were differentially expressed with 894 genes up-regulated and 308 genes down regulated in the Δ*sakA* sample in comparison to that of wild-type (Eaton *et al.*, 2010). Of the up-regulated genes, many of these encoded hydrolytic enzymes and transporters (Eaton *et al.*, 2010). In contrast, the down-regulated genes included genes involved in production of secondary metabolites such as peramine and lolitrem production (Eaton *et al.*, 2010). As a result of the RNAseq analysis the variation of the genes that are differentially expressed shows the large number of contributors to the control of the symbiotic interaction. To refine the data set analysis additional RNAseq analysis of two symbiotic mutants previously identified, Δ*noxA* and a transcription factor Δ*proA*, was carried out by Eaton *et al.* (unpublished). This experiment identified a core set of 182 genes important in the symbiotic association. Within the up regulated genes in the Δ*sakA* data were two genes encoding adhesins, *adsA* and *adsB*, which have been identified in other fungal systems as proteins that are

important in adherence and virulence. In the three-way RNAseq analysis only *adsB* was significantly up-regulated in all three symbiotic mutant associations.

1.3. Adhesins

Adhesins have been extensively studied and characterised in prokaryotes and yeast. Adhesins have a general structure of a N-terminal carbohydrate or peptide binding domain, central serine or threonine rich glycosylated domains and C-terminal region mediating covalently cross linking to the cell wall by modified glycophosphatidylinositol (GPI) anchors (Dranginis *et al.*, 2007). It has been shown that these proteins are important for adherence to cellular surfaces. This is important in development, symbiosis and pathogenicity (Dranginis *et al.*, 2007). Yeast adhesin proteins are anchored on the outer cell wall surface by the GPI anchor and from here the proteins can interact with the immediate environment. The mode of action of attachment due to the adhesin protein is by two different modes. The first being a lectin-like (sugar sensitive) adhesion and the second sugar-insensitive (Verstrepen & Klis, 2006). These proteins play an important role in mating of different yeast cells and in pathogenicity (Dranginis *et al.*, 2007). However, less is known about the role adhesins play in filamentous fungi. Adhesin genes have been identified and functionally characterised in *Metarhizium robertsii* (Wang & St Leger, 2007; Barelli *et al.*, 2011; Wyrebek & Bidochka, 2013) and recently studied in *Beauveria bassiana* (Xiao *et al.*, 2012).

1.3.1. Adhesins –filamentous fungi

The insect pathogen *Metarhizium robertsii* (formerly *Metarhizium anisopliae*) has two adhesin genes that were shown to be important in colonisation and/or pathogenicity (Barelli *et al.*, 2011). The first adhesin-like protein, Mad1, has been shown to play an important role in the fungal adherence to the insect cuticle (Wang & St Leger, 2007). Whereas, the second adhesin-like protein, Mad2, has been shown to play a role in the colonisation of plant roots (Wang & St Leger, 2007). Wang and St Leger (2007) have shown that *Mad1* also plays an important role in the cell cycle, in respect to the organisation of the cytoskeleton and cell

division. When deletion mutants of *Mad1* were generated the notable phenotypic difference was the decrease in virulence in comparison to that of wild-type (Barelli *et al.*, 2011). Results gained by Barelli *et al.* (2011) showed that the regulation of *Mad2* was comparable to that of known stress related genes. These expression patterns were seen under conditions such as nutrient starvation and other stress activators (Barelli *et al.*, 2011).

Phylogenetic analysis of *Mad1* and *Mad2* suggests that the association with the host plants plays a greater role in the evolution rather than that of the insect host (Wyrebek & Bidochka, 2013). However, overall both *Mad1* and *Mad2* are relatively well conserved within the *Metarhizium spp.* Several putative transcriptional elements associated with the *Mad2* promoter were identified; stress responsive elements (STRE), post diauxic shift element (PDS), degenerative TATA box element and TATA-like element (Wyrebek & Bidochka, 2013). The STRE element activates genes under various environmental stresses, for example glucose starvation. In response to nutrient limitation the PDS mediates transcriptional activation. The presence of these elements is consistent with expression patterns seen by Barelli *et al.* (2011). Presence of *M. robertsii* has been shown to play a role in root hair development of the host plant (Sasan & Bidochka, 2012). The number of Δ*Mad2* conidia attached to the roots was lower than that of wild-type (Sasan & Bidochka, 2012). Sasan and Bidochka (2012) also showed that when plants were treated with Δ*Mad2* conidia there was little root hair development, suggesting that attachment of conidia is important in root hair development.

Adhesin homologues have also been identified in *B. bassiana* (Xiao *et al.*, 2012). However, the mechanism of attachment used by *B. bassiana* has been shown to involve hydrophobins. Hydrophobins play a role in the cell surface hydrophobicity and virulence (Zhang *et al.*, 2011). The functional role of hydrophobins was shown by the reduction of conidia adherence when the individual genes were deleted (Zhang *et al.*, 2011). This finding suggests a possible redundancy for physical attachment of filamentous fungi to their host plants.

1.4. Aims of this study

To date the mode of attachment of *E. festucae* hyphae to the host tissue has not been identified. Due to the highly controlled growth of the hyphae *in planta* identifying the genes involved in attachment of the hyphae will shed light on the symbiotic association. Based on the work in *M. robertsii* and the up-regulation of adhesins in the RNAseq data (Eaton *et al.*, 2010) the aim of this study was to determine if adhesins play a similar role in the *E. festucae*/*L. perenne* association.

The first objective of this study was to determine the effect of deleting *adsA* and *adsB* and determine whether they are required for normal axenic culture growth. The second objective was to determine the effect on the symbiotic association of *E. festucae* and *L. perenne* when either *adsA* or *adsB* were deleted. The third objective was to test whether *adsA* or *adsB* confer adherence to plant surfaces by expression in a non-adherent yeast strain.

2. Materials and Methods

2 Materials and Methods

2.1. Biological materials

Bacterial and fungal strains, plasmids and plant material used this study are listed below in Table 2.1.

Table 2.1. Organisms and plasmids used in this study

Organism/Strain	Relevant Characteristic(s)	Reference
E. coli		
PN4138	DH5α/pRS426	(Christianson *et al.*, 1992)
PN4142	DH5α/pCE53; Amp^R	This Study
PN4414	DH5α/pCE55; Amp^R	This Study
PN4232	DH5α/pPC2; Amp^R	This Study
PN2966	DH5α/pYES2, Amp^R	Invitrogen
PN4220	DH5α/pCE87; Amp^R	This Study
PN4221	DH5α/pCE88; Amp^R	This Study
PN2019	DH5α/pREP-Cgfp, Amp^R	Hagan I., UK
S. cerevisiae		
PN2806 (FY834)	MATα; *his*3Δ200; *ura*3-52; *leu*2Δ1; *lys*2Δ202; *trp*1 Δ 63	(Winston *et al.*, 1995)
PN2932 (INVSC1)	MATa *his*3Δ1 *leu*2 *trp*1-289 *ura*3-52/MATα *his*3Δ1 *leu*2 *trp*1-289 *ura*3-52	Invitrogen
PN3030 (*adsA*#1)	PN2932/pCE87,pREP-Cgfp; Ura^+, Leu^+	This study
PN3031 (*adsA*#2)	PN2932/pCE87,pREP-Cgfp; Ura^+, Leu^+	This study
PN3032 (*adsB*#3)	PN2932/pCE88,pREP-Cgfp; Ura^+, Leu^+	This study
PN3033 (*adsB*#4)	PN2932/pCE88,pREP-Cgfp; Ura^+, Leu^+	This study
PN3029 (pYES2 + EGFP)	PN2932/pYES2, pREP-Cgfp; Ura^+, Leu^+	This study
PN3028 (INVSc1+ EGFP)	PN2932/pREP-Cgfp; Leu^+	This study
E. festucae		
PN2278 (Fl1)	WT	(Young *et al.*, 2005)
PN2893 (Δ*adsA* 6-4)	PN2278/pCE55; Hyg^R	This Study
PN2966 (Δ*adsA* 7-3)	PN2278/pCE55; Hyg^R	This Study
PN2894 (Δ*adsA* 8-9)	PN2278/pCE55; Hyg^R	This Study
PN2895 (Δ*adsB* 11-8)	PN2278/pCE53; Hyg^R	This Study
PN2896 (Δ*adsB* 14-2)	PN2278/pCE53; Hyg^R	This Study

PN3044 (Δ*adsB* 11-8/*adsB* #9)	PN2895/pPC2; Hyg^R; Gen^R	This Study
PN3045 (Δ*adsB* 11-8/*adsB* #22)	PN2895/pPC2; Hyg^R; Gen^R	This Study
PN3046 (Δ*adsB* 14-2/*adsB* #13)	PN2896/pPC2; Hyg^R; Gen^R	This Study
PN3047 (Δ*adsB* 14-2/*adsB* #14)	PN2896/pPC2; Hyg^R; Gen^R	This Study
L. perenne		
L. perenne cv. Samson	-	AgResearch
Plasmids	Relevant Characteristic(s)	Reference
pCE53	pRS426 containing 5'*adsB*-P*trpC-hph*-3'*adsB*; Amp^R , Hyg^R	This Study
pCE55	pRS426 containing 5'*adsA*-P*trpC-hph*-3'*adsA*; Amp^R, Hyg^R	This Study
pPC2	pRS426 containing P*adsB-adsB*-T*adsB*; Amp^R	This Study
pCE87	pYES2 containing *adsA*	This Study
pCE88	pYES2 containing *adsB*	This Study
pREP-Cgfp	pREP containing Cgfp	Hagan I., UK

2.2. Media and growth conditions

Unless otherwise specified, all media were prepared with Nanopure water supplied by a Barnstead NANOpure ultrapure water purification system (Thermo Scientific), sterilised and autoclaved at 121°C for 20 min.

2.2.1. *E. coli*

E. coli cultures containing plasmids (Table 2.1) were grown overnight at 37°C in LB (Luria-Bertani) broth, with shaking (200 rpm) or on LB agar containing 100 µg/ml ampicillin as previously described (Miller & Anderson, 1962). For short-term storage of *E. coli* strains, cultures were streaked onto LB plates and stored at 4°C. For long term storage cultures were stored in 50% (v/v) glycerol at -80°C.

2.2.1.2. Luria-Bertani (LB) medium

LB liquid medium (Miller & Anderson, 1962) contained 5 g/L tryptone, 10 g/L yeast extract and 5 g/L NaCl, pH 7.0-7.5. For solid media, agar was added at 15 g/L.

2.2.1.3. SOC medium

SOC medium (Dower *et al.*, 1988) contained 20 mM glucose, 10 mM $MgCl_2$, 10 mM $MgSO_2.7H_2O$, 10 mM NaCl, 2.5 mM KCl, 20 g/L tryptone and 5 g/L yeast extract.

2.2.2. *S. cerevisiae*

S. cerevisiae cultures (Table 2.1) were grown on synthetic defined drop-out medium (2.2.2.1) or Yeast-extract Peptone Dextrose (YPD) medium (2.2.2.3) at 30°C for three days, unless otherwise specified. Expression of the GAL1 promoter of the pYES2 vector was induced by addition of filter sterilised 2% (w/v) galactose and 2% (w/v) raffinose or repressed with the addition of 2% (w/v) glucose to the medium after autoclaving. For short-term storage of *S. cerevisiae* strains, cultures were streaked on to synthetic complete (SC) plates and stored at 4°C. For long term storage cultures were stored in 20% (v/v) glycerol at -80°C.

2.2.2.1. Synthetic defined uracil drop-out (SD-Ura) medium

SC-Ura medium contained 1 M sorbitol, 0.67% (w/v) yeast nitrogen base without amino acids and 0.08% (w/v) uracil dropout supplement (Clontech #630416), with pH adjusted to 5.8. Glucose was added to a final concentration of 2% (w/v) after autoclaving. For solid media, agar was added at 15 g/L

2.2.2.3. Synthetic complete uracil and leucine drop-out (SC-Ura-Leu) medium

SC-Ura-Leu medium contained 0.67% (w/v) yeast nitrogen base without amino acids, 0.08% (w/v) uracil and leucine drop out mix (2.2.2.2.1), pH adjusted to 5.6. The carbon source (glucose, galactose or raffinose) was added to a final concentration of 2% after autoclaving. For solid media, agar was added at 15 g/L.

2.2.2.3.1. Synthetic Complete uracil and leucine drop-out mix

SC-Ura-Leu drop-out mix contained 0.06% (w/v) adenine hemisulfate, arginine HCl, histidine HCl, lysine HCl, methionine, tyrosine; 0.09% (w/v) phenylalanine, tryptophan, 0.18% (w/v) homoserine and 0.27% (w/v) valine. Amino acid powder stocks were combined and ground with a sterile mortar and pestle to a fine powder and stored at 4°C.

2.2.2.4. Yeast-extract peptone dextrose (YPD) medium

YPD medium contained 2% (w/v) peptone and 0.5% (w/v) yeast extract, with pH adjusted to 5.8. Glucose was added to a concentration of 2% (w/v) after autoclaving.

2.2.3. *E. festucae* growth conditions

2.2.3.1. Potato dextrose (PD) medium

PD medium contained 2.4% (w/v) potato dextrose (Difco), pH 6.5. For solid media agar was added at 15 g/L. For antibiotic selection hygromycin or geneticin were added to final concentrations of 150 μg or 200 μg/mL respectively.

2.2.3.3. Regeneration (RG) medium

RG medium contained 2.4% (w/v) potato dextrose (Difco), 0.8 M sucrose, with pH adjusted to 6.5. Agar was added to a final concentration of 8 g/L for soft overlays and 15 g/L for base agar layers.

2.2.3.4. Water agar medium

Water agar contained 15 g/L (w/v) agar.

2.2.3.5. Water agarose medium

Water agarose contained 15 g/L (w/v) low melt agarose.

2.2.4. *L. perenne* growth conditions

2.2.4.1. Water agar medium

Water agar medium contained 3 g/L agar.

2.2.4.2. Seedling growth conditions

Surface sterilised ryegrass seeds were transferred to water agar plates where the seeds and allowed to germinate for 7 days at 22°C in continuous darkness prior to inoculation. Inoculated seedlings were returned to the dark for a further 7 days to continue etiolation, then transferred to continuous light for a final 7 days before planting the seedlings containing commercial fungicide free potting mix.

2.2.4.3. Plant growth conditions

Ryegrass plants were incubated in a temperature (19°C) and light controlled (16 h/8 h light/dark cycle) growth room. Plants were regularly watered, and when required treated with insecticides and *Epichloë spp.* safe fungicides.

2.3. DNA isolation

2.3.1. *E.coli* plasmid DNA

For plasmid isolation from *E. coli*, the bacteria were grown overnight at 37°C with shaking at 200 rpm. Plasmid DNA was isolated by alkaline lysis and extraction using the High Pure Plasmid Isolation Kit (Roche) according to the manufacturers instructions.

2.3.2. *S. cerevisiae* plasmid DNA

For plasmid isolation from *S. cerevisiae*, a single yeast colony was inoculated into YPD broth and grown overnight at 30°C with shaking at 200 rpm. The cells were pelleted (15s; 13,000 rpm) and, to the pellet, 100 µL lysis buffer (150 mM EDTA, 50 mM Tris-HCl, 1% (w/v) SLS, pH8), 100 µL chloroform and 100 µL of glass beads were added. The mixture was vortexed for 2 min and centrifuged (10 min; 13,000 rpm). The supernatant was transferred to a fresh tube and then 10 µL of 3 M KOAc and 250 µL of isopropanol were added. The suspension was incubated at room temperature for 10 min, the cells pelleted (5 min; 13,000 rpm) and the pellet washed with 1 mL of 70% ethanol, air-dried and resuspended in 50 µL H_2O. DNA was used neat for PCR screening.

2.3.3. Fungal Genomic DNA

2.3.3.1. DNA purification

2.3.3.1.1. Byrd method

Pure, high molecular weight fungal genomic DNA was extracted from freeze dried mycelium by the method of Byrd *et al*. (1990). About 100 mg of freeze-dried mycelium was ground to a fine powder in liquid nitrogen and resuspended in 10 mL of lysis buffer containing 2 mg/mL Proteinase K. Samples were incubated at 37°C for 30 min the centrifuged at 4,000 rpm for 10 min at 4°C. The supernatant

was transferred to a fresh tube and 1 volume phenol was added, this was then mixed and centrifuged (15 min, 10,000 rpm, 4°C). The clear aqueous phase was transferred to a fresh tube and 0.5 volume phenol and 0.5 volume chloroform was added, this was then mixed and centrifuged (15 min, 10,000 rpm, 4°C). The clear aqueous phase was transferred to a fresh tube and 1 volume of chloroform was added, this was then mixed and centrifuged (15 min, 10,000 rpm, 4°C). The clear aqueous phase was transferred to a fresh tube and 1 volume isopropanol was added, this was mixed well and DNA was allowed to precipitate for 15 minutes at room temperature. The DNA was pelleted at 8,000 rpm for 10 min at 4°C. The supernatant was removed and the DNA pellet was resuspended in 5 mL of 1 M NaCl, this was mixed well and centrifuged (5 min, 10,000 rpm, 4°C). The supernatant was transferred to a fresh tube and 5 mL isopropanol was added then mixed well and stored at -20°C for 15 minutes and then centrifuged (30 min, 13,000 rpm, 4°C). The supernatant was removed and the pellet was washed with 70% ethanol. The pellet was air dried at 37°C for 20 min and resuspended in 500 µL sterile H_2O.

2.3.3.1.2. Rapid genomic DNA extraction

For small scale, rapid extraction of genomic DNA, a 2 mm square of agar free mycelia was macerated with the tip of a scalpel blade in a mircocentrifuge tube containing 150 µL lysis buffer and incubated at 70°C for 30 min. The lysate was neutralised by the addition of 1 volume of 5 M potassium acetate. Samples were incubated on ice for 10 min and centrifuged (20 min, 13,000 rpm). DNA was isolated from the aqueous phase by precipitation with 0.7 volumes of 4°C isopropanol and centrifugation at 13,000 rpm for 20 min. The pellet was air dried and resuspended in 20 µL sterile H_2O. Samples were stored at 4°C and used neat for PCR screening.

2.3.3.2. DNA concentration

When required, genomic DNA was concentrated by adding 0.1 volume of 3M sodium acetate and 2 volume 95% ethanol to the samples and incubated at -20°C

overnight. The DNA was pelleted by centrifugation (20 min, 13,000 rpm) and the resulting pellet was washed with 70% ethanol (v/v), then air-dried and resuspended in H_2O.

2.4. PCR amplification

PCR assays for screening were performed in 50 µL PCR tubes and stored at 4°C until analysed. Sequences of PCR primers are provided in the Table 2.2.

Table 2.2 Primers used in this study

Name	Sequence 5'-3'	Used for
adsA1	GTCTCCTGCCACAAGATCAAG	*adsA* Screening
adsA2	AAAGTGGTGACAAAGGTGGTG	*adsA* Screening
adsA3	TTCACCTTGTCACCGCCATC	*adsA* Screening
adsA4	TCCATTGTCGTTCCTGTTCC	*adsA* Screening
adsA5	GTGTGGCAACTCGTGTAAGTG	*adsA* Screening
adsA6	GCATACATTGGCGTAATCTCC	*adsA* Screening
adsB1	AAGTCTGCTGTCCTCGCTGTC	*adsB* Screening
adsB2	TGGTGAGGAGGGTGCCAGAC	*adsB* Screening
adsB3	TCTTTGCTGGAGAACGAGACC	*adsB* Screening
adsB4	CAGCCTGTAATCATAGCGAAG	*adsB* Screening
adsB5	TTTCGCACTACCCGTCCACTC	*adsB* Screening
adsB6	TCTGCGTGACGGTGGAAGTTC	*adsB* Screening
adsB7	GGATGCTGGTTACACGAAGTG	*adsB* Complementation
adsB8	TAGCTAGGATTACGATCTAGG	*adsB* Complementation
adsB9	TCTGAGAAGCACCAGCGATG	*adsB* Complementation
adsB10	CAACACTCAGGCTCCTTCTCC	*adsB* Complementation/ Screening
pRS426-PadsB-F	GTAACGCCAGGGTTTTCCCAGTCACGATCG TGTCTTGTCTGCCACCTC	*adsB* Complementation
TadsB-pRS426-R	GCGGATAACAATTTCACACAGGAAACAGC TCACCAAGGACGACAGTATCG	*adsB* Complementation

2.4.1. Standard PCR

Standard PCR amplification was performed with *Taq* DNA polymerase (Roche). The reaction mixture contained 5 µL of 10× Taq reaction buffer, 1 µL (0.2 µM final concentration) of each primer, 2.5 µL dNTPs (200 µM final concentration), 1 ng template DNA and 1 U of Taq polymerase. The following conditions were used: one

cycle at 94°C for 2 min; 35 cycles at 94°C for 30 s, 45-68°C for 30 sec and 72°C for 1 min per kb. Final extension consisted of one cycle at 72°C for 10 min.

2.4.2. High fidelity PCR

When proofreading activity was required the Expand High Fidelity™ PCR system (Roche) or Phusion® High Fidelity DNA Polymerase (Thermo Fisher) was used.

For amplification using the Expand High Fidelity™ PCR system the reaction mixture contained 5 µL of 10× Expand High Fidelity Buffer 1 µL (0.2 µM final concentration) of each primer, 2.5 µL dNTPs (200 µM final concentration), 1 ng template DNA and 1.75 U of Expand High Fidelity Enzyme mix. The following conditions were used: one cycle at 94°C for 2 min; 35 cycles at 94°C for 30 s, 45-68°C for 30 sec and 72°C for 1 min per kb. Final extension consisted of one cycle at 72°C for 10 min. Final extension consisted of one cycle at 72°C for 10 min.

For amplification using the Phusion® High Fidelity DNA Polymerase the reaction mixture contained 10 µL of 5× Phusion® HF Reaction Buffer 2.5 µL (0.5 µM final concentration) of each primer, 2.5 µL dNTPs (200 µM final concentration), 1 ng template DNA and 1 U of Phusion® polymerase. The following conditions were used: one cycle at 98°C for 30 s; 10 cycles at 98°C for 10 s, 55°C for 30 sec and 72°C for 15 s per kb; 20 cycles at 98°C for 10 s, and 72°C for 15 s per kb Final extension consisted of one cycle at 72°C for 10 min. Final extension consisted of one cycle at 72°C for 10 min.

2.5. DNA manipulation

2.5.1. DNA quantification

Plasmid DNA was quantified with a NanoPhotometer (Implen) according to the manufacturer's instructions.

Genomic DNA concentrations were estimated by comparing the fluorescent intensity of 1 µL samples of uncut genomic DNA with a series of Lambda (λ) DNA (Fermentas) mass standards (10-200 ng) in agarose gels (1% w/v) stained with ethidium bromide. Samples were visualised using a Molecular Imager® Gel DocTM XR+ System with Image Lab software #170-8195 (Bio-Rad).

2.5.2. Restriction endonuclease digestion

Plasmid DNA was digested at 37°C for 1-4 h. Digests containing ≤ 100 ng DNA was performed in 10 µL final volumes with 2 U of restriction enzyme. Digests containing ≥ 100 ng DNA were performed in a final volume of 50 µL with 20 U of enzyme/µg, the optimal buffer was used for each enzyme. For Southern blot analysis 2 µg of *E. festucae* genomic DNA was digested overnight at 37°C in a final volume of 100 µL containing 10 µL 10× optimal buffer and 30 U of restriction enzyme. Reactions were stopped by the addition of SDS loading dye.

2.5.3. Agarose gel electrophoresis

DNA was separated on 0.7-2% argarose gels in 1× Tris/Borate/EDTA (TBE) buffer (89 mM Tris, 89 mM boric acid, 2 mM Na_2EDTA, pH 8.2) with voltage of 90-100 V. DNA solution was loaded into gels diluted 1:4 with SDS loading dye (0.02% (w/v) Bromophenol blue, 20% (w/v) sucrose, 1% (w/v) SDS and 5 mM EDTA). Gels were stained with ethidium bromide (1 µg/mL) for 10-30 min. Bands were visualised using a Molecular Imager® Gel Doc™ XR+ System with Image Lab software #170-8195 (Bio-Rad). 1 kb Plus DNA ladder (Invitrogen) was used as the DNA marker.

2.5.4. Purification of DNA and PCR product

Ethidium bromide-stained DNA bands were visualised and excised on a Dark Reader™ Non-UV transilluminator DR-88M (400-500 nm). DNA was purified from agarose slices or from PCR reactions using the Wizard® SV Gel and PCR Clean-Up System (Promega).

2.5.5. Southern blotting

For Southern blot analysis (Southern, 1975), genomic digests were separated in a 0.8% agarose gel at 30 V overnight and visualised with ethidium bromide staining. Gels were soaked in 0.25 M HCl for 15 min (depurination step) followed by 0.5 M NaOH/5 M NaCl for 30 min (denaturation step), and 0.5 M Tris, pH 7.4, 2.0 M NaCl for 30 min (neutralisation step). Gels were washed in 2× saline-sodium citrate buffer (SSC; 0.3 M NaCl, 30 mM Na^+ citrate) for 2 min and assembled onto the blotting stand prepared as follows: 2× 3MM paper wick soaked in 20× SSC; covered in plastic wrap with a hole slightly smaller than the gel; gel placed on top and overlaid with a nylon membrane; 2× 3MM sheets pre-soaked in 2× SSC; 2× dry 3MM sheets, followed by a stack of paper towels and an evenly positioned weight. The DNA was transferred to the membrane overnight. The membrane was washed in 2× SSC and the DNA was fixed by UV light cross-linking in a Cex-800 UV light cross-linker (Ultra-Lum) at 254 nm for 2 min.

2.5.6. DNA hybridisation

The PCR amplified replacement fragments used to replace *adsA* and *adsB* were used as probes to screen the putative knock-out transformants. 30 ng of each fragment was boiled for 3 min and placed on ice immediately to obtain single stranded fragments. These fragments were radioactively labeled with [α-^{32}P]dCTP (3000 Ci/mmol; Amersham Biosciences) using the High Prime Kit (Roche). Hybridisations were carried out according to the manufacturer's instructions and visualised by autoradiography.

2.5.7. Yeast Recombinational cloning

A single FY834 colony from a fresh YPD plate was inoculated into 5 mL of YPD and grown overnight at 30°C, shaking at 200 rpm. 1 mL of the overnight culture was used to inoculate 50 mL YPD and grown at 30°C, shaking at 200 rpm for a further 4-5 h. The cells were pelleted (5 min; 2,500 rpm) and washed with sterile H_2O, repelleted then suspended in 1 mL of 100 mM LiAc. The cells were pelleted

(15 s; 13,000 rpm) and, to the pellet 240 µL 50% PEG 4000, 36 µL 1 M LiAc, 10 µL 2 mg/mL single stranded carrier DNA and 300 ng of each DNA fragment to under go recombination was added. This suspension was vortexed and incubated at 30°C for 30 min then mixed by inverting and transferred to 42°C for 30 min. The cells were pelleted (15 s; 13,000 rpm) twice and resuspended in 1 mL H_2O. Finally the cells were pelleted (15 s; 13,000 rpm) and resuspended in 50 µL H_2O. SD-Ura plates were spread with 30 µL aliquots of transformed yeast cells and incubated (30°C; 3-4 days).

2.5.7.1. Yeast 'smash and grab'

Transformed FY834 colonies were scrubbed from plates with 2 mL YPD. The cells were pelleted (15 s; 13,000 rpm) and to the pellet, 100 µL lysis buffer, 100 µL chloroform, 100 µL phenol and 100 µL glass beads. The suspension was vortexed for 2 min then centrifuged (10 min; 13,000 rpm). The supernatant was transferred to a fresh tube and 10 µL of 3 M KOAc and 250 µL of isopropanol were added. The suspension was incubated at room temperature for 10 min. The DNA was pelleted (5 min, 13,000 rpm) and the pellet washed with 1 mL of 70% ethanol, air dried and resuspended in 50 µL H_2O.

2.5.8. DNA sequencing

DNA for sequencing was sent to the Massey Genome Service. The BigDye™ Terminator (version 3.1) Ready Reaction Cycle Sequencing Kit (Applied Biosystems) was used. Samples were sent in 20 µL total volumes containing 4 pmol primers and 100-200 ng plasmid DNA or 5-100 ng DNA from PCR reactions. Sequence data was assembled and analysed using the MacVector sequence assembly software, version 12.6.0.

2.7. Bacterial transformation

2.7.1. Chemically competent *E. coli*

50 mL of super optimal broth (SOB; 2% (w/v) tryptone, 0.5% (w/v) yeast extract, 0.05 % (w/v) NaCl, 2.5 mM KCl, 2 mM $MgCl_2$, adjusted to pH 7) was inoculated with fresh overnight culture of *E. coli* and incubated (18°C; 20-50 h; 200 rpm) until mid-log phase was reached (A600 = 0.4-0.8). Cells were chilled on ice for 10 min and centrifuged (10 min 6,000 rcf; 4°C) and resuspended in 17 mL ice-chilled transformation buffer (TB; 10 mM PIPES, 15 mM $CaCl_2$, 0.25 M KCl, pH 6.7, and 0.18 M $MnCl_2$, 0.45 µm filter-sterilised) and incubated on ice for 10 min. The cells were again centrifuged at 4°C for 10 min at 6,000 rcf then resuspended in 4 mL ice-chilled TB. 300 mL of DMSO was added, mixed well, and 100 µL aliquots of cell suspension were flash-frozen in liquid nitrogen and stored at -80°C.

2.7.2. Electrocompetent *E. coli*

600 mL of LB broth was inoculated with 6 mL of overnight culture of *E. coli* and incubated (5 h; 250 rpm; 37°C) until mid-log phase was reached (A_{600} = 0.4-0.8). The culture was chilled on ice for 10 min and centrifuged (15 min; 6,000 rcf; 4°C) and resuspended in 600 mL ice-chilled sterile 10% (v/v) glycerol. The cells were pelleted by three subsequent centrifugations (15 min; 6,000 rcf; 4°C) and resuspended in 300 mL, 12 mL, and finally 1.2 mL of 10% (v/v) glycerol. 50 µL aliquots of cell suspension were flash-frozen in liquid nitrogen and stored at -80°C.

2.7.3. *E. coli* transformation

Plasmids were transferred into Chemically-competent DH5α *E. coli* by the heat shock method. 2-5 µL of DNA (10-100 ng vector DNA) was added to the 50 µL of cells and incubated on ice for 20 min. Cells were heat shocked by incubation in a 42°C water bath for 30 s and immediately transferred back to ice. 250 µL of 37°C SOC medium was added then the cells were incubated at 37°C with shaking

(225 rpm) for 1 h. The cells were spread on LB agar with or without antibiotic selection and incubated overnight at 37°C.

Plasmids were transformed into electrocompetent DH5α *E. coli* by the electroporation method. 1 µL of the yeast plasmid DNA prepared by the 'smash and grab' method (Section 2.5.7.1) was added to 50 µL of cells and the cell-DNA mixture was transferred to a cold 1 mm-electroporation cuvettes. The cuvettes were placed in the electroporator and pulsed at 2.0 kV, 200 Ω and 2.5 µF. 250 µL 37°C SOC medium was added, the suspension was incubated at 37°C with shaking (225 rpm) for 1h. The cells were spread on LB agar containing selective antibiotic as required and incubated overnight at 37°C.

2.7.3.1. CloneChecker™ system

Transformed *E. coli* clones were screened for recombinant plasmids using the CloneChecker™ System (Invitrogen). Colonies were resuspended in 8 µL of lysis solution (Green solution; proprietary components). Samples were heated at 99°C for 30 s in a thermal cycler then cooled to room temperature. 1µL of 10× restriction buffer and 10 U of restriction enzyme was added and incubated for 15-30 min at 37°C. The restriction digest was stopped by added 2 µL SDS loading dye and plasmid DNA digestion was analysed by agarose gel electrophoresis.

2.8. Preparation of complementation constructs

Phusion® High-Fidelity DNA Polymerase was routinely used for amplification requiring proof reading. For difficult templates that Phusion® could not amplify Expand High Fidelity Enzyme mix was used.

2.8.1. *E. festucae adsB* gene complementation construct

The *adsB* complementation construct, pPC2, was prepared by initial PCR amplifications of a 1,808 bp fragment 3' of *adsB* with primer pair pRS426-PadsB-F/adsB6 from WT Fl1 genomic DNA; and a 1,826 bp fragment 5' of *adsB* (inclusive

of *adsB* gene) with primer pair adsB5/TadsB-pRD426-R from WT Fl1 genomic DNA. Purified PCR products and pRS426 vector (digested with *Eco*RI and *Xho*I) were assembled by yeast recombinational cloning (Section 2.5.7). Plates that had more growth than the negative controls were scrubbed and smash and grab (Section 2.5.7.1) was carried out. The resulting DNA was transformed into *E. coli* by electroporation (Section 2.6.3). Ampicillin resistant colonies were selected and screened by the CloneChecker™ System (Section 2.6.3.1) for the correct banding pattern. Colonies with the correct banding pattern were grown overnight in LB+Amp and DNA was extracted using alkaline lysis and purification (Section 2.3.1). The DNA was sent, with appropriate primers for sequencing (Section 2.5.8). A plasmid that contained no base pair changes was used to transform Δ*adsB* protoplasts.

2.9. Fungal transformation

2.9.1. Transformation of *S. cerevisiae* INVSc1

S. cerevisiae INVSc1 (Invitrogen) variant strain transformation with pYES2 (Invitrogen) and pREP-Cgfp was carried out as per the manufactures instructions. INVSc1 cells were transformed sequentially with pYES2/*adsA* or *adsB* then pREP-Cgfp. Transformants were grown on SD-Ura or SD-Ura-Leu respectively.

2.9.1.1. Screening of INVSc1 transformants

Colonies were selected by growth on uracil dropout SD media; in addition to this colonies were screened by PCR before transformation with pREP-Cgfp. pYES2/*adsA* INVSc1 transformants were screen by PCR with primer pair adsA1 and adsA2 yielding a 332 bp fragment. pYES2/*adsB* INVSc1 transformants were screened by PCR with primer pair adsB1 and adsB2 yielding a 221 bp fragment. After transformation with pREP-Cgfp transformants were selected by growth on uracil and leucine dropout SD media and GFP fluorescence using a Dark Reader™ Non-UV transilluminator DR-88M (400-500 nm).

2.9.3. Transformation of *E. festucae*

2.9.3.1. *E. festucae* protoplast preparation

E. festucae protoplasts were prepared using a method described by Young *et al*. (2005). Mycelia were harvested from liquid cultures grown for 4 days at 22°C shaking at 150 rpm. Mycelia were filtered with a sterile nappy liner and washed three times with sterile H_2O then rinsed with osmotic medium (OM) buffer (100 mM Na_2HPO_4, 100 mM NaH_2PO_4, 1.2 M $MgSO_4$, 100 mM Na_2HPO_4). The collected mycelia (~5g wet weight) was suspended in 50 mL of Lysing Enzyme solution (10 mg/mL *Trichoderma harzianum* (Sigma L1412) in OM buffer; filter sterilised, 45 µm filter) and incubated overnight at 22°C, shaking at 80 rpm. Protoplasts were filtered with a sterilised nappy liner and 5 mL aliquots of protoplasts were overlaid with 2 mL of ST buffer (0.6 M sorbitol, 1 M Tris-HCl, pH 8) and centrifuged (10 min; 4,300 rpm; 4°C). Protoplasts were harvested from the lysing enzyme solution- ST buffer interface and subsequently washed three times and resuspended in STC buffer (1 M sorbitol, 50 mM $CaCl_2$, 1 M Tris-HCl, pH 8) to a final concentration of 1.25 x 10^8 protoplasts/mL. For long-term storage 80 µL protoplast aliquots were mixed with 20 µL PEG solution (40% (w/v) PEG 4000, 50 mM $CaCl_2$, 1 M sorbitol, 50 mM Tris-HCl, pH 8).

2.9.3.2. Transformation of *E. festucae* protoplasts

Protoplasts were transformed with DNA using the method previously described by Itoh *et al.* (1994). Approximately 1.25 x 10^7 protoplasts in 100 µL aliquots (80 µL protoplasts + 20 µL PEG solution) were mixed with 1-5 µg DNA, 2 µL spermidine (50 mM) and 5 µL heparin (5 mg/mL) and incubated on ice for 30 min. For complementation protoplasts were co-transformed with geneticin resistance cassette vector pII99 (Figure 6.5). 900 µL of 40% (w/v) PEG solution was added, mixed well and incubated on ice for a further 30 min. 50 µL of the protoplast suspension was added to 3.5 mL of soft overlay RG agar (0.8%) maintained at 50°C. The soft overlay containing protoplasts was immediately poured over a layer of presolidfied RG agar (1.6%) and incubated at 22°C overnight. The regenerating

protoplasts were then overlaid with an additional 5 mL soft agar containing the relevant antibiotic. After solidification of the top layer of agar, the plates were incubated at 22°C for 10-14 days until transformants grew through the antibiotic layer of agar. Antibiotic resistant transformants were transferred to geneticin-containing PD media and nuclear purified by three rounds of subculturing onto antibiotic containing media (Young *et al.*, 2005).

2.9.3.2.1. Screening of *E. festucae* transformants

Putative *adsA* replacement mutants were screened by PCR using primers that flank the gene (adsA5 and adsA6; 2.379 kb WT, 1.576 kb replacement). Putative *adsB* replacement mutants were screen by PCR using primers that flank the gene (adsB5 and adsB4; 1.604 kb WT, 2.756 kb replacement).

Reintroduction of *adsB* was confirmed by PCR using the primer pair adsB10 and adsB4 yielding a 986 bp fragment.

2.10. Plant Inoculation and growth

2.10.1. Seed sterilization

Endophyte free seeds of *L. perenne* cv. Samson were surfaced sterilized by the method adapted from Latch and Christensen (1985). Seeds were soaked in 50% (v/v) sulfuric acid for 20 min, rinsed in sterile H_2O, soaked in 2.5% (v/v) sodium hypochlorite (commercial bleach), rinsed well in sterile H_2O and air dried in a laminar flow cabinet on sterile Whatmann 3MM filter paper.

2.10.2. Seedling inoculation

Sterile rye grass seedlings were artificially infected using the seedling inoculation technique outlined by Latch and Christensen (1985), whereby fungal mycelia are introduced into the seedling via a small incision across the shoot apical meristem.

2.10.3. Detection of endophyte infection by immunoblotting

Inoculated plants were tested for infection by immunoblot detection using polyclonal rabbit antibodies, raised to homogenized mycelia of *E. festucae var. lolii* Lp5 (Gwinn *et al.*, 1991). Tillers were transversely cut close to the base of the pseudostem and printed on a nitrocellulose membrane (BDH). The membrane was incubated in blocking solution (20 mM Tris, 10 mM HCl, 50 mM NaCl, 0.5% (w/v) non-fat milk powder, pH 7.5) at room temperature for 2 h with gentle shaking then blocking solution containing anti-*N. lolii* antibody diluted 1/1000 overnight at 4°C with gentle shaking. Membranes were rinsed with blocking solution and then incubated with blocking solution containing anti-rabbit alkaline phosphatase-conjugated secondary antibody (Sigma) diluted 1/2000 for 2 h at room temperature with gentle shaking. The alkaline phosphatase reaction was developed with Fast Red chromogen (Sigma) for 15 min.

2.11. Yeast adhesion assay

For analysis of adhesion yeast clones were cultured for two days in SD-Ura-Leu broth with 2% (w/v) glucose as a carbon source at 30°C with shaking (200 rpm) to an OD_{600} of ~0.6-0.8. 1 mL was removed and transferred to a sterile tube then centrifuged (15 s, 13,000 rpm) twice and rinsed with SD broth. The cell pellet was resuspended in 1 mL SD broth, 500 µL of cell suspension was transferred to 5 mL fresh SD media containing 2% (w/v) raffinose. The remaining 500 µL was transferred to 5 mL fresh SD media containing 2% (w/v) galactose. These cultures were incubated for 12 h at 30°C with shaking (200 rpm). After 12 h growth cultures were aliquoted into petri dishes containing sections of onion epidermis and incubated at room temperature at 30 min. The cell suspension was removed from the petri dish and the onion epidermis/plate was washed with 0.05% (v/v) Tween-20 for 30 s. The onion epidermis was transferred to a glass slide and observed using an inverted microscope (Section 2.10.1). Images were taken across various areas of the sample and cells expressing GFP were counted.

2.12. Microscopy

Cultures to be analysed by microscopy were inoculated onto a thin layer of water agarose (1.5% w/v) layered on top of a sterile glass slide placed on a pre solidified base layer of water agar (1.5% w/v).

2.12.1. Light and fluorescence microscopy

Transverse 1 µM fixed plant pseudostem tissue sections were stained with toluidine blue as outlined by Christensen *et al*. (2002) and analysed using a compound light microscope (Zeiss Axiophot, 40 x objective) fitted with a CDD camera (Leica Microsystems).

E. festucae culture phenotype was observed by DIC microscopy (Olympus IX83, 40 x objective). Cultures were grown for 7 days. To observe the hyphae the glass slide was cut from the overlay and a 22 x 60 glass cover slip was placed on the agar with 20% (v/v) glycerol. Photographs were taken with a Hamamatsu ORCA-ER C4742-80 digital CCD camera (Hamamatsu Corporation).

Adherent *S. cerevisiae* INVSc1 transformed cells were observed by DIC and fluorescence microscopy using an Olympus IX83 (40 x objective). GFP expressing cells were observed under UV light. Photographs were taken with a Hamamatsu ORCA-ER C4742-80 digital CCD camera (Hamamatsu Corporation).

2.12.2. Confocal microscopy

In planta lateral growth analysis was carried out using a Leica SP5 DM6000B (Leica Microsystems) confocal microscope. An excitation wavelength of 405 nm and acquisition window of 449 nm to 555 nm was set for aniline blue. An excitation wavelength of 488 nm and acquisition window of 498 nm to 558 nm was set for Alexafluor® (WGA-AF488). Images were obtained of 14-17 µm-thick z-distances with a step size recommended by LAS (Leica Application Suite 4.1) software. Images were processed with LAS as a maximum projection (z-stack).

2.12.2.1. Alexafluor ®(WGA-AF488) and aniline blue staining

Pseudostem sheath tissue peels from endophyte infected plants were stained with aniline blue and AlexaFluor® (WGA-AF488) to visulalise *in planta* growth in the pseudostem region of *L. perenne*. The tissue was soaked in 95% (v/v) ethanol at 4°C overnight or for several weeks prior to analysing. Samples were transferred to 10% (v/v) KOH and incubated for 3 h. Samples were washed with PBS (8 g/L, NaCl; 0.2 g/L, KCl; 1.44 g/L, Na_2HPO_4; 0.24 g/L, KH_2PO_4; pH 7.4) then incubated in staining solution (aniline blue (Sigma), 0.2 mg/mL; WGA-AF488 (Molecular Probes), 1 mg/mL; Tween 20 (Invitrogen), 0.02%) for 30 min at room temperature followed by a 10 min vacuum infiltration.

2.12.3. Transmission electron microscopy (TEM)

To examine hyphal ultrastructure and surrounding plant tissue, small disks (0.5 mm thick) of pseudostem tissue from 8-12 week old endophyte infected plants were fixed in 3% glutaraldehyde and 2% formaldehyde in 0.1 M phosphate buffer, pH7.2 for 1h and then transverse sections prepared for light microscopy and TEM as outlined by Spiers & Hopcroft (1993). Fixed samples were analysed with a Philips CM10 (Eindhoren, The Netherlands) transmission electron microscope (Olympus SIS Morada digital camera) or a FEI Tecnai G^2 Spirit BioTWIN transmission electron microscope (Olympus SIS Veleta digital camera).

2.13. Bioinfomatics

2.13.1. Acquisition of sequence data

E. festucae genes boundaries were identified mRNA sequencing data (Eaton *et al.*, 2010) of the *E. festucae* Fl1 (strain 894) and mapped against the genome (http://csbio-l.csr.uky.edu/ef894-2011/). All other fungal sequences used for alignments and phylogenetic analyses were retrieved from the NCBI GenBank database (http://www.ncbi.nlm.nih.gov/) or the Broad Institute

(http://www.broad.mit.edu). Where homologues were identified by BLASTp analysis an E-value threshold of $1x10^{-3}$ was applied.

Gene annotation and naming are given in accordance with the Broad *Apergillus* Comparative Database. The *E. festucae* genome sequence data, as curated by C.L. Schardl at the University of Kentucky are available at http://www.endophyte.uky.edu (Schardl *et al.*, 2013).

2.13.2. Identity and similarity scores

Identity and similarity scores were calculated by Crustal pairwise alignments of sequences using MacVactor version 12.6.0.

2.13.3. Multiple sequence alignments

Amino acid sequence alignments were generated using ClustalW implemented with MacVector (12.6.0). Aligned sequences were trimmed as necessary and used for phylogenetic analysis in MacVector (12.6.0).

2.13.4. Construction of dendrogram

The dendrogram was constructed in MacVector (12.6.0) using the Maximum Likelihood method with 10,000 bootstrap replicates.

2.13.5. Protein domain predictions

Protein domains were predicted using the InterProScan (version 5) server (Jones *et al.*, 2014) http://www.ebi.ac.uk/interpro/search/sequence-search. Signal peptides were predicted using the SignalP (version 4.1) server (Petersen *et al.*, 2011) http://www.cbs.dtu.dk/services/SignalP/. GPI anchor sites were predicted using big-PI Fungal Predictor GPI Modification Site Prediction in Fungi (Eisenhaber *et al.*, 2004) http://mendel.imp.ac.at/gpi/fungi_server.html.

2.14. Statistical analysis

2.14.1. Generalised linear mixed effects model (Poisson data)

The model used for analyzing yeast adhesion count data was adapted from the generalised linear mixed effects model (poisson data) outlined by Breslow and Clayton (1993) (μij ~ Poisson) using RStudio (http://www.rstudio.org/). Effects being analysed were as follows; gene (*adsA*, *adsB* or pYES2), treatment (induced or not induced) and day the experiment was carried out. Day was set as a random effect as it could not be replicated. Base lines set for analysis of the effects were pYES2 for gene and non-induced for treatment. The code written by Poppy Miller is provided in Section 6.3. Raw count data was used for initial analysis (Table 6.1) Outliers that were identified were removed and the modified data was used for the second analysis.

Analysis of cumulative effects was calculated from the output results from RStudio. Equation used: $\log(\mu ij) = \alpha + \beta_{Treatment(i)} + \beta_{Gene(j)}$
Where μ = mean count, i = treatment, j = gene and β = coefficient for effect. Thus, to determine the equation was rearranged, $\mu ij = e^{\alpha+\beta T+\beta G}$.

3. Results

3 Results

3.1. Bioinfomatic analysis of *adsA* and *adsB*

To determine the genome organisation and gene structure of *adsA* (EfM2.037020) and *adsB* (EfM2.037530) a search of the *E. festucae* Fl1 genome was carried out through http://www.endophyte.uky.edu/. Both *adsA* and *adsB* were found to map to the same supercontig with 25 genes separating them (Figure 3.1).

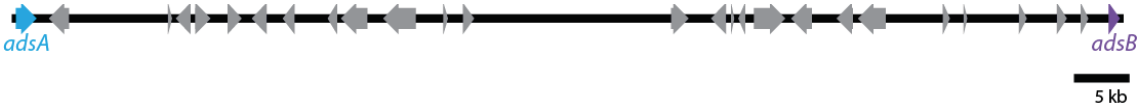

Figure 3.1 Gene linkage map of *adsA* and *adsB* in *E. festucae* Fl1. Schematic of the region between *adsA* and *adsB* on supercontig-6 of the *E. festucae* Fl1 genome sequence. Total distance between *adsA* and *adsB* is 98,124 bp.

Analysis of *adsA* gene structure using the *Epichloë spp*. GBrowse (http://www.endophyte.uky.edu/ef894-2011/) predicts a single open reading frame (ORF) of 1,887 nucleotides with a transcription start site (TSS) 274 bp upstream and a polyadenylation (polyA) 193 bp downstream, both determined from RNAseq data (Eaton *et al.*, 2010) (Figure 3.2). Analysis of *adsB* gene structure predicted a single ORF of 1,014 nucleotides with a TSS 194 bp upstream and polyA 152 bp downstream (Figure 3.2).

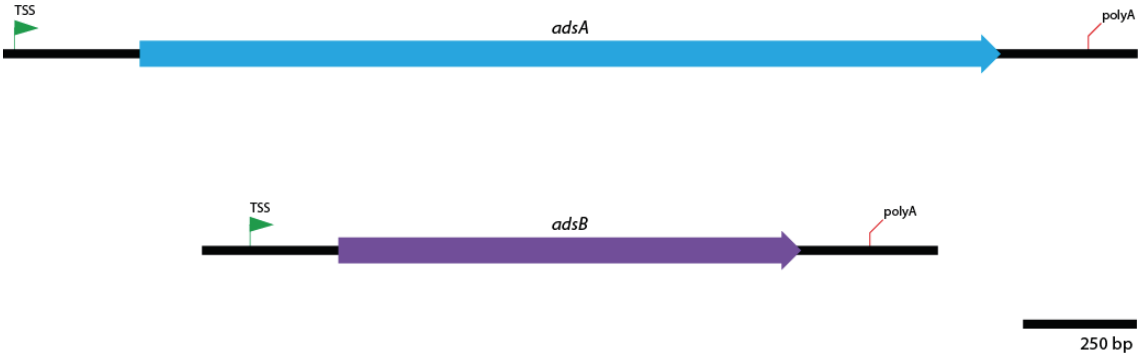

Figure 3.2 Gene structure of *E. festucae adsA* and *adsB*. Schematic of *adsA* nucleotide sequence of 1,887 bp, upstream transcription-start-site (TSS) indicated by green arrow and downstream

termination-site (polyA) indicated by red line. Schematic of *adsB* nucleotide sequence of 1,014 bp, upstream TSS indicated by green arrow and downstream polyA indicated by red line.

Conceptual translation of *adsA* gives rise to a 628 amino acid (aa) polypeptide with a predicted signal peptide, an extra cellular membrane (CFEM) domain and a GPI anchor site (Figure 3.3). The hydrophobic/glycine (G) rich, threonine rich and proline rich regions were identified by analysing the amino acid sequence and an alignment with *M. roberstii* Mad1, which has been functionally characterised (Wang & St Leger, 2007). The conceptual translation of *adsB* gives rise to a 337 aa polypeptide, with a predicted signal peptide and a GPI anchor site. Hydrophobic/glycine (G) rich, threonine rich and proline rich regions were identified and found to be conserved with *M. robertsii* Mad2.

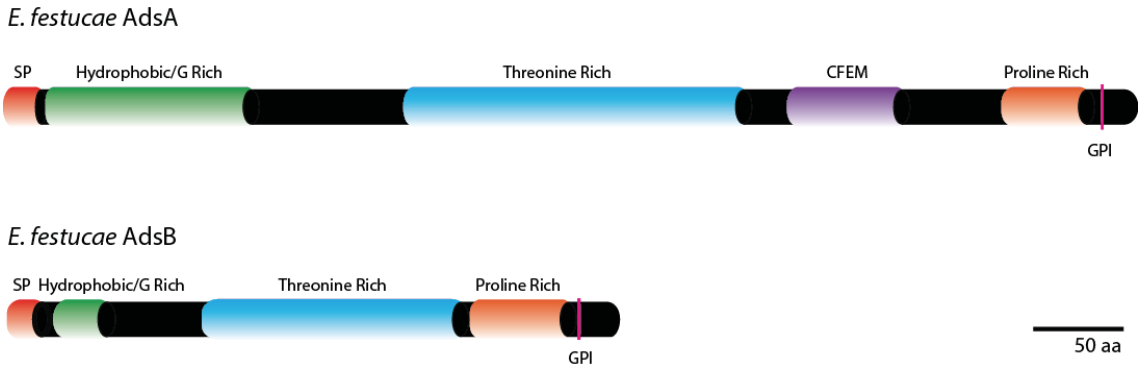

Figure 3.3 Schematic of *E. festucae* AdsA and AdsB. Signal peptide predictions from SignalP 4.1 indicated for both AdsA and AdsB (red shading). CFEM domain predicted by InterPro for AdsA is also indicated. Fungal GPI anchor site predictions for AdsA and AdsB are indicated by pink line. Regions of hydrophobic/glycine (G) rich (green), threonine rich (blue) and proline rich (orange) are indicated. AdsA total length is 629 amino acids. AdsB total length is 338 amino acids.

E. festucae AdsA shares 53% sequence identity with *M. robertsii* Mad1, and greater than 40% identity with homologues from other filamentous fungi (Figure 3.4). Sequence similarity exists through out the entire length of the protein, however *F. graminearum* appears to have some small insertions in the sequence. *E. festucae* AdsB shares 62% sequence identity with *M. robertsii* Mad2 (Figure 3.5). There were no other significant hits outside the Hypocreomycetidae, a subclass of the Sordariomycetes. The *N. haematococca* sequence has a large internal insertion, however the remaining regions of the protein appear to be conserved.

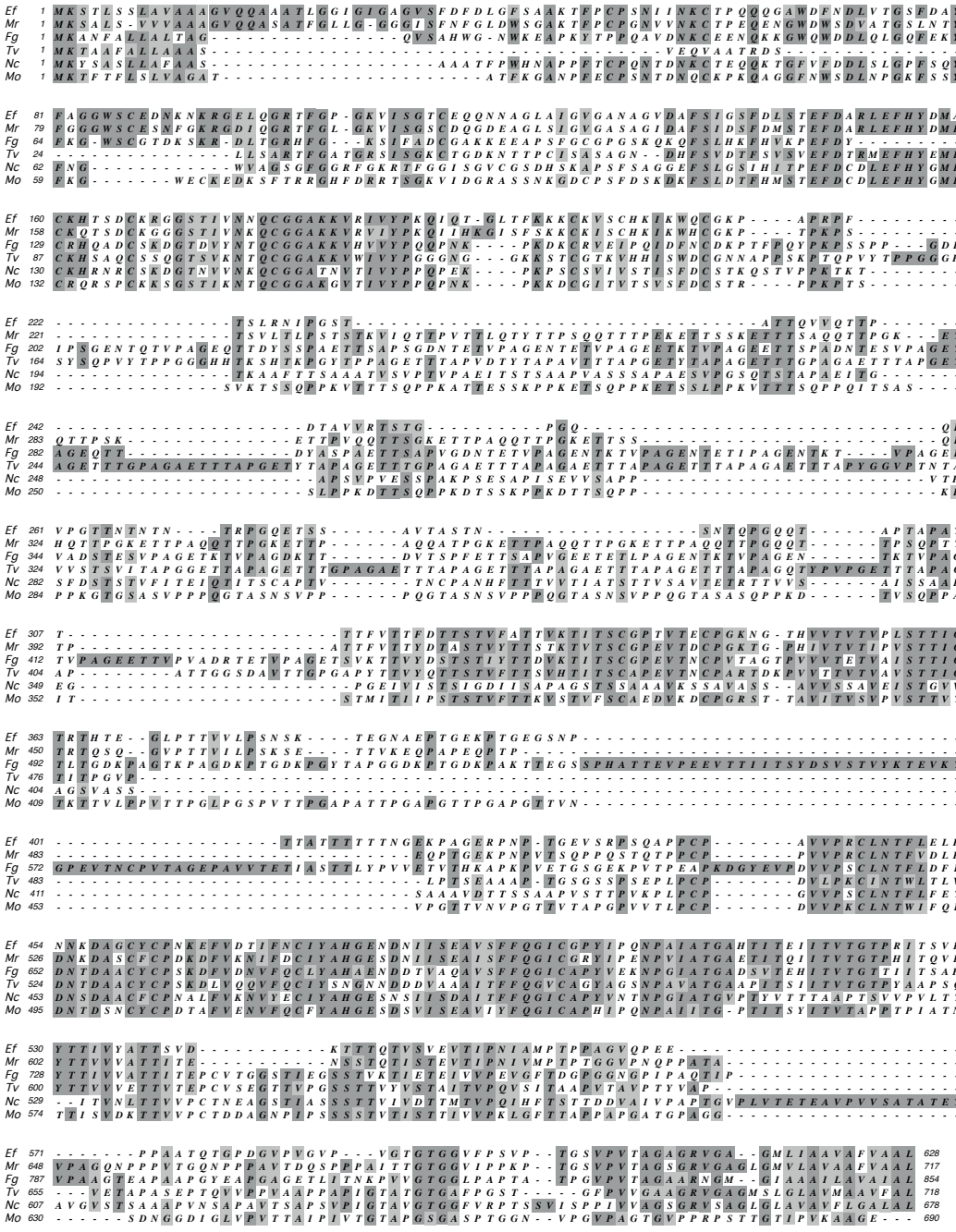

Figure 3.4 Multiple sequence alignment of filamentous fungal AdsA proteins. Amino acid sequences from Ef, *E. festucae* (EfM2.037020), Mr, *M. robertsii* (AGF41723.1); Fg, *F. graminearum* (XP_389020.1); Tv, *T. virens* (EHK22589.1); Nc, *N. crassa* (XP_001728567.1); Mo, *M. oryzae* (XP_003720615.1). Regions of identity are shaded dark grey. Regions of similarity are shaded light grey.

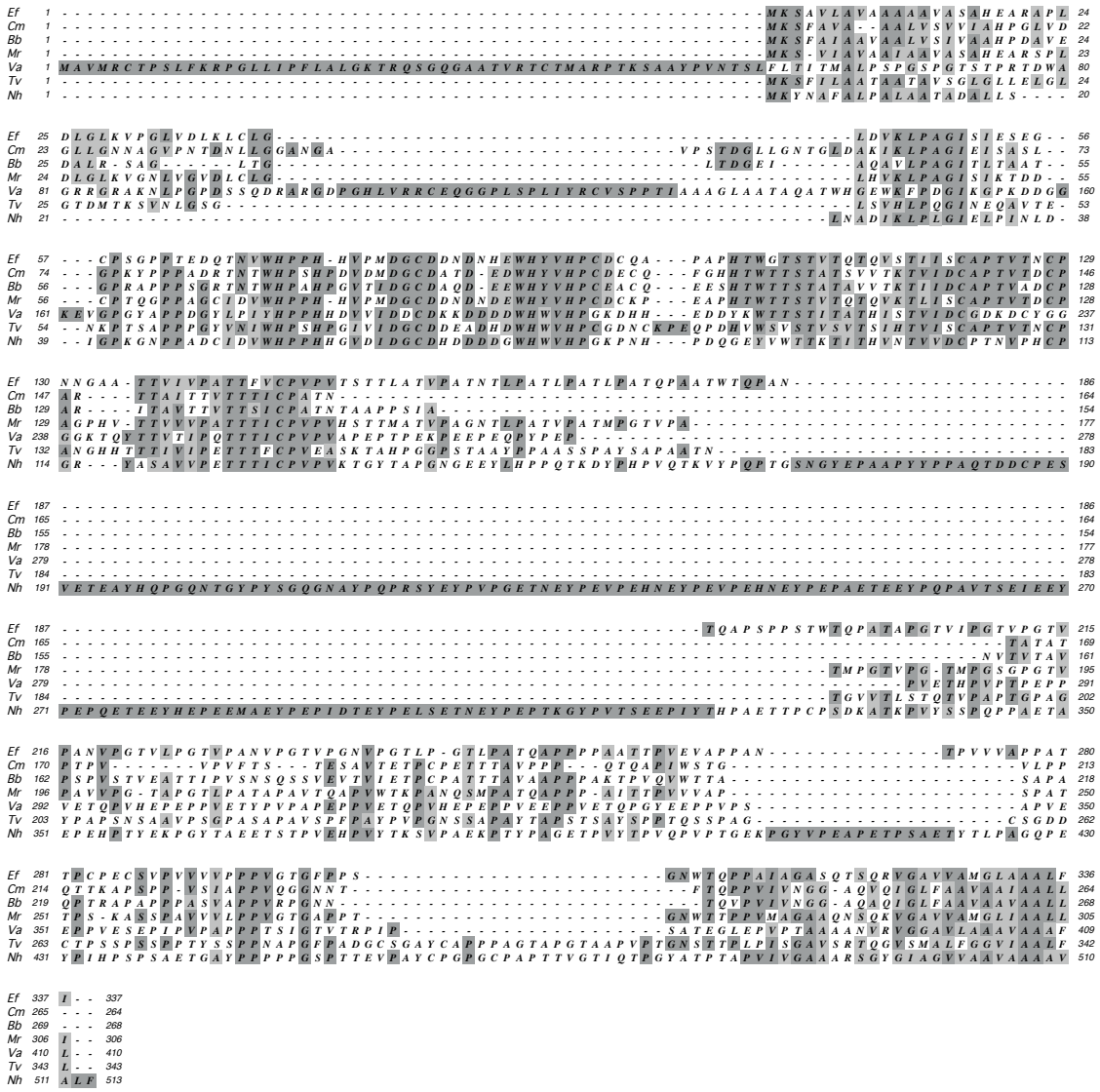

Figure 3.5 Multiple sequence alignment of filamentous fungal AdsB proteins. Amino acid sequences from Ef, *E. festucae* (EfM2.037530); Cf, *C. militaris* (EGX95318.1); Bb, *B. bassiana* (EJP68377.1); Mr, *M. robertsii* (ABC655822.1); Va, *V. alfalfae* (XP_003007547.1); Tv, *T. virens* (EHK22696.1); Nh, *N. haematococca* (XP_003052720.1). Regions of identity are shaded dark grey. Regions of similarity are shaded light grey.

Due to the similar protein structure between AdsA and AdsB and their homologues within the Hypocreomycetidae, phylogenetic analysis was performed to determine if AdsA groups with AdsB. In addition to the sequences used for the multiple sequence alignments (Figures 3.4 and 3.5), additional sequences were retrieved from fungal databases and *E. festucae* AdsA was used as the query. When all the AdsA and AdsB full-length protein sequences were aligned there was very little similarity. Each AdsA sequence was trimmed at both ends to reduce 'noise' and maximise evolutionary divergence. The trimmed sequences of AdsA homologues were aligned with the AdsB full-length protein sequences (Figure 6.9). This resulted in an alignment that generated regions with sequence identity. This alignment was used to construct a maximum-likelihood dendrogram (Figure 3.6).

The dendrogram clearly illustrates that AdsA sequences indicated by blue text group separately to AdsB; a result strongly supported by bootstrap values. However, *N. crassa* and *A. niger* are indicated as a subgroup of AdsA with a lower bootstrap value of 70. AdsB sequences group separately to all AdsA sequences. This grouping is also supported by high bootstrap values. *N. haematococca* was an out group for this dendrogram most likely due to the large internal insertion. Due to the limited sequences available a phylogenetic tree cannot be constructed thus, it cannot be determined how AdsB arose.

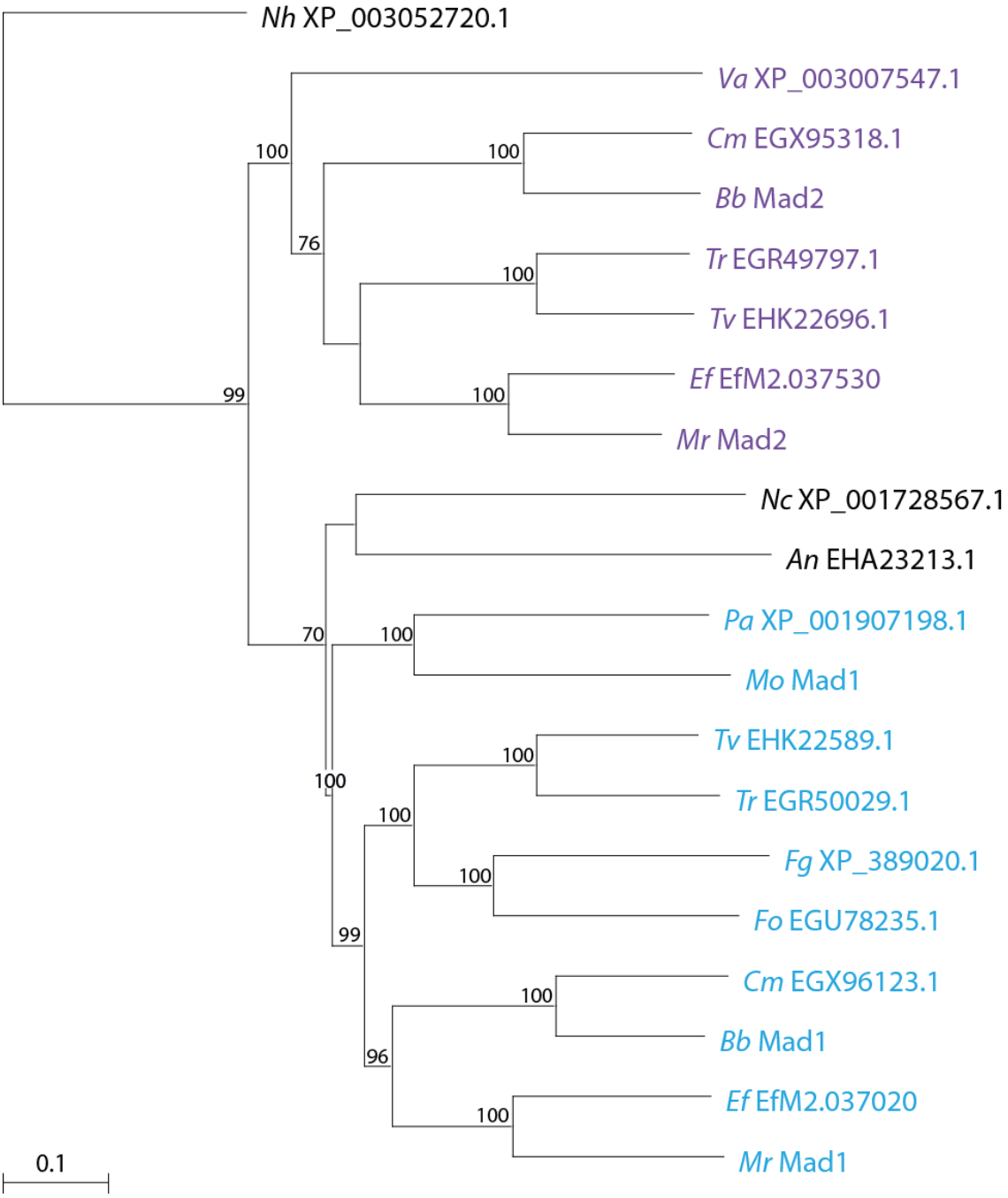

Figure 3.6 Maximum-likelihood dendrogram of filamentous fungal AdsA and AdsB proteins. Values above the branches indicate bootstrap values based on 10,000 replicates. AdsA protein grouping indicated by blue text, AdsB protein grouping indicated by purple text. Gene IDs with associated GenBank accession numbers are as follows: Nh, *N. haematococca* (XP_003052720.1); Va, *V. alfalfae* (XP_003007547.1); Cm, *C. militaris* (EGX95318.1); Bb, *B. bassiana* Mad2 (EJP68377.1); Tr, *T. reesei* (EGR49797.1); Tv, *T. virens* (EHK22696.1); Ef, *E. festucae* (EfM2.037530); Mr, *M. robertsii* Mad2 (ABC655822.1); Nc, *N. crassa* (XP_001728567.1); An, *A. niger* (EHA23213.1); Pa, *P. anserina* (XP_001907198.1); Mo, *M. oryzae Mad1* (XP_003720615.1); Tv, *T. virens* (EHK22589.1), Tr, *T. reesei* (EGR50029.1); Fg, *F. graminearum* (XP_389020.1); Cm, *C. militaris* (EGX96123.1); Bb, *B. bassiana* Mad1 (EJP68417.1); Ef, *E. festucae* (EfM2.037020); Mr, *M. robertsii* (AGF41723.1).

3.2. Molecular analysis of *adsA*

To determine if *E. festucae* adhesins *adsA* and *adsB* are important for growth and development in culture and *in planta,* deletion constructs were prepared for each to generate knock-out mutants (Eaton, unpublished). Hygromycin resistant transformants of *adsA* were initially screened by PCR using primer pair adsA5/adsA6 flanking the deleted region. This PCR screen identified three putative *adsA* deletion mutants Δ*adsA* 6-4, Δ*adsA* 7-3 and Δ*adsA* 8-9 (Figure 3.7).

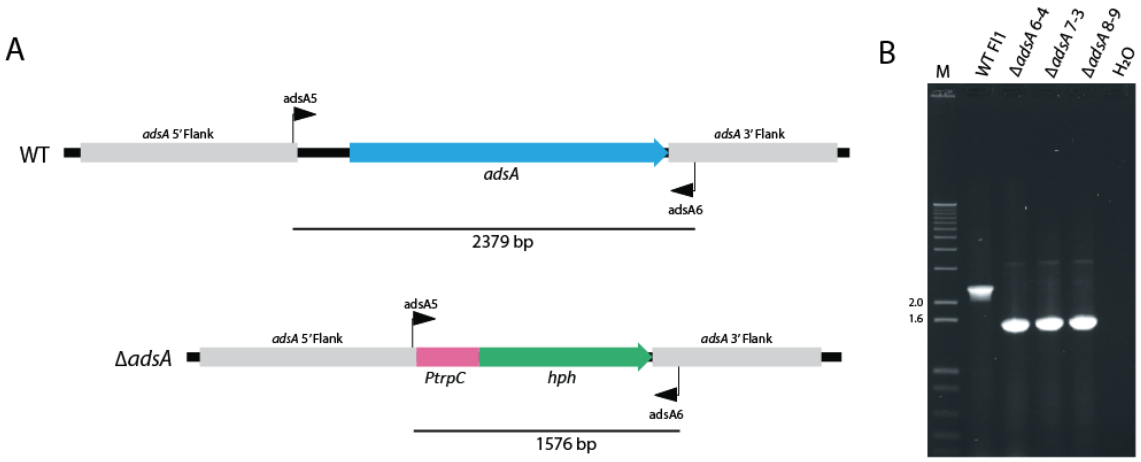

Figure 3.7 PCR to confirm *E. festucae adsA* deletion. (A) Schematic of wild-type (WT) *adsA* locus and replacement of the corresponding region with the *hph* resistance cassette in the Δ*adsA* mutant. (B) PCR screening of *adsA* gene replacement strains. Primer pair adsA5/adsA6 flanks the *adsA* gene and yields a 2,379 bp product for wild-type and a 1576 bp product for Δ*adsA* mutants. M = 1 kb+ ladder, H_2O = water only negative control.

Southern blot analysis of the putative *adsA* deletion mutants was carried out to identify 'clean' deletion mutants. Genomic DNA of wild-type, Δ*adsA* 6-4, Δ*adsA* 7-3 and Δ*adsA* 8-9 was digested with *Xba*I or *Nde*I and separated by gel electrophoresis. A Southern blot of this gel probed with [^{32}P]-labeled linearised pCE55, showed a *Xba*I pattern of hybridisation consistent with a 'clean' single copy replacement for *adsA* 6-4 and *adsA* 8-9 (Figure 3.8); bands of 3.31 kb and 6.84 kb. Δ*adsA* 7-3 has an additional band of 3.68 kb indicating that the deletion cassette has been inserted in tandem. Other unidentified bands in Δ*adsA* 7-3 are due to an ectopic insertion of the replacement cassette elsewhere in the genome. The presence of an *Nde*I pattern of hybridisation provided further evidence of 'clean' replacements in adsA 6-4 and adsA 8-9; bands of 1.80 kb and 4.0 kb. Δ*adsA* 7-3 has an additional band of 6.4 kb confirming the tandem insertion and multiple

unidentified bands again are due to ectopic insertion. The additional bands of 3 kb and 1kb (red asterisks, Figure 3.8B), the sum of the 4 kb fragment, are indicative of *Nde*I star activity resulting in digestion at a non-canonical site.

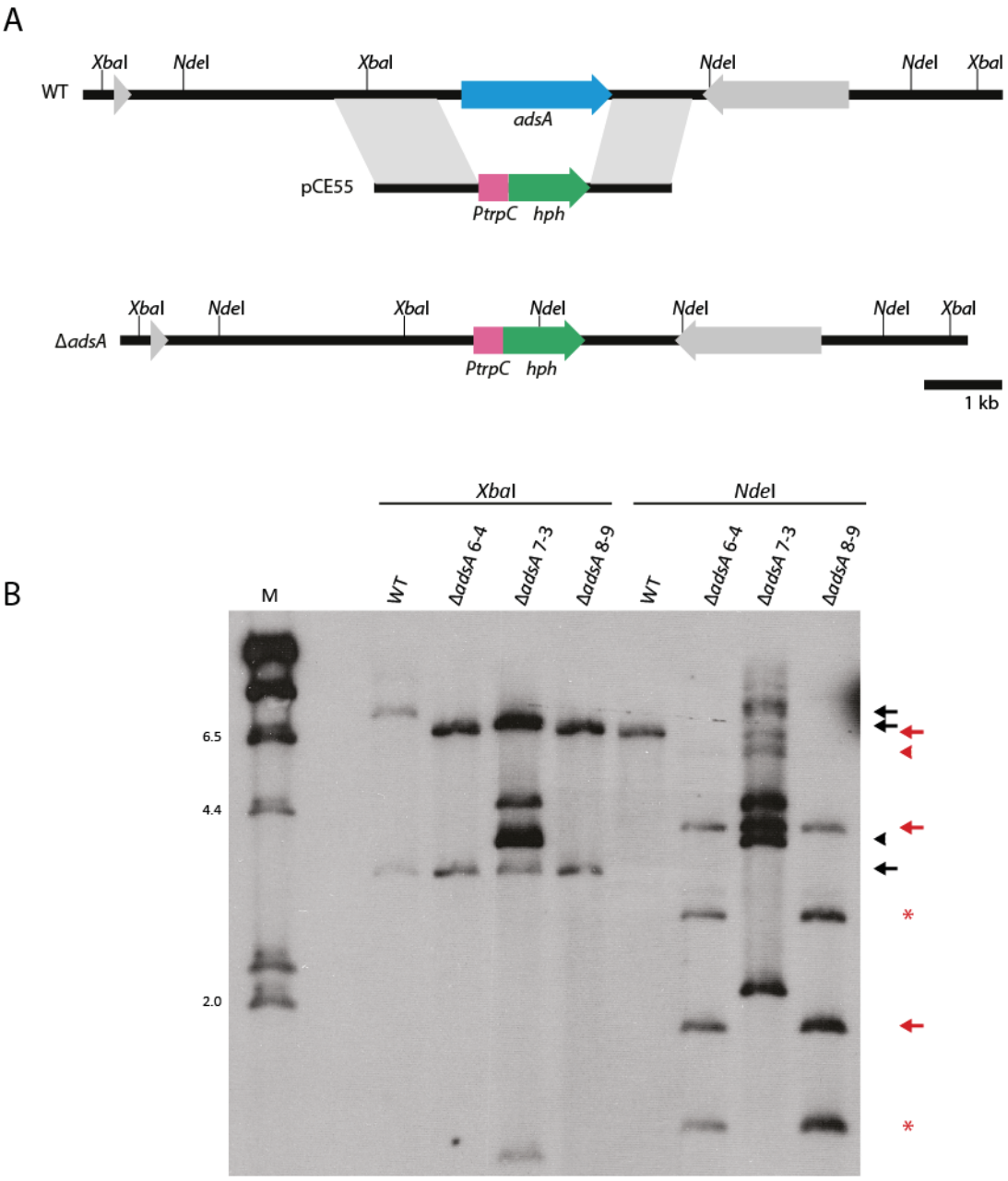

Figure 3.8 Southern blot analysis to confirm *E. festucae adsA* deletion. (A) Schematic of the wild-type *adsA* locus, linearised replacement construct (pCE55) and Δ*adsA* mutant genomic locus. Regions of recombination between homologous sequences flanking the *adsA* locus and *hph* resistance cassette are indicated by grey shading. (B) Autoradiograph of Southern blot of *Xba*I digests (1 µg) of *E. festucae* WT (lane 3), Δ*adsA* 6-4 (lane 4), Δ*adsA* 7-3 (lane 5), Δ*adsA* 8-9 (lane 6) and *Nde*I digests (1µg) of WT (lane 7), Δ*adsA* 6-4 (lane 8), Δ*adsA* 7-3 (lane 9), Δ*adsA* 8-9 (lane 10) genomic DNA, probed with [^{32}P] labeled linear fragment of pCE55. Expected fragment sizes for *Xba*I digests are 3.31 kb and 7.65 kb (black arrows) for *E. festucae* wild-type, 3.31 kb and 6.84 kb (black arrows) for deletion mutant, an additional band of 3.68 kb (black arrow head) is seen in

Δ*adsA* 7-3 due to tandem insertion of replacement construct. Additional unidentified bands are due to the replacement construct being inserted ectopically as well. Expected fragment sizes for *Nde*I digests are 6.60 kb (red arrow) for *E. festucae* wild-type, 1.80 kb and 4.0 kb (red arrows) for deletion mutant, an additional band of 6.40 kb (red arrow head) is seen in Δ*adsA* 7-3 due to tandem insertion of replacement construct. Additional unidentified bands in Δ*adsA* 7-3 are due to the replacement construct being inserted ectopically as well. Presence of a 3 kb and 1 kb (red asterisk) bands in Δ*adsA* 6-4 and Δ*adsA* 8-9 are due to *Nde*I starring. M = λ DNA/*Hind*III.

3.3. Molecular analysis of *adsB*

Hygromycin resistant transformants of *adsB* were initially screened by PCR using primer pair adsB5/adsB4 that flank the deleted region. This PCR screen identified five putative *adsB* deletion mutants; Δ*adsB* 4-4, Δ*adsB* 4-5, Δ*adsB* 11-8, Δ*adsB* 14-2 and Δ*adsB* 14-5 (Figure 3.9).

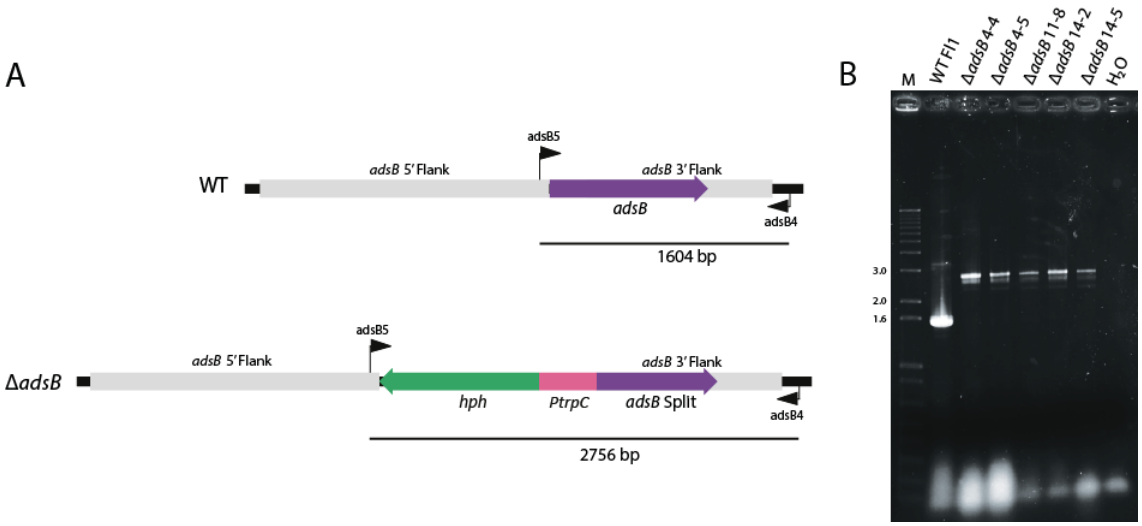

Figure 3.9 PCR to confirm *E. festucae adsB* deletion. (A) Schematic of wild-type *adsB* locus and replacement construct of the corresponding region with the *hph* resistance cassette in the *adsB* mutant. (B) PCR screening of the *adsB* gene replacement strains. Primer pair adsB5/adsB4 flanks the *adsB* gene and yields a 1,604 bp product for wild-type and a 2,756 bp product for *adsB* mutants. M = 1 kb+ ladder, H_2O = water only negative control.

Southern blots of the putative *adsB* deletion mutants were carried out to identify 'clean' deletion mutants. Genomic DNA of wild-type, Δ*adsB* 4-4, Δ*adsB* 4-5, Δ*adsB* 11-8, Δ*adsB* 14-2 and Δ*adsB* 14-5 was digested with *Pvu*I and separated by gel electrophoresis. A Southern blot of this gel probed with [^{32}P]-labeled linearised pCE53, showed a *Pvu*I pattern of hybridisation consistent with a 'clean' single copy replacement for Δ*adsB* 14-2 (Figure 3.10B); bands of 3.6 kb and 10 kb. Δ*adsB* 11-8 and Δ*adsB* 4-4 showed an additional band of 4.4 kb indicating that the deletion cassette has been inserted in tandem. The remaining putative deletion mutants contain unidentified bands that are due to an ectopic insertion elsewhere in the genome as well as the target. Genomic DNA of putative *adsB* deletion mutants was also digested with *Nde*I and separated on an agarose gel. The presence of a *Nde*I hybridisation pattern provided further evidence of *adsB* 14-2 containing a single 'clean' replacement (Figure 3.10C); bands 13.5 kb and 7.9 kb. Δ*adsB* 11-8 and

Δ*adsB* 4-4 have an additional band of 4.4 kb confirming the tandem insertion, however the amount of DNA present for Δ*adsB* 11-8 is very low compared to other lanes resulting in very faint bands at 13.5 kb and 7.9 kb. The remaining putative knockouts contain unidentified bands due to ectopic insertion. Since just one 'clean' knockout was identified the tandem insertion mutant Δ*adsB* 11-8 was also carried forward for phenotype analysis.

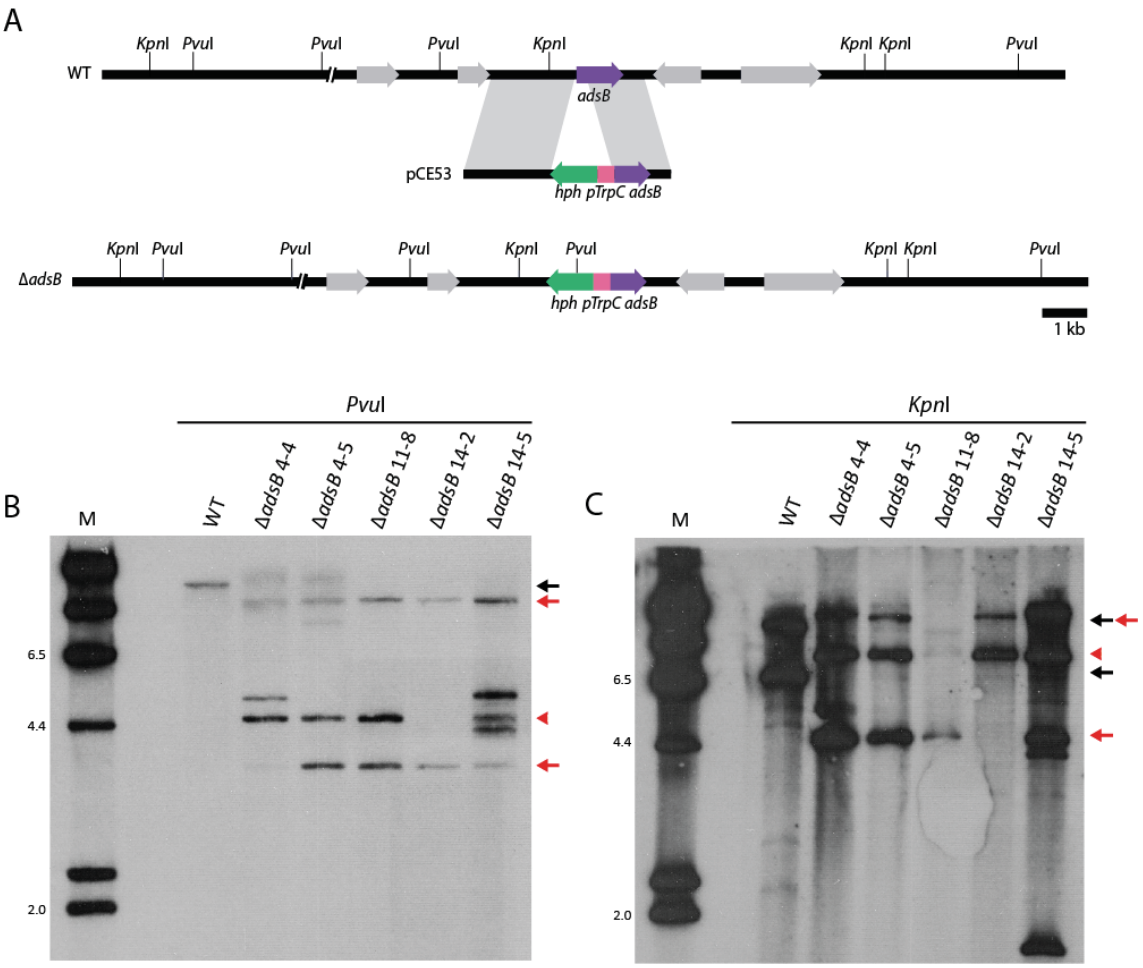

Figure 3.10 Southern blot analysis to confirm *E. festucae adsB* deletion. (A) Schematic of the wild-type *adsB* locus, linearised replacement construct (pCE53), Δ*adsB* mutant genomic locus. Regions of recombination between homologous sequences flanking the *adsB* locus and *hph* resistance cassette are indicated by grey shading. The dashed lines indicate where 5 Kb has been removed from the schematic. (B) Autoradiograph of Southern blot of *Pvu*I digests (1μg) of *E. festucae* WT (lane 3), Δ*adsB* 4-4 (lane 4), Δ*adsB* 4-5 (lane 5), Δ*adsB* 11-8 (lane 6) Δ*adsB* 14-2 (lane 7) and Δ*adsB* 14-5 (lane 8) genomic DNA, probed with [^{32}P] labeled linear fragment of pCE53. The expected fragment sizes are 12.5 kb (black arrow) for wild-type, 3.6 kb and 10 kb (red arrows) for 'clean' deletion mutant. An additional band of 4.4 kb (red arrow head) is seen if *hph* resistance cassette has been inserted in tandem. Additional unidentified bands are present due to the replacement construct being inserted ectopically as well. (C) Autoradiograph of Southern blot of *Kpn*I digests (1μg) of *E. festucae* WT (lane 3), Δ*adsB* 4-4 (lane 4), Δ*adsB* 4-5 (lane 5), Δ*adsB* 11-8 (lane6), Δ*adsB* 14-2 (lane7) and Δ*adsB* 14-5 (lane 8) genomic DNA, probed with [^{32}P] labeled

pCE53. The expected sizes are 6.8 kb and 13.5 kb (black arrows) for wild-type, 13.5 kb and 7.9 kb (red arrows) for 'clean' deletion mutant. An additional band of 4.4 kb (red arrow head) is seen if *hph* resistance cassette has been inserted in tandem. Additional unidentified bands are present due to the replacement construct being inserted ectopically as well. M = λ DNA/*Hind*III.

3.4. Δ*adsA* maintains wild-type growth in culture

No differences were observed in radial growth or colony morphology of the Δ*adsA* mutants compared to the wild-type (Figure 3.11). DIC light microscopy analysis showed that the culture phenotype of the Δ*adsA* mutants was indistinguishable from wild-type. On the edge of the colony hyphae were adhered to one another to form bundles of unbranched hyphae (Figure 3.12). Toward the centre of the colony hyphal coils were observed, some of these had conidiophores (Figure 3.12).

In axenic culture *E. festucae* forms a hyphal network by a series of lateral cell fusions. These arise by fusion of a growing hyphal tip with the lateral cell wall of an adjacent hyphae followed by repolarisation and ongoing growth (Becker, unpublished). Δ*adsA* mutants retained the ability to form these lateral cell fusions (Figure 3.13).

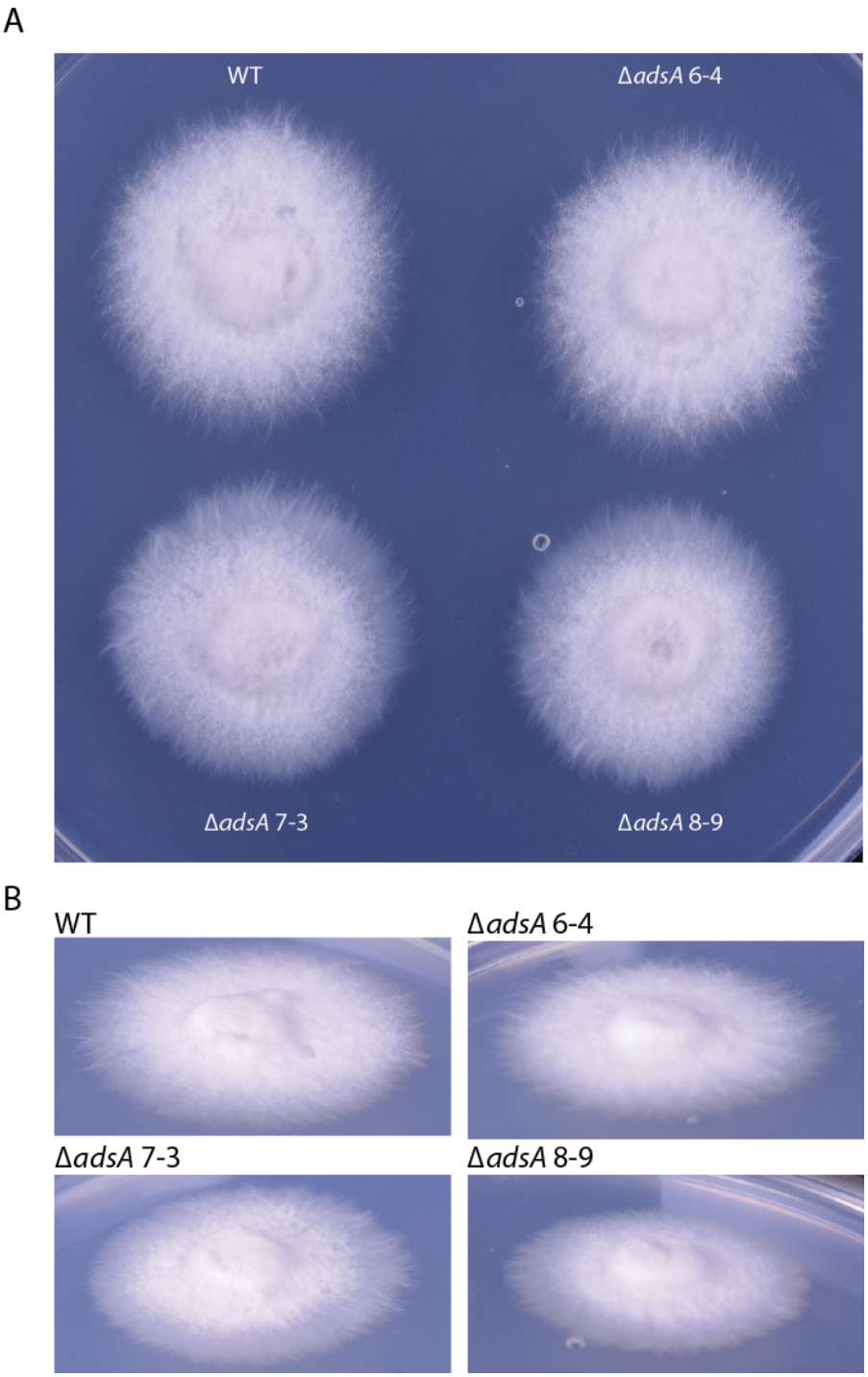

Figure 3.11 Colony morphology of *E. festucae* Δ*adsA* mutant strains. (A) Aerial image of wild-type and Δ*adsA* mycelia plugs 5 mm in diameter. These were inoculated onto 2.4% potato dextrose agar and grown at 22°C for 7 days. (B) Side angle image of wild-type and Δ*adsA* mutant strains depicting aerial hyphal growth.

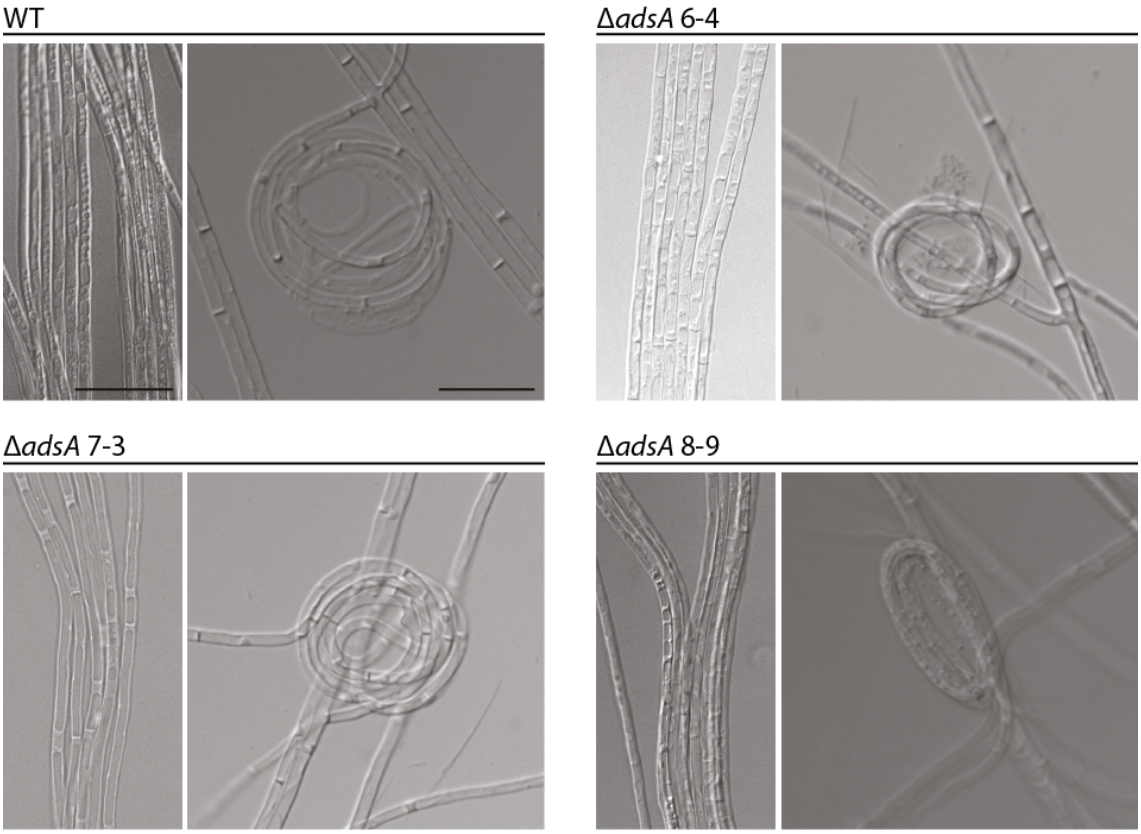

Figure 3.12 Bundle formation and development of hyphal coils in *E. festucae* Δ*adsA* mutant strains. Hyphal bundles and coil structures in wild-type and *adsA* mutants. Mycelia were grown on water agarose overlays for 7 days at 22°C. Images were taken on an inverted light microscope using DIC. Bars = 20 µm.

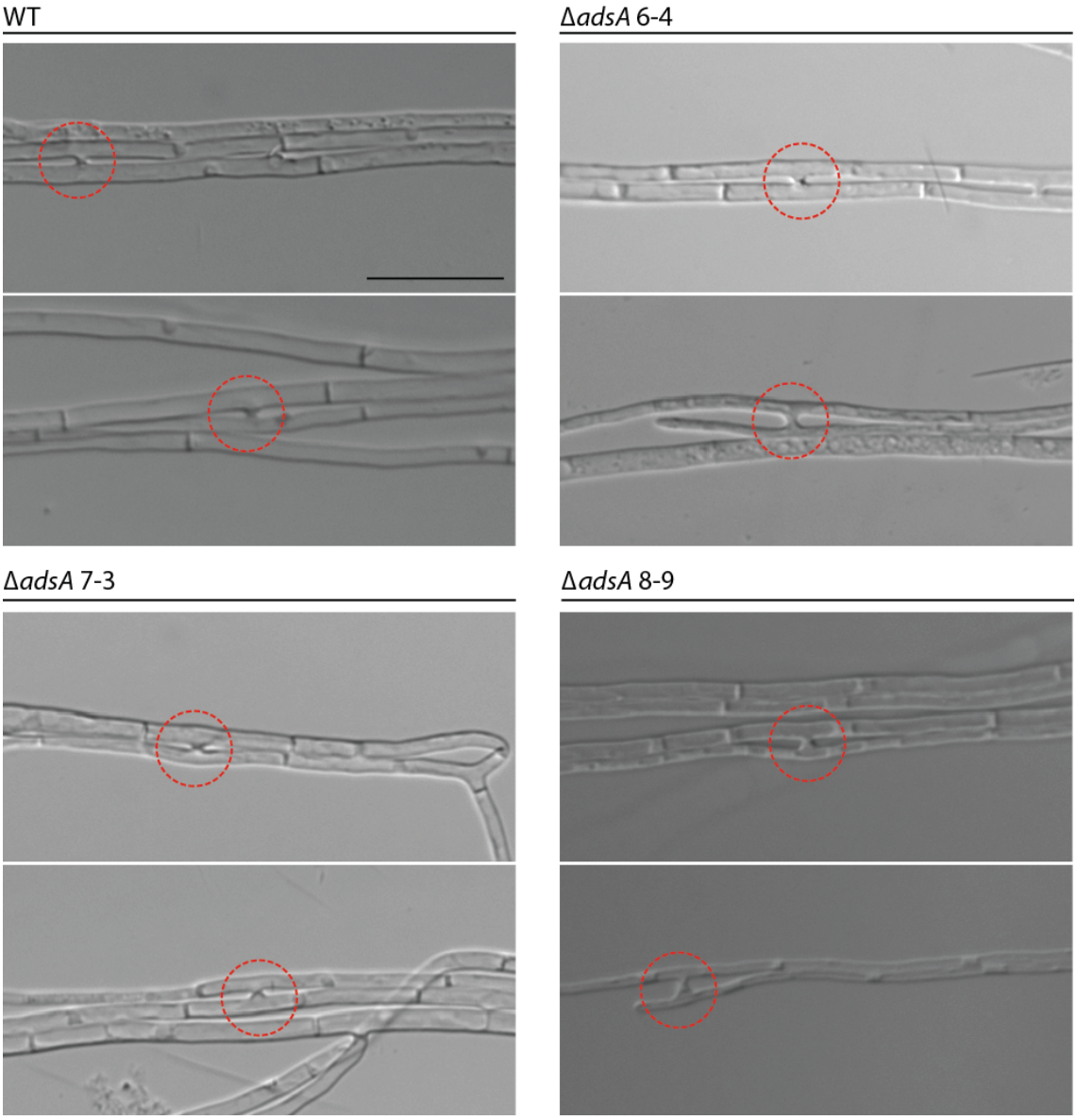

Figure 3.13 Hyphal fusion in *E. festucae* Δ*adsA* mutant strains. Hyphal fusion events in wild-type and Δ*adsA* mutants are indicated by red dashed circles. Mycelia were grown on water agarose overlays for 7 days at 22°C. Images were taken on an inverted light microscope using DIC. Bar = 20 µm.

3.5. Δ*adsB* maintains wild-type growth in culture

Similar to Δ*adsA* mutants there was no difference in radial growth for Δ*adsB* deletion mutants. However, Δ*adsB* deletion mutants showed a reduction in aerial hyphae at the outmost edge of the colony (Figure 3.14). As observed with Δ*adsA* mutants, Δ*adsB* mutants were indistinguishable from wild-type by DIC light microscopy (Figures 3.15 and 3.16).

A

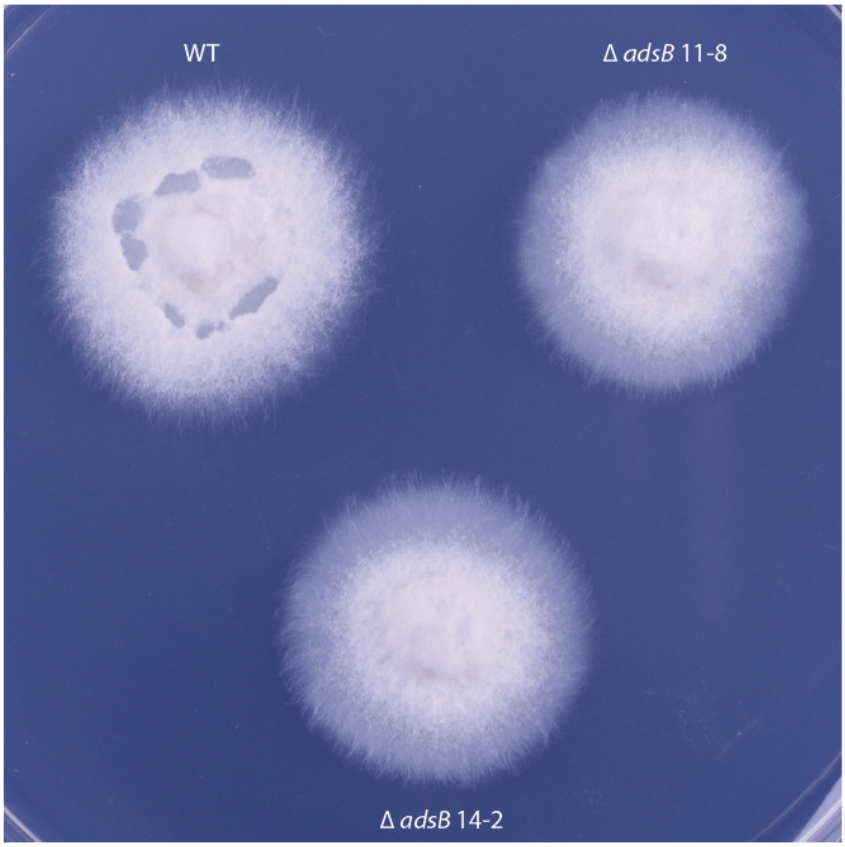

B

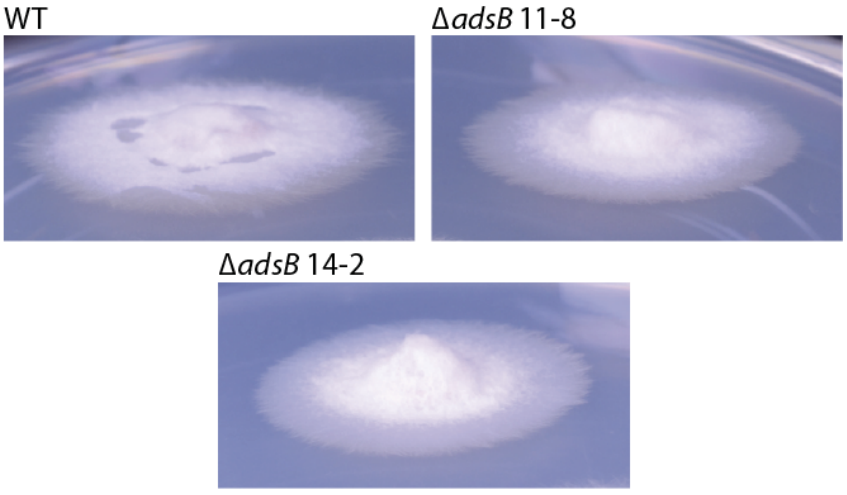

Figure 3.14 Colony morphology of *E. festucae* Δ*adsB* mutant strains. (A) Aerial image of wild-type and Δ*adsB* mycelia plugs 5 mm in diameter. These were inoculated onto 2.4% potato dextrose agar and grown at 22°C for 7 days. (B) Side angle image of wild-type and Δ*adsB* mutant strains depicting aerial hyphal growth.

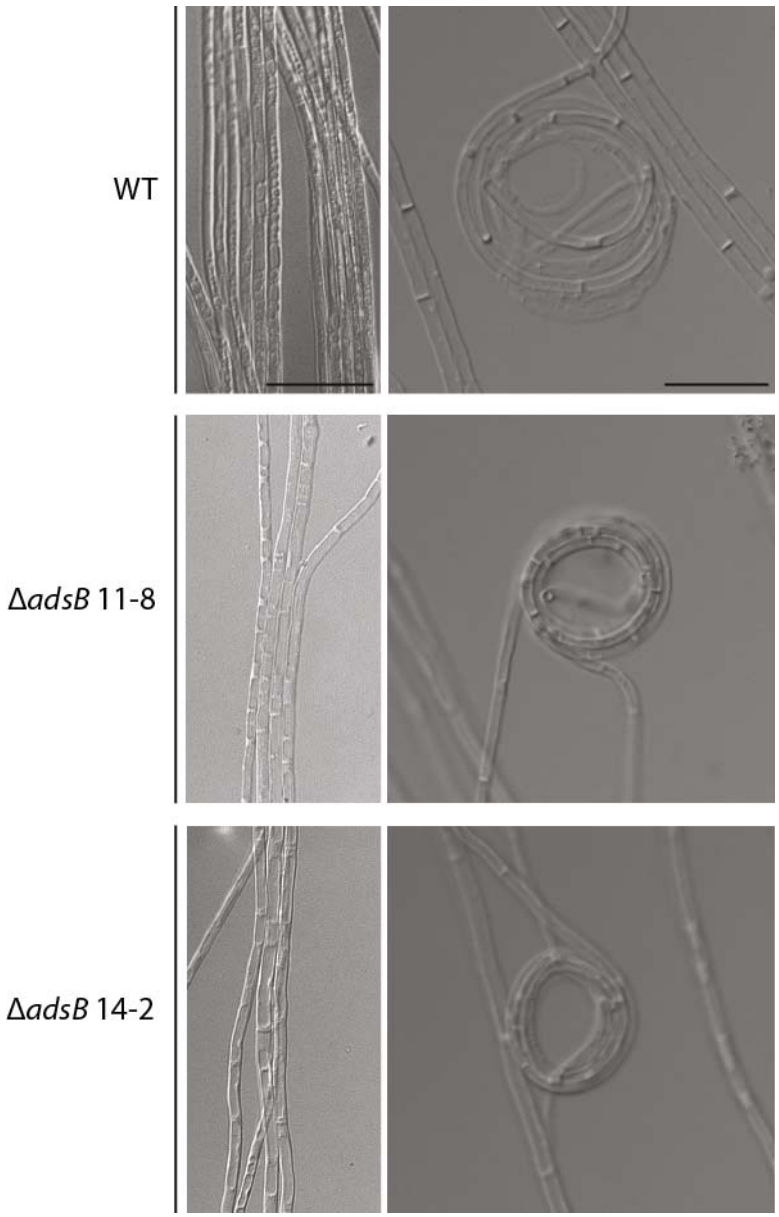

Figure 3.15 Bundle formation and development of hyphal coils in *E. festucae* Δ*adsB* mutant strains. Hyphal bundles and coil structures in wild-type and Δ*adsB* mutants. Mycelia were grown on water agarose overlays for 7 days at 22°C. Images were taken on an inverted light microscope using DIC. Bars = 20 μm.

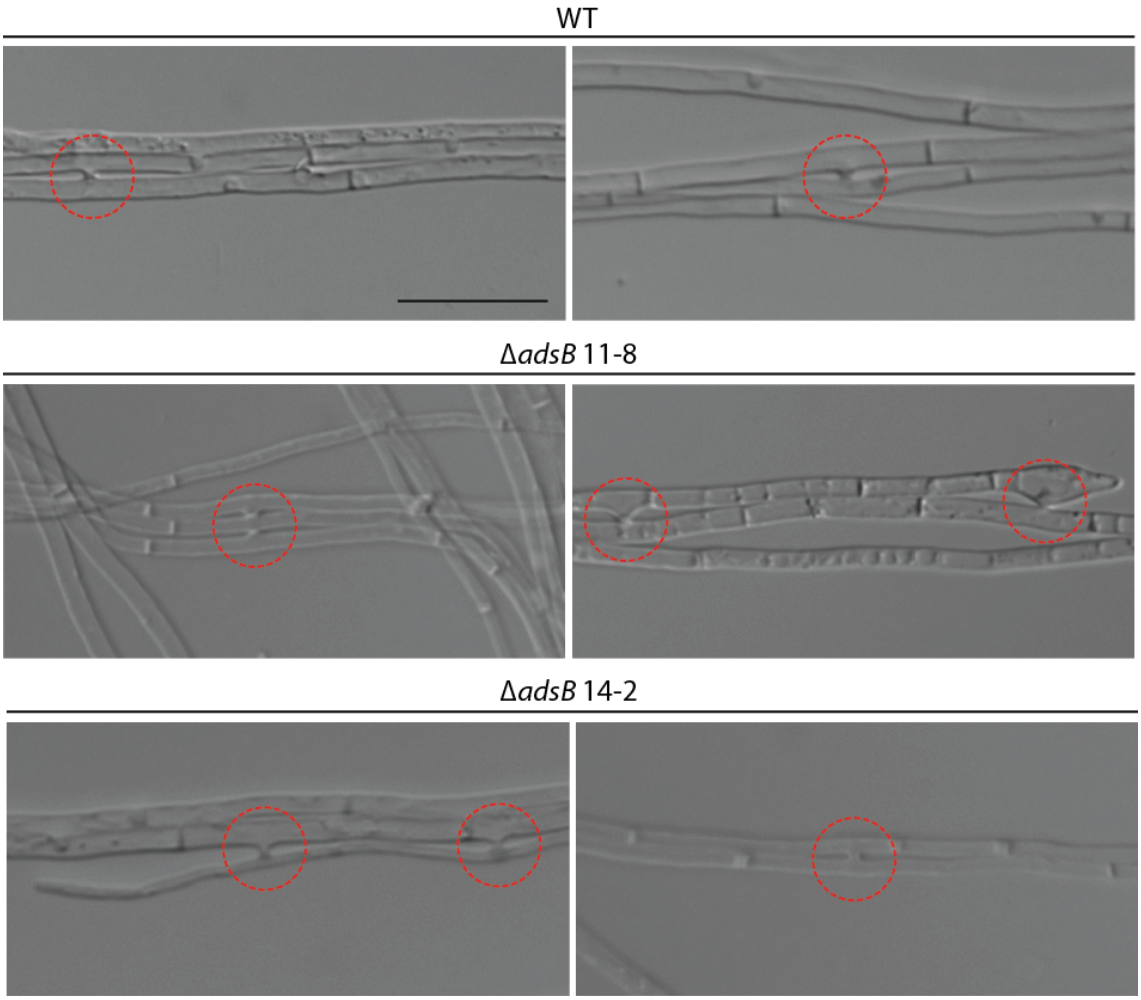

Figure 3.16 Hyphal fusion in *E. festucae* Δ*adsB* mutant strains. Hyphal fusion events in wild-type and Δ*adsB* mutants are indicated by red dashed circles. Mycelia were grown on water agarose overlays for 7 days at 22°C. Images were taken on an inverted light microscope using DIC. Bar = 20 µm.

3.6. Δ*adsA* exhibits wild-type growth *in planta*

To investigate the role *adsA* plays in the symbiotic association of *E. festucae* and *L. perenne* Δ*adsA* mutants were inoculated into sterile *L. perenne* seedlings. No difference was seen for the whole plant phenotype for Δ*adsA* mutants when compared to wild-type (Figure 3.17). Wild-type hyphae were restricted to growth between plant cells parallel to the leaf axis, seldom branched with regularly spaced septa. Confocal microscopy showed that the *in planta* phenotype of Δ*adsA* mutants was indistinguishable from wild-type (Figure 3.18).

Light microscopy analysis of plant tissue infected with Δ*adsA* mutants had the same distribution as wild-type with no colonisation of the vascular bundles (Figure 3.19). Hyphae are frequently present in the sclerenchyma region of the large and small vascular bundles in WT and Δ*adsA* mutants. However, hyphae are not seen in the phloem or xylem tissue in the large vascular bundles, nor are they seen in the phloem of the small vascular bundles for WT or Δ*adsA* mutants.

The presence of only one or two hyphae per intercellular space in WT and Δ*adsA* mutants was observed by transmission electron microscopy (TEM) (Figure 3.20). Hyphae were firmly attached to plant cells in all layers of the pseudostem for WT and Δ*adsA* mutants shown in the second column of intercellular growth. Epiphyllous hyphae were present on the leaf surfaces of plants infected with both WT and Δ*adsA* mutants; these are identified by growth outside the thick plant cuticle layer.


A
WT
ΔadsA 6-4


B
WT
ΔadsA 7-3

Figure 3.17 Whole plant analysis of the *E. festucae* Δ*adsA* mutants and *L. perenne* association. Phenotypes of *L. perenne* infected with the following strains: (A) wild-type (WT) and Δ*adsA* 6-4 mutant strain, (B) WT and Δ*adsA* 7-3 mutant strain, (C) WT and Δ*adsA* 8-9 mutant strain. Photographs were taken at 12 weeks post inoculation with the same set of WT plants.

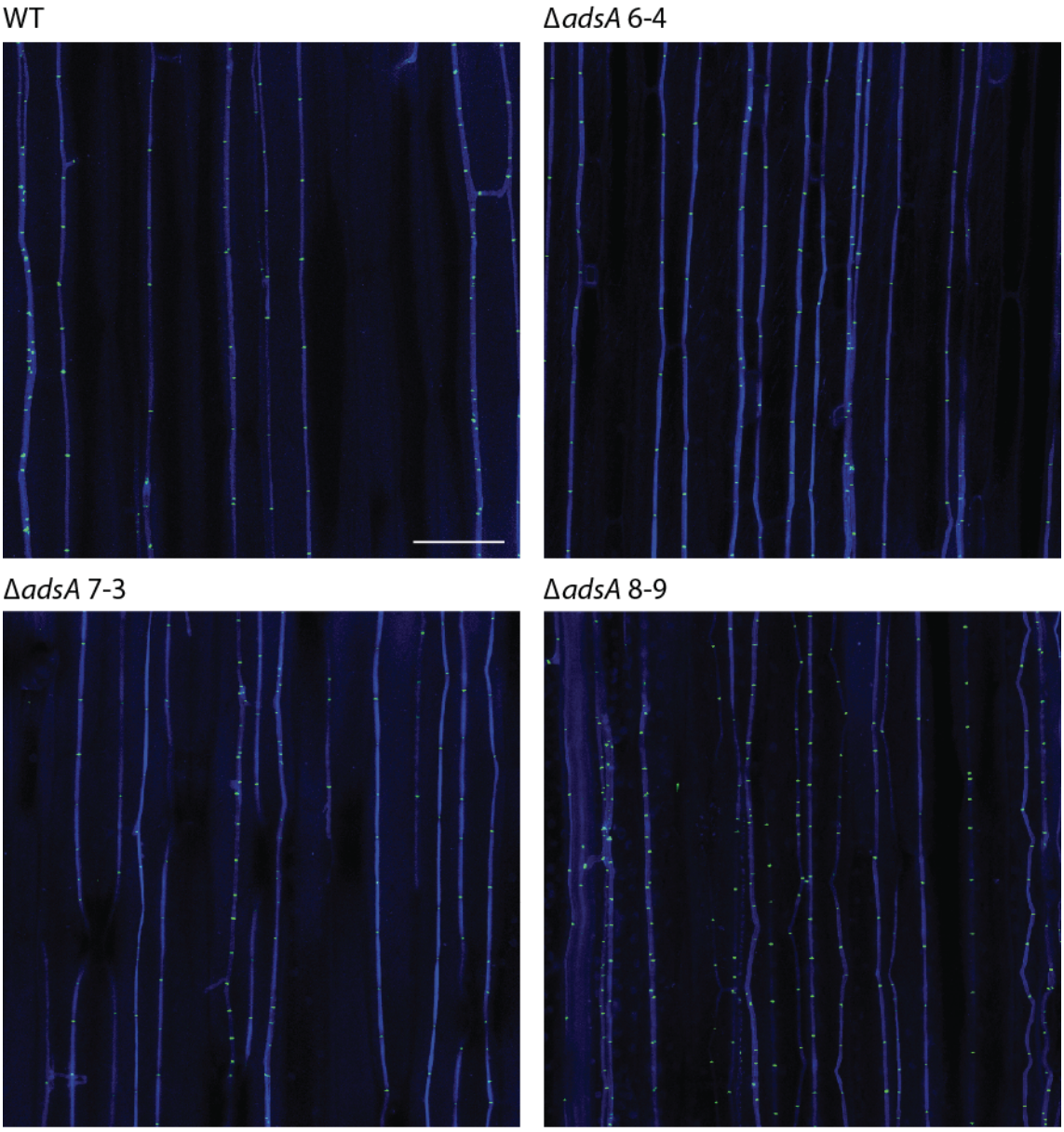

Figure 3.18 Confocal analysis *of E. festucase* Δ*adsA* mutant strains growth *in planta*. Confocal depth series images of longitudinal sections through *L. perenne* pseudostem tissue, infected with *E. festucae* strains as indicated: wild-type (WT), Δ*adsA* 6-4, Δ*adsA* 7-3 and Δ*adsA* 8-9. Aniline blue and Alexafluor® 488-WGA stains were used to visualise hyphae, stained blue, and septa, stained green respectively. Images were generated by maximum intensity projection of 10× 1 µm confocal z-stacks. Bar = 50 µm

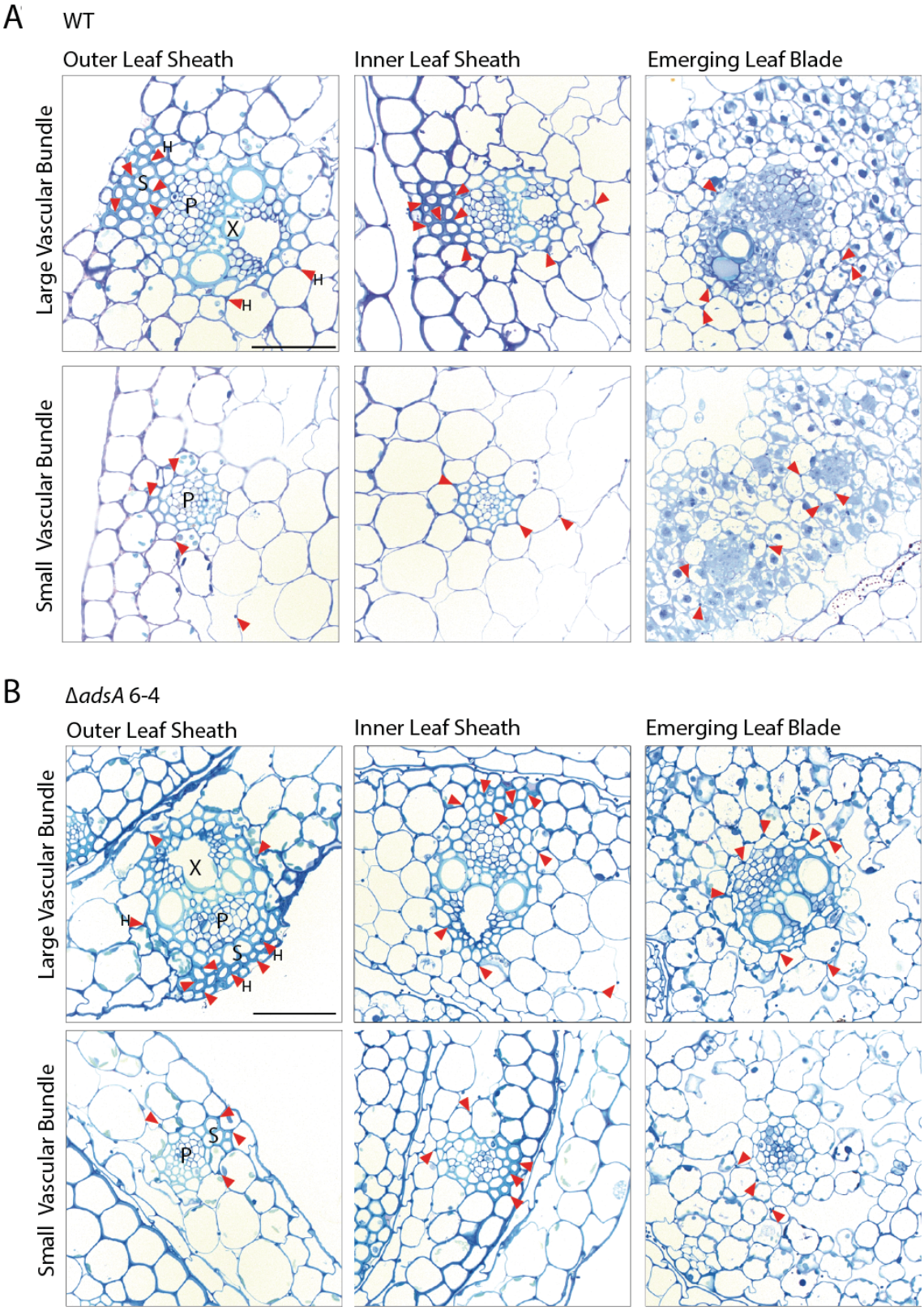
A
WT
Outer Leaf Sheath
Inner Leaf Sheath
Emerging Leaf Blade
Large Vascular Bundle
Small Vascular Bundle
H
S
P
X
B
ΔadsA 6-4
Outer Leaf Sheath
Inner Leaf Sheath
Emerging Leaf Blade
Large Vascular Bundle
Small Vascular Bundle

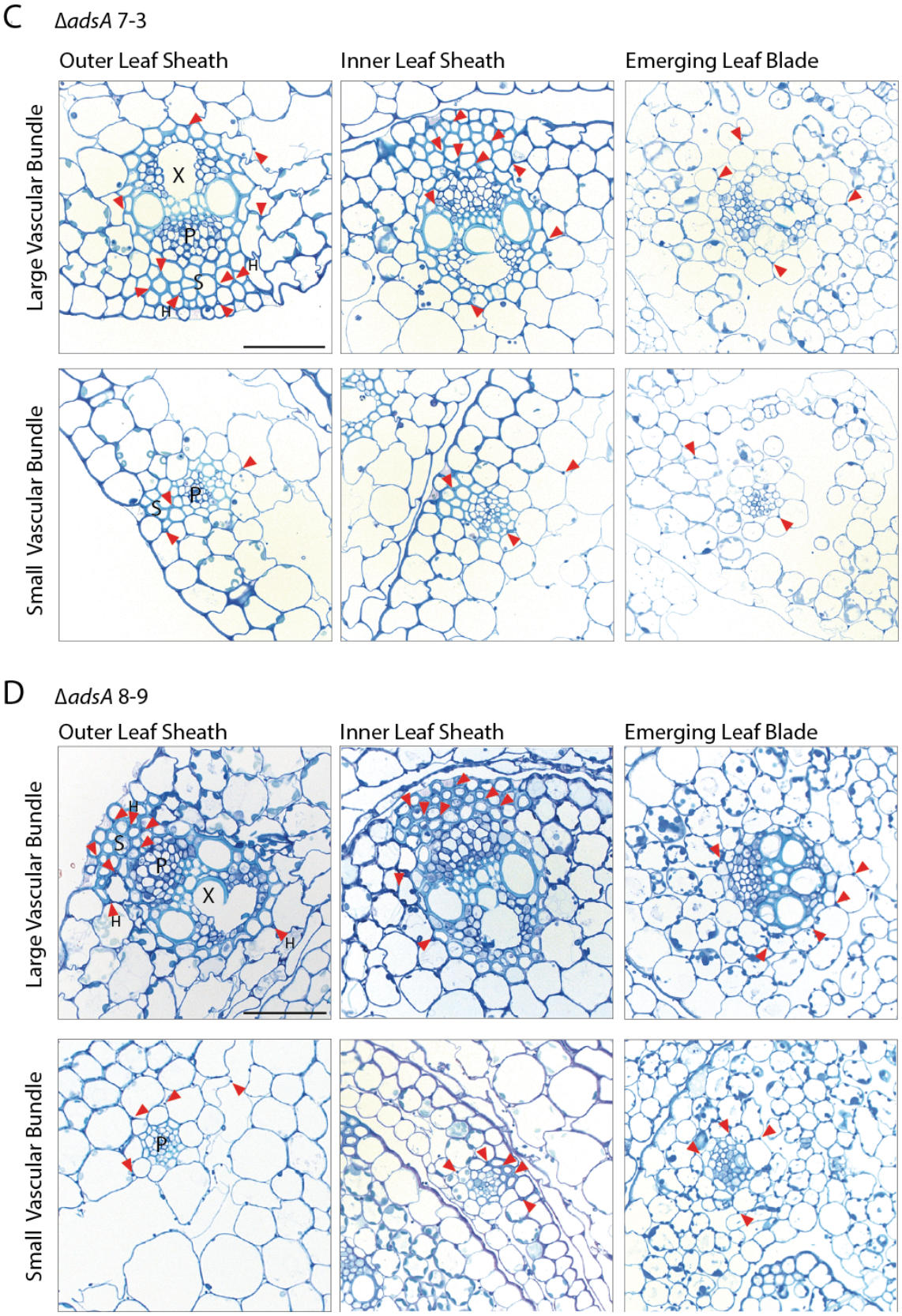

Figure 3.19 Light microscopy analysis of *E. festucae* Δ*adsA* mutant strains within *L. perenne* vascular tissue. Transverse sections of *L. perenne* pseudostem tissue infected with (A) wild-type (WT) , (B) Δ*adsA* 6-4, (C) Δ*adsA* 7-3 and (D) Δ*adsA* 8-9, stained with toluidine blue. Samples were taken from plants 12 weeks post inoculation. S = sclerenchyma, P = phloem, X = xylem and H = hyphae. Vertical hyphae are indicated by red arrow-heads. Bars = 20 µm

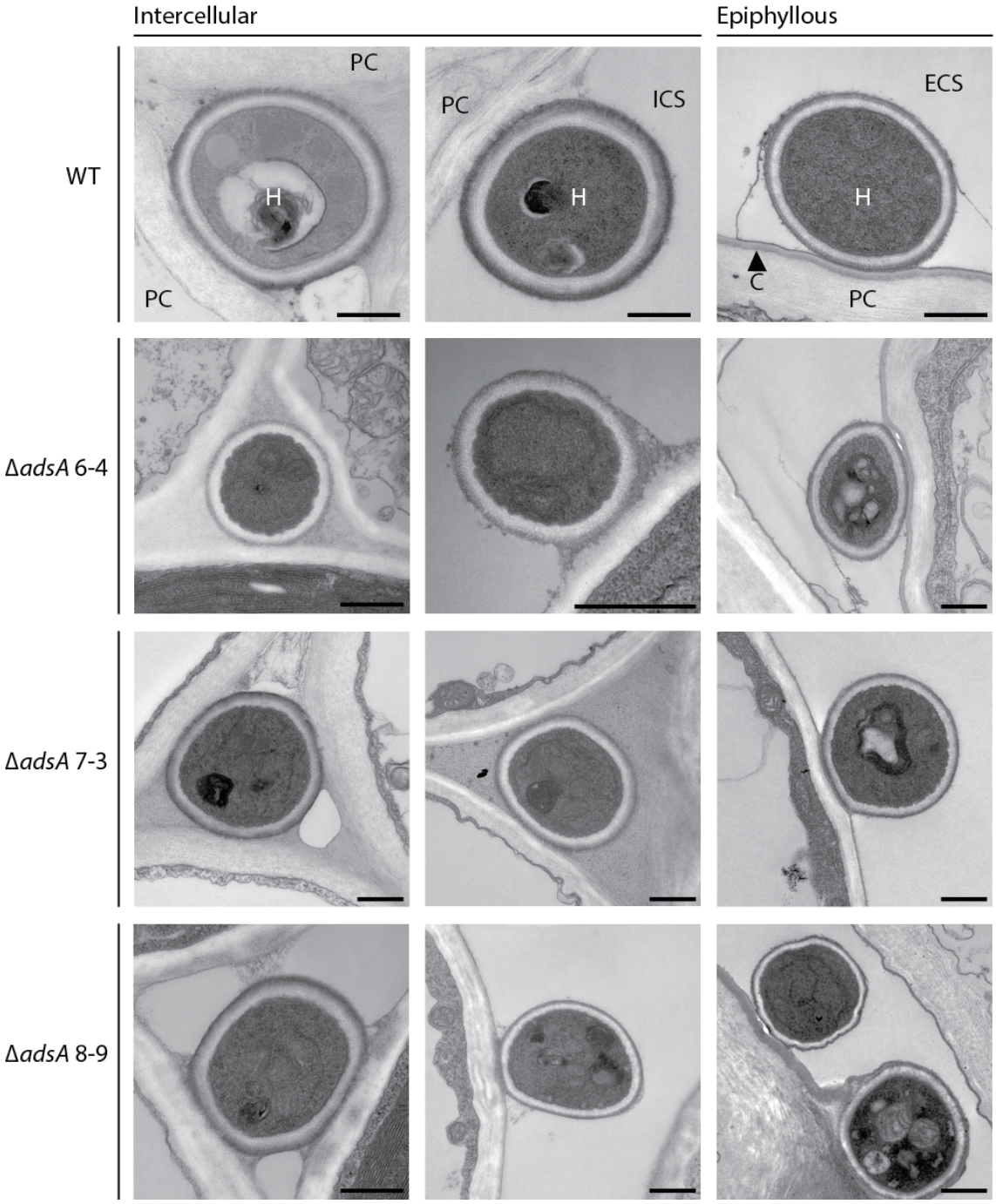

Figure 3.20 Transmission electron micrographs of *E. festucae* Δ*adsA* mutant strains within *L. perenne*. Transverse sections of pseudostem tissue containing hyphae of wild-type and Δ*adsA*. Intercellular hyphae are identified by surrounding plant cells and attachment to plant cells. Epiphyllous hyphae are identified by thick plant cuticle layer. H = hyphae, PC = plant cell, ICS = intercellular space, ECS = extra cellular space and C = plant cuticle, indicated with black arrow. Black bars = 500 nm.

3.7. *adsB* plays a role in the symbiotic association

To investigate the role that *adsB* plays in the symbiotic association of *E. festucae* and *L. perenne* Δ*adsB* mutants were inoculated into sterile *L. perenne* seedlings. A mild phenotype of reduced aerial growth and root development is seen for *adsB* mutants when compared to wild-type (Figure 3.21). Similar to wild-type and Δ*adsA* mutants confocal analysis showed that Δ*adsB* mutants had restricted growth *in planta* in the tissue between vascular bundles (Figure 3.22).

Light microscopy of transverse sections of pseudostem tissue infected with Δ*adsB* mutants the hyphae colonised the large vascular bundles in the sheath tissue and the emerging leaf (Figures 3.23 and 3.24) – a feature seldom seen in wild-type associations. The main (older) large vascular bundles had more hyphae in comparison to newly emerging large vascular bundles. There was an increase in hyphal load in the sclerenchyma intercellular space in the Δ*adsB* mutants in comparison to wild-type. Whereas, there was no colonisation of the small vascular bundles, this indicated that the hyphae were entering the large vascular bundle at the growth apex of the tiller when it was developing.

As seen in wild-type and Δ*adsA* mutant associations the growth and attachment of the hyphae was comparable for Δ*adsB* mutants outside the vascular bundles (Figure 3.25). Colonisation of the large vascular bundles in Δ*adsB* mutant associations was supported by TEM microscopy (Figure 3.25). Electron dense hyphae were surrounding and colonising the large vascular bundles for Δ*adsB* mutants. Hyphae were distinguishable from plant phloem cells as they were smaller, more electron dense and the fungal cell was also visible.


A
WT
ΔadsB 11-8

Figure 3.21 Whole plant analysis of the *E. festucae* Δ*adsB* mutant strains and *L. perenne* association. Phenotypes of *L. perenne* infected with the following strains: (A) wild-type (WT) and Δ*adsB* 11-8 mutant strain. (B) WT and Δ*adsB* 14-2 mutant strain. Photographs were taken at 12 weeks post inoculation with the same set of WT plants.

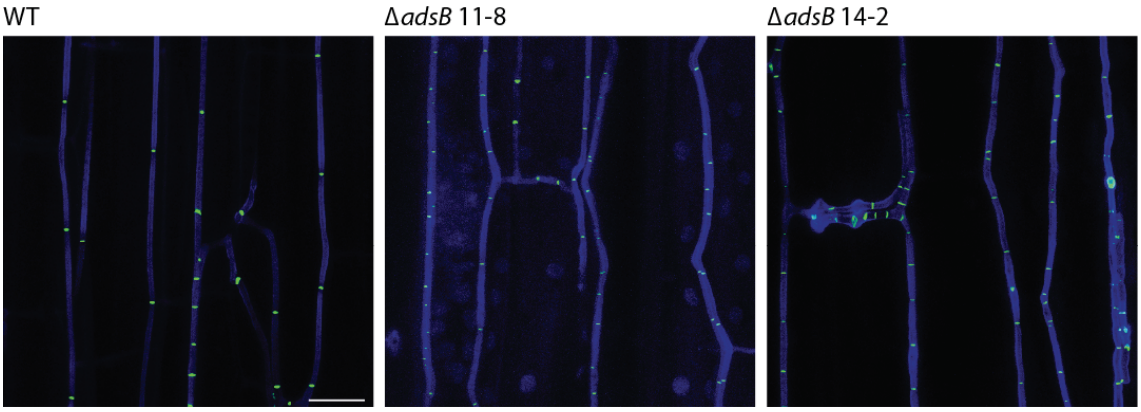

Figure 3.22 Confocal analysis of *E. festucae* Δ*adsB* mutant strains growth *in planta*. Confocal depth series images of longitudinal sections through *L. perenne* pseudostem tissue, infected with *E. festucae* strains as indicated: wild-type (WT), Δ*adsB* 11-8 and Δ*adsB* 14-2. Aniline blue and Alexafluor® 488-WGA stains were used to visualise hyphae, stained blue, and septa, stained green respectively. Images were generated by maximum intensity projection of 10× 1 µm confocal z-stacks. Bar = 20 µm.

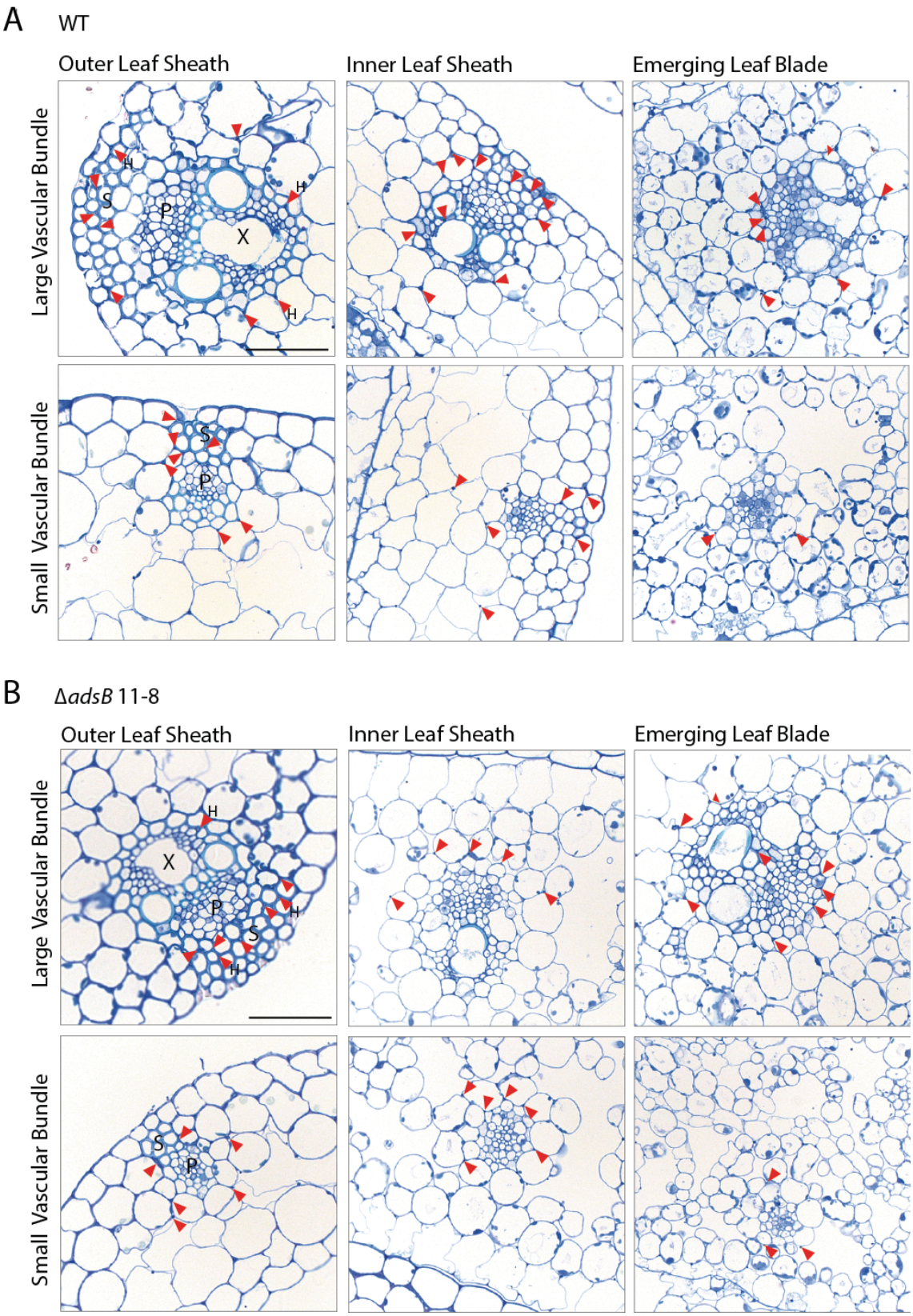

Figure 3.23 Light microscopy analysis of *E. festucae* Δ*adsB* 11-8 mutant strain within *L. perenne* vascular tissue. Transverse sections of *L. perenne* pseudostem tissue infected with (A) wild-type (WT) and (B) Δ*adsB* 11-8, stained with toluidine blue. Samples were taken from plants 8 weeks post inoculation. S = sclerenchyma, P = phloem, X = xylem and H = hyphae. Hyphae are indicated by red arrow-heads. Bars = 20 µm.

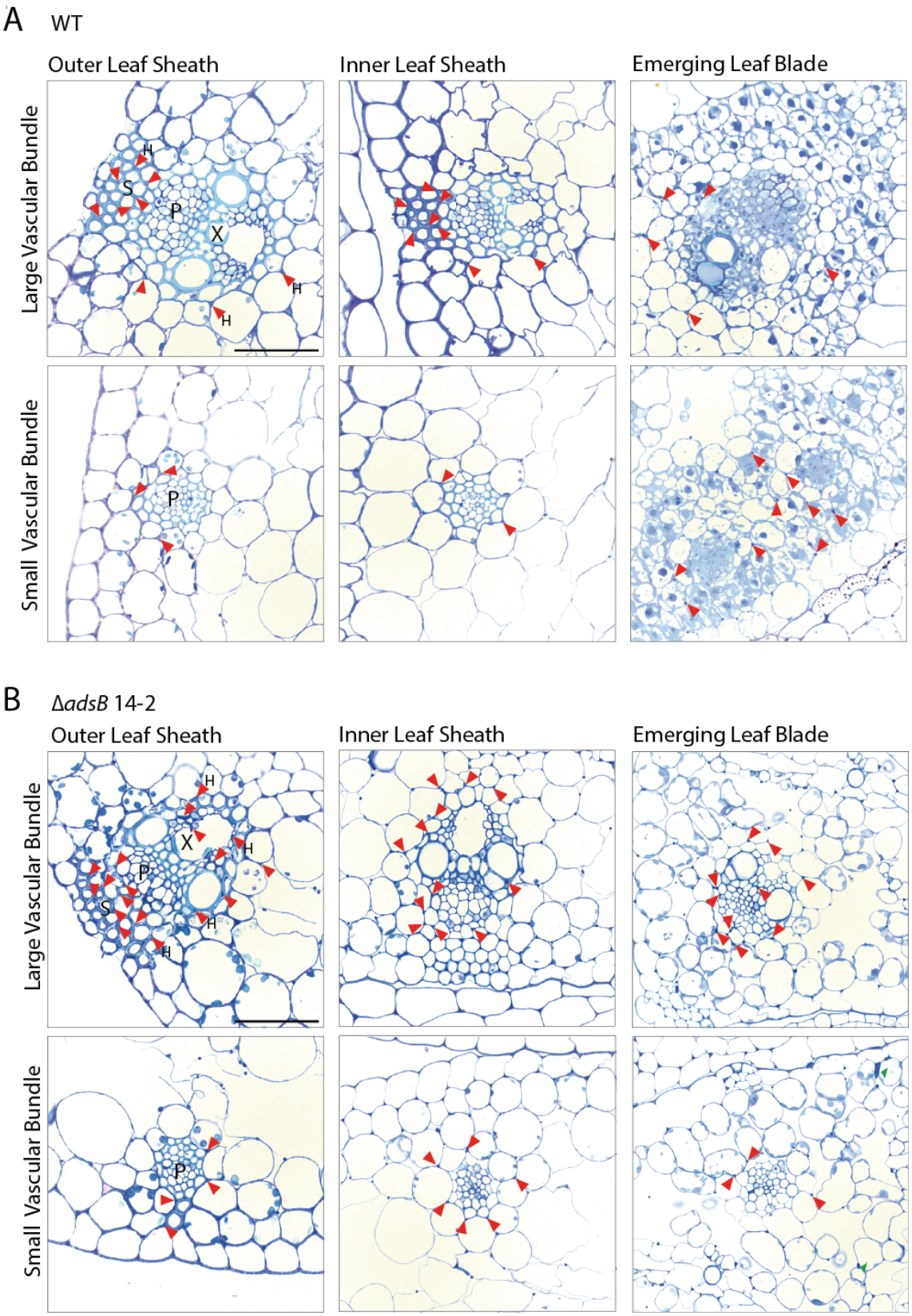

Figure 3.24 Light microscopy analysis of *E. festucae* Δ*adsB* 14-2 mutant strain within *L. perenne* vascular tissue. Transverse sections of *L. perenne* pseudostem tissue infected with (A) Wild-type (WT) and (B) Δ*adsB* 14-2, stained with toluidine blue. Samples were taken from plants 12 weeks post inoculation. S = sclerenchyma, P = phloem, X = xylem and H = hyphae. Hyphae are indicated by red arrow-heads. Bars = 20 µm.

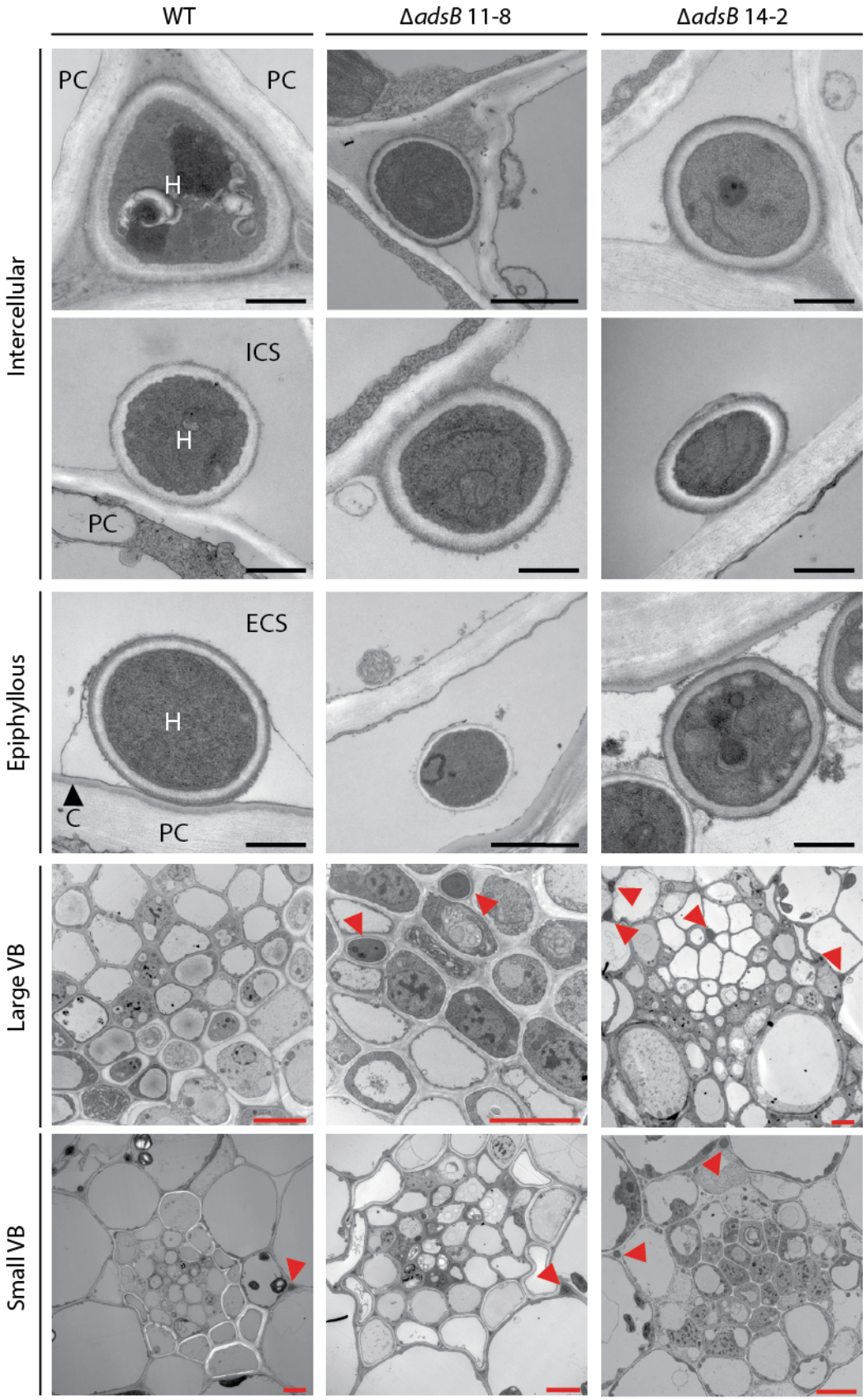

Figure 3.25 Transmission electron micrographs of *E. festucae* Δ*adsB* mutant strains within *L. perenne*. Transverse sections of pseudostem tissue containing hyphae of wild-type and Δ*adsB*. Intercellular hyphae are identified by surrounding plant cells and attachment to plant cells is shown. Epiphyllous hyphae are identified by thick plant cuticle layer. Large and small vascular

bundle (VB) phloem tissue is also shown; hyphae are indicated by red arrow heads. H = hyphae, PC = plant cell, ICS = intercellular space, ECS = extracellular space and C = plant cuticle, indicated with black arrow. Black bars = 500 nm. Red bars = 5 µm.

3.8. Complementation of *E. festucae* Δ*adsB*

To determine if the mild plant stunting and large vascular bundle colonisation phenotypes was due to the deletion of *adsB* the native gene was reintroduced. Complementation constructs were made my PCR amplification of the native gene and yeast recombinational cloning. Both Δ*adsB* 11-8 and Δ*adsB* 14-2 were transformed with the *adsB* complementation vector pPC2 (Figure 6.4) and pII99 (Figure 6.5). Geneticin and hygromycin resistant colonies were screened by PCR using the primer pair adsB10/adsB4. Two Δ*adsB* 11-8/*adsB* complementation transformants were identified along with three Δ*adsB* 14-2/*adsB* complementation transformants.

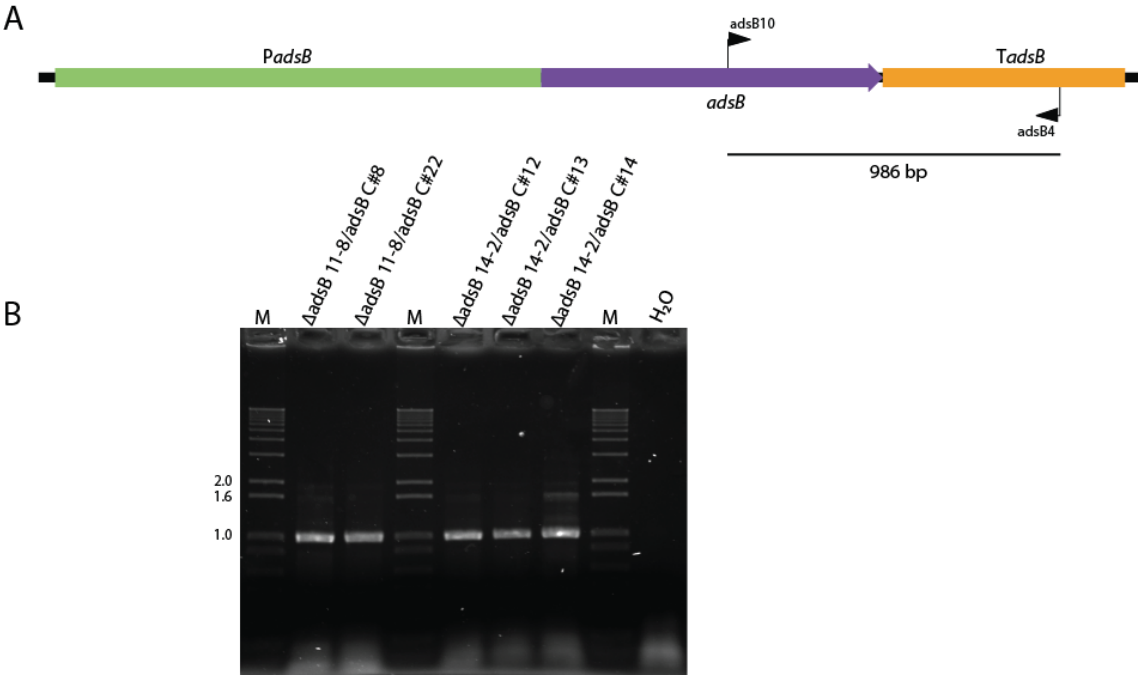

Figure 3.26 Complementation construct design for Δ*adsB* and PCR confirmation. (A) Schematic of *adsB* complementation (pPC2) design including 1 kb of native promoter (P*adsB*, green) and 0.5 kb of native terminator (T*adsB*, orange). (B) PCR screening of complementation strains. Primer pair asdB10/adsB4 amplifies from the centre of *adsB* to the centre of the native terminator and yields a 986 bp product for complemented strains. M = 1 kb+ ladder; H_2O = water only negative control.

Reintroduction of the native *adsB* gene into Δ*adsB* 11-8 partially complemented the whole plant phenotype (Figure 3.27) for both complementation strains (C#9 and C#22). Complementation strains like wild-type no longer colonised the large vascular bundles (Figure 3.28), with the exception two hyphae seen in

Δ*adsB* 11-8/*adsB* C#22 large vascular bundle in the outer leaf sheath. Incomplete complementation could be due to altered gene expression as a result of ectopic insertion of *adsB* when reintroduced.

Reintroduction of the native *adsB* gene into Δ*adsB* 14-2 complemented the whole plant phenotype (Figure 3.29) for complementation strains Δ*adsB* 14-2/*adsB* C#13 and Δ*adsB* 14-3/*adsB* C#14. Both complementation strains restored the wild-type phenotype of no large vascular bundle colonisation (Figure 3.30). Hyphae were present in the intercellular spaces of the sclerenchyma and the surrounding tissue but not within the phloem or xylem tissue. Complementation of the 'clean' *adsB* deletion mutant Δ*adsB* 14-2 confirms that the mild plant stunting and large vascular bundle colonisation is due to the deletion of *adsB*.

Figure 3.27 Whole plant complementation of Δ*adsB* 11-8. Phenotypes of *L. perenne* infected with the following strains: (A) wild-type (WT), Δ*adsB* 11-8 and Δ*adsB*/*adsB* C#9, (B) wild-type (WT), Δ*adsB* 11-8 and ΔadsB/*adsB* C#22. Photographs were taken at 8 weeks post inoculation with the same set of WT plants.

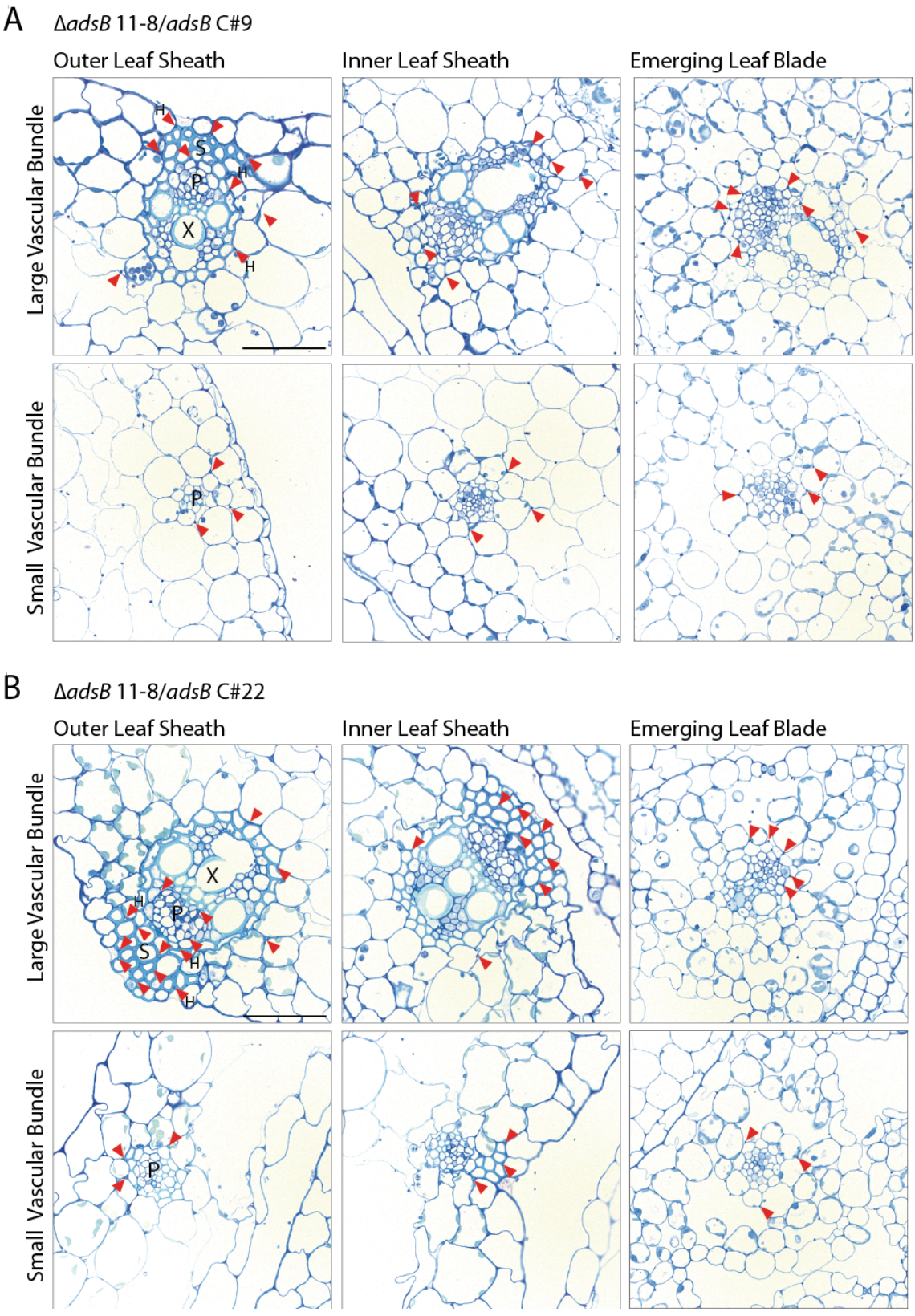

Figure 3.28 Light microscopy analysis of *E. festucae* Δ*adsB* 11-8 complementation strains within *L. perenne* vascular tissue. Transverse sections of *L. perenne* pseudostem tissue infected with (A) Δ*adsB*/*adsB* C#9 and (B) Δ*adsB*/*adsB* C#22, stained with toluidine blue. Samples were taken from plants 8 weeks post inoculation. S = sclerenchyma, P = phloem, X = xylem and H = hyphae (red arrow heads). Bars = 20 µm.


A
WT
ΔadsB 14-2
ΔadsB 14-2/adsB C#13

Figure 3.29 Whole plant complementation of Δ*adsB* 14-2. Phenotypes of *L. perenne* infected with the following strains: (A) wild-type (WT), Δ*adsB* 14-2 and Δ*adsB*/*adsB* C#13, (B) WT, Δ*adsB* 14-2 and Δ*adsB*/*adsB* C#14. Photographs were taken at 12 weeks post inoculation with the same set of WT plants.

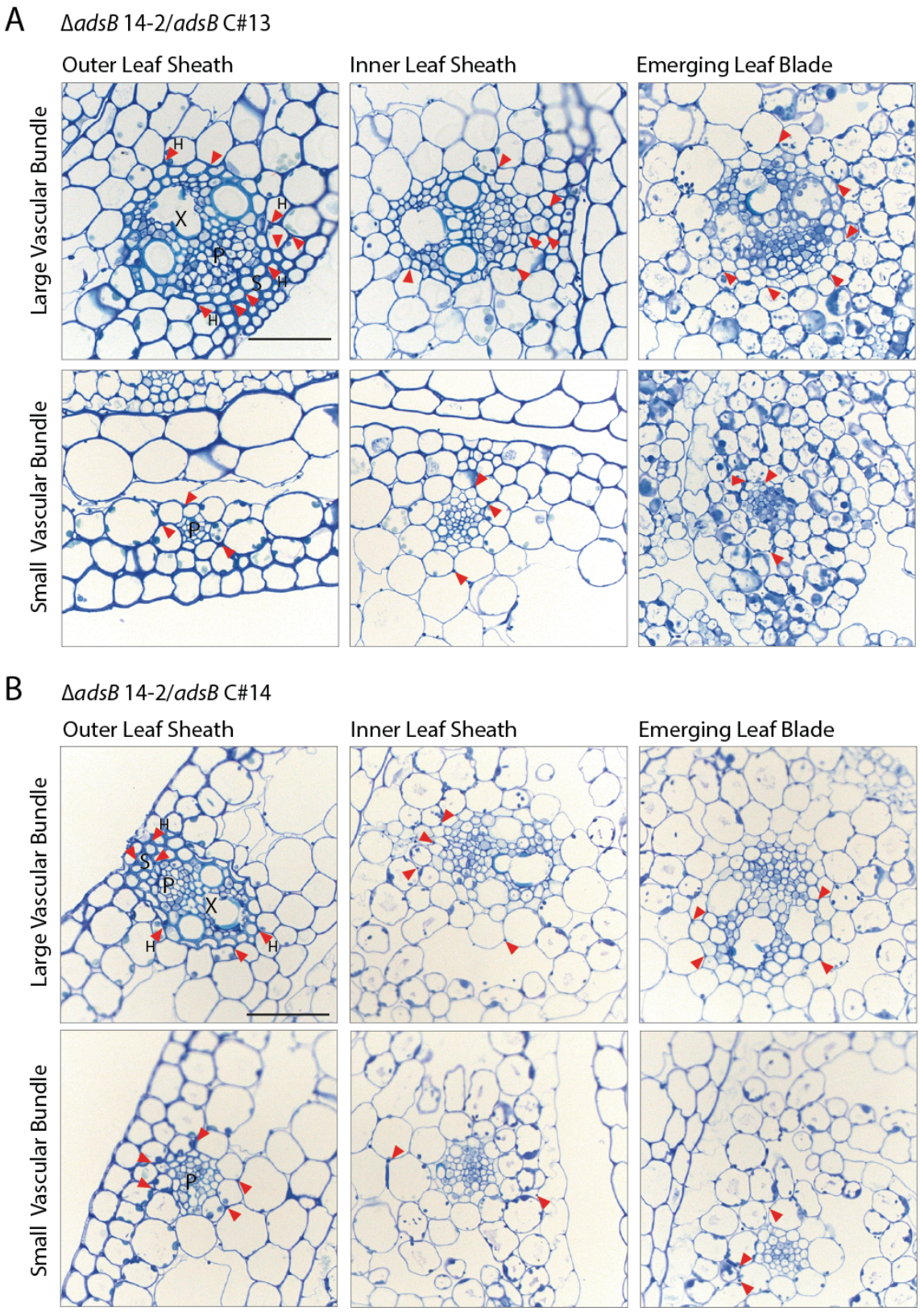

Figure 3.30 Light microscopy of *E. festucase* Δ*adsB* 14-2 complementation strains within *L. perenne* vascular tissue. Transverse sections of *L. perenne* pseudostem tissue infected with (A) Δ*adsB*/*adsB* C#13 and (B) Δ*adsB*/*adsB* C#14, stained with toluidine blue. Samples were taken from plants 12 weeks post inoculation. S = sclerenchyma, P = phloem, X = xylem and H = hyphae (red arrow heads). Bars = 20 µm.

3.9. Adhesion Assay

To determine if *E. festucae adsB* conferred a specificity to plant adherence a yeast adhesion assay was developed based on that used previously by Wang *et al.* (2007) in *M. robertsii*. The *E. festucae adsA* and *adsB* genes were cloned into the pYES2 vector (Figure 6.6) under the inducible promoter GAL1 (Figure 3.31A). pYES2/*adsA* transformants that were able to grow on SD-Ura plates were screened by PCR with primer pair adsA1/adsA2 (Figure 3.31B). This PCR identified two yeast colonies containing *adsA*. pYES2/*adsB* transformants that were able to grow on SD-Ura plates were screened by PCR with primer pair adsB1/adsB2 (Figure 3.31C). This PCR identified three yeast colonies containing *adsB*. Two colonies for each gene were selected as biological replicates for the assay, *adsA*#1, *adsA*#2 and *adsB*#3, *adsB*#4.

The initial assay was carried out by looking for cells adhered to the onion epidermis using DIC microscopy. However, adhered cells were difficult to identify. Thus, a construct that constitutively expresses GFP was transformed into the two strains of *adsA* and *adsB*. Transformants were identified by growth on SD-Ura-Leu and GFP fluorescence.

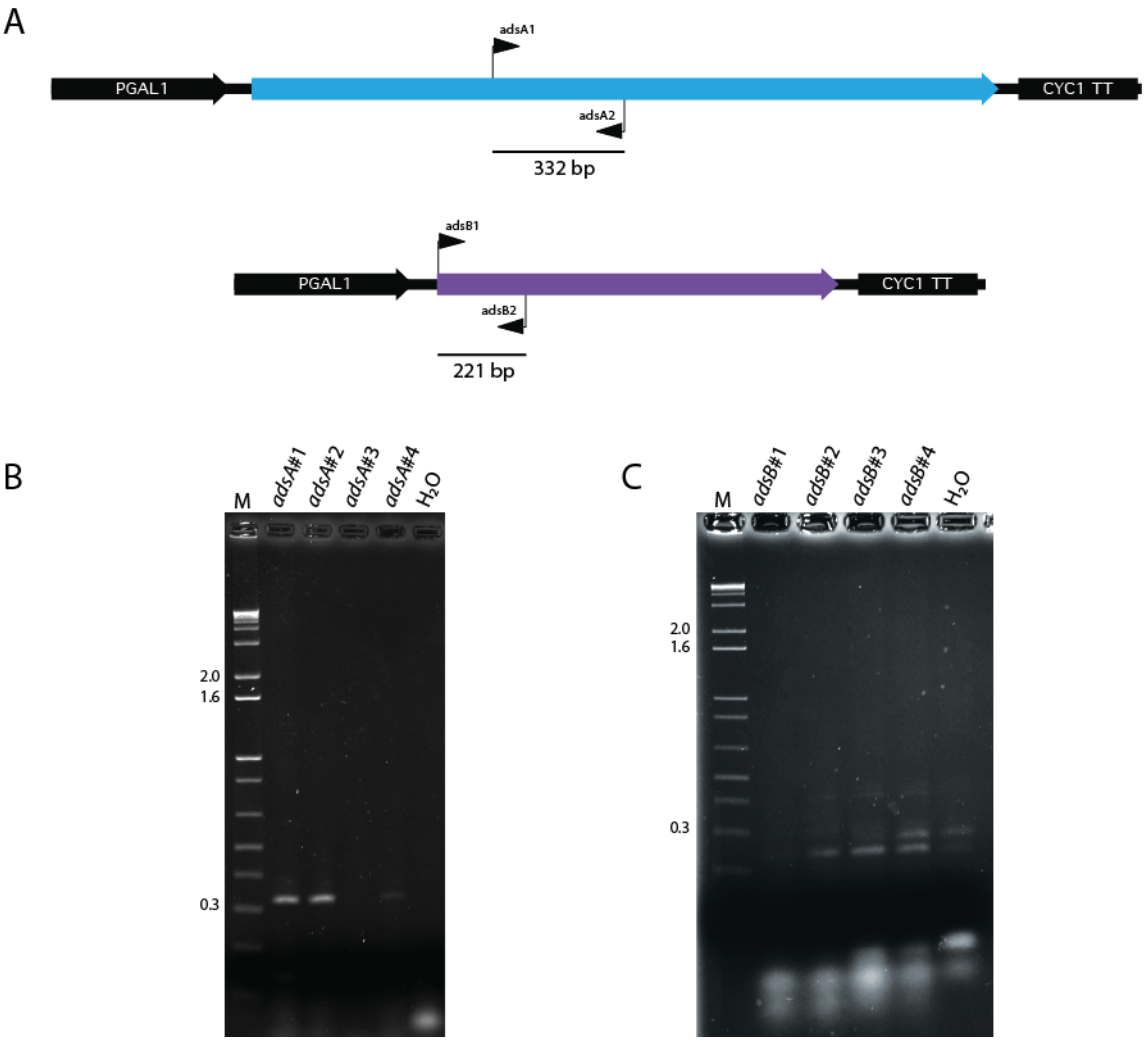

Figure 3.31 Yeast adhesion assay construct design and PCR confirmation. (A) Schematic of pYES2:*adsA* (pCE87) and pYES2:*adsB* (pCE88). (B) PCR screening of single yeast colonies transformed with pYES2/*adsA*. Primer pair adsA1/adsA2 amplifies an internal fragment of *adsA* and yields a product of 332 bp. (C) PCR screening of single yeast colonies transformed with pYES2/*adsB*. Primer pair adsB1/adsB2 amplifies an internal fragment of *adsB* yields a product of 221 bp. M = 1 kb+ ladder; H_2O = water only negative control

Cells expressing *adsA* and GFP were seen on the onion epidermal tissue incubated with galactose-induced cultures (Figure 3.32). The total number of GFP expressing cells was counted for each image taken. The yeast adhesion assay was replicated four times with both biological replicates and unmodified vector controls.

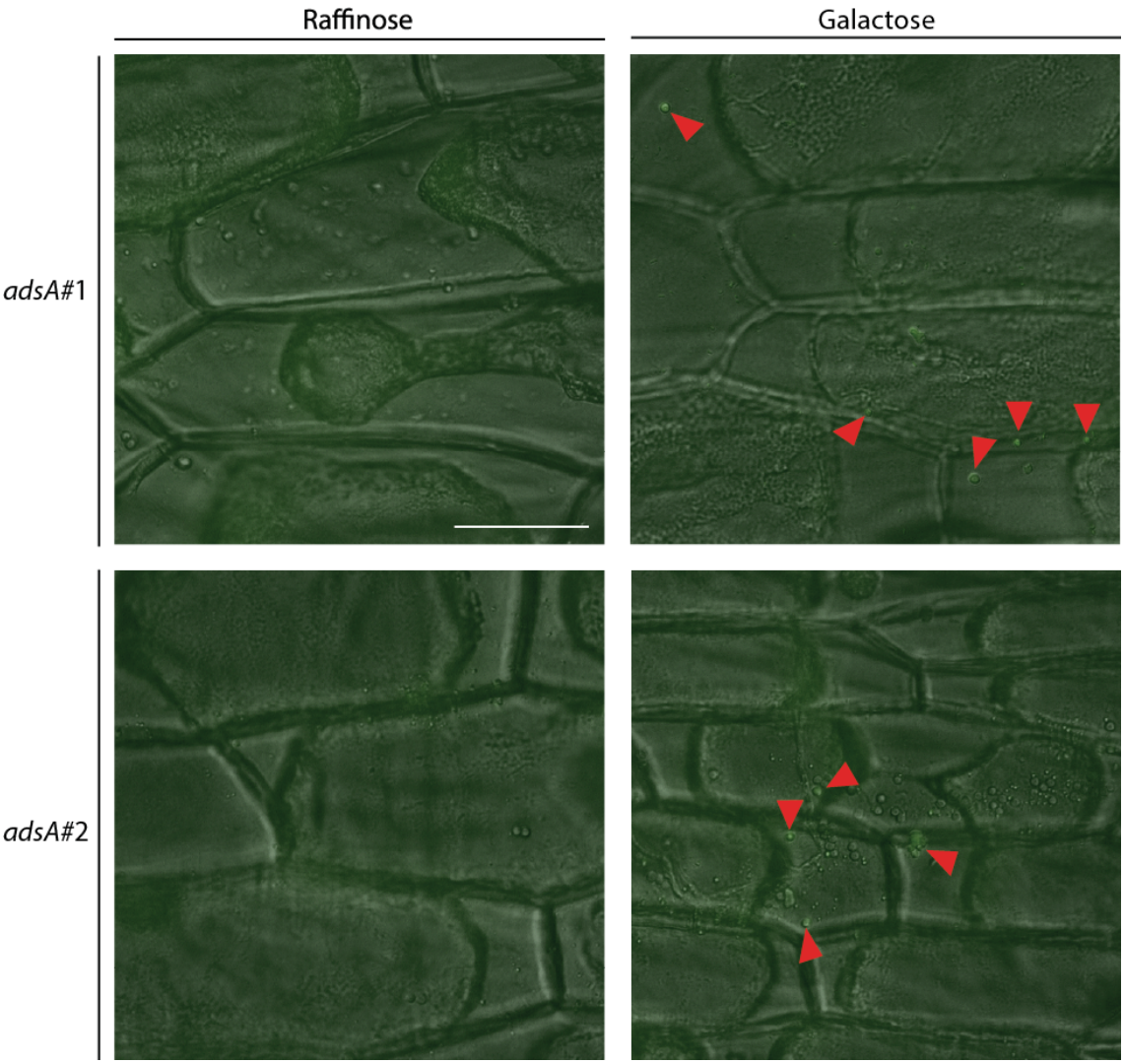

Figure 3.32 *adsA* yeast adhesion to onion epidermis assay. Fluorescence and DIC image overlays of *S. cerevisiae* INVSc1 variant strain expressing *adsA* under the control of the GAL promoter. *adsA* expressing cultures induced by galactose adhered to onion epidermal peels. All samples were prepared in duplicate and images are representative of 4 experimental replicates. Bar = 20 μm.

Similar to the *adsA* adhesion assay, adherent cells expressing *adsB* and GFP was seen on the onion epidermal sections incubated with galactose-induced cultures (Figure 3.33). The onion epidermal tissue was imaged at various locations across the sample and total cells expressing GFP were counted. Low counts of cells expressing GFP were observed for some of the controls. This was replicated four times with both biological replicates.

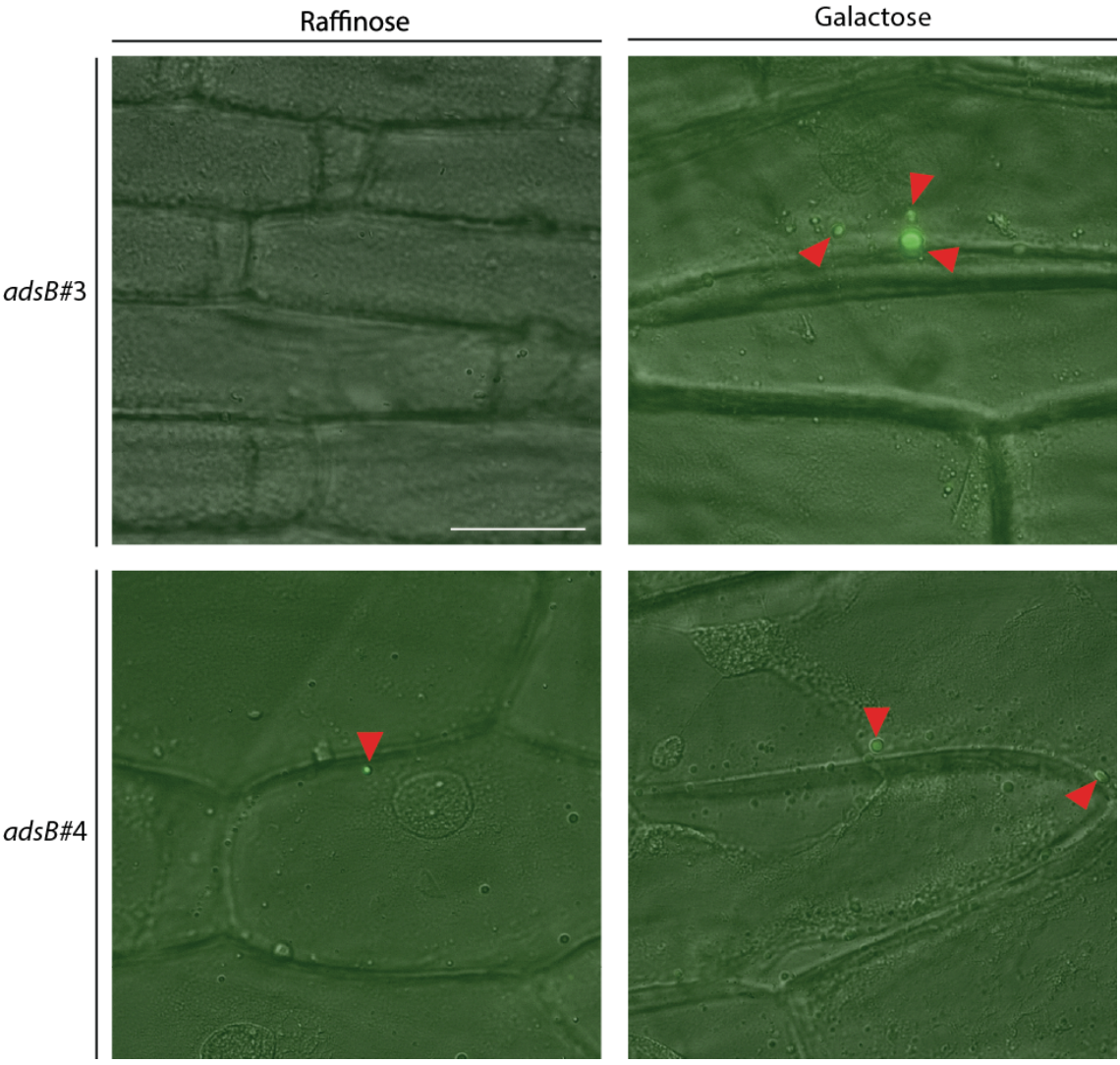

Figure 3.33 *adsB* yeast adhesion to onion epidermis assay. Fluorescence and DIC image overlays of *S. cerevisiae* INVSc1 variant strain expressing *adsB* under the control of the GAL promoter. *adsB* expressing cultures induced by galactose adhered to onion epidermal peels. All samples were prepared in duplicate and images are representative of 4 experimental replicates. Bar = 20 µm.

Count data for *adsA* and *adsB* adherence to onion epidermis was similar. However, some counts appeared to be outliers. Statistical analysis of the raw data (Table 6.1) was carried out to identify if the outliers changed the resulting data significantly. The statistics model used was the Generalised Linear Mixed Effects Model (Poisson data). The code for analysing count data with various fixed effects using this model was written by Poppy Miller (Section 6.3). In addition to the fixed effects, treatment (induced or non-induced) and gene (*adsA*#1, *adsA*#2, *adsB*#3, *adsB*#4 or pYES2), day was used as a random effect as it could not be replicated and outliers were identified based on the Pearson residuals. For the analysis of the data within the code the base lines were adjusted to be pYES2 (unmodified vector) for the gene and non-induced for the treatment. The remaining data was compared to these set baselines.

The output from RStudio showed that the presence of *adsA* and *adsB* were both statistically significant (Table 3.1). Additionally the effect of the induced treatment was statistically significant. The correlation between *adsA* and *adsB* genes was also high (Table 3.2). To determine if the outliers that were identified by the model significantly affected the data the correlation between the genes was compared. When the two outliers identified were removed and the model was run again there was no significant difference in the correlation between the genes, therefore the outliers were not removed.

	Estimate	Std. Error	z value	Pr (>|z|)
(Intercept)	-3.6095	0.6553	-5.508	3.63E-08
TreatmentInduced	2.0689	0.2050	10.09	< 2E-16
GeneadsA1	1.9781	0.4292	4.609	4.05E-06
GeneadsA2	2.9540	0.4169	7.085	1.39E-12
GeneadsB3	2.5356	0.4256	5.958	2.55E-09
GeneadsB4	3.1456	0.4172	7.539	4.73E-14

Table 3.1 Fixed effects of yeast adhesion assays. Fixed effects of yeast adhesion assay output from RStudio. Pr (>|z|) = p-values. Base lines set: gene = pYES2 (unmodified vector) and treatment = non-induced. Day is random effect.

	(Intr)	TrtmntI	GndsA1	GndsA2	GndsB3	GndsB4
TrtmtnIndcd	-0.273					
GeneadsA1	-0.576	-0.029				
GeneadsA2	-0.593	-0.029	0.926			
GeneadsB3	-0.584	-0.026	0.903	0.929		
GeneadsB4	-0.600	-0.007	0.921	0.947	0.939	

Table 3.2 Correlation of fixed effects of yeast adhesion assays. Correlation of fixed effects output from RStudio. Base lines set: gene pYES2 (unmodified vector) and treatment – non-induced. Day is random effect.

To determine the cumulative effect of presence of a gene and being induced the calculation for Generalised Linear Mixed Effects Model, μij ~Poisson (μij). The equations that were used are shown below:

$\mu_{\text{treated, Gene } adsA} = e^{\alpha+\beta_T+\beta_{\text{gene}adsA}} = e^{\alpha}e^{\beta_T}e^{\beta_A}$

$\mu_{\text{treated, Gene } adsB} = e^{\alpha+\beta_T+\beta_{\text{gene}adsB}} = e^{\alpha}e^{\beta_T}e^{\beta_B}$

The fold change due to induction and presence of either gene was high for both *adsA* and *adsB* (Table 3.3). Based on statistical analysis of the count data both *adsA* and *adsB* have the ability to confer adherence to plant surfaces in *E. festucae*, a result different to that seen in *M. robertsii* (Wang & St Leger, 2007). However, due to variation seen caused by experimental error because of the nature of the experiment, many more replicates need to be carried out to obtain definitive results.

	Non-Induced	Induced	Fold Change
adsA#1	0.1962	1.5488	7.89
adsA#2	0.5192	2.7319	5.26
adsB#3	0.3417	2.7047	7.92
adsB#4	0.6288	4.9779	7.92

Table 3.3 Calculations of cumulative fixed effects. Calculations of cumulative effects for presence of gene or induction with the presence of a gene. Non-induced (e^{α} $e^{\beta G}$), Induced (e^{α} $e^{\beta G}$ $e^{\beta T}$) and Fold change (Induced – Non-induced).

4. Discussion

4 Discussion

To determine the role adhesins play in the symbiotic associations targeted gene deletions of *adsA* and *adsB* were carried out (Eaton, unpublished). Homologues of *adsA* and *adsB* in *M. robertsii*, *Mad1* and *Mad2* respectively, have been shown to play a role in insect pathogenesis and attachment to plant surfaces (Wang & St Leger, 2007). RNAseq analysis of a stress activated MAP kinase (*sak*A) mutant in comparison to wild-type found that both *adsA* and *adsB* are up-regulated in the mutant association (Eaton *et al.*, 2010). Additional RNAseq analysis of two symbiotic mutants, a transcription factor (*proA*) and a NADPH oxidase (*noxA*), showed that across the three symbiotic mutants *adsB* is up-regulated in all three data sets whereas, *adsA* is only up-regulated in *sak*A (Eaton *et al*. unpublished). The increased expression of *adsB* across the three mutants suggests that it plays a role in the symbiotic association of *E. festucae* and *L. perenne*.

Using a range of bioinformatic tools, both *adsA* and *adsB* were shown to map to the same region of the genome, separated by 25 genes. *adsA* was shown to be conserved among filamentous fungi whereas; *adsB* is restricted to the Hypocreomycetidae, a subclass of the Sordariomycetes. The distinct grouping of *adsA* and *adsB* sequences separate to each other is highly supported. As the distribution of adhesin homologues is relatively narrow the evolutionary distance between *E. festucae adsA* and *adsB* cannot be determined thus, it cannot be determined how *adsB* arose. Based on functional characterisation of adhesins in *M. robertsii* and their conservation within *Metarhizium spp*. (Wyrebek & Bidochka, 2013) it was hypothesised that *E. festucae* adhesins would have similar functions. This prediction was based on sequence identity and protein domain structure of AdsA and AdsB compared to Mad1 and Mad2 respectively. Like, Mad1 and Mad2 both AdsA and AdsB contain signal peptides and a GPI anchor site. Further analysis of the amino acid make up of both AdsA and AdsB showed the same regions containing hydrophobic/glycine, threonine and proline rich regions as seen in *M. robertsii* (Wang & St Leger, 2007). When analysing the sequences no obvious tandem repeats were seen as in *M. robertsii* (Wang & St Leger, 2007). Given that

both AdsA and AdsB are predicted to have GPI anchors indicates that they have a functional role on the outside of the fungal hyphae or conidia.

In culture Δ*adsA* mutants form bundles of unbranched hyphae, form cell-cell fusions and form coil structures that frequently have conidiophores. *In planta* Δ*adsA* hyphae grow within the intercellular spaces of the host cells and do not colonise the vascular tissue, as shown by confocal, light and TEM microscopy. The phenotypes seen are comparable to that of wild-type. With the support of up-regulation in only one symbiotic mutant (*sakA*) of the three-way RNAseq data (Eaton *et al.* unpublished) it can be determined that *adsA* deletion does not play a detectable role in the symbiotic association with *L. perenne*. With no detectable phenotype seen in culture, specifically the formation of the hyphal coils and fusion events, it appears that *adsA* does not play a significant role in the organisation of the cytoskeleton and cell division unlike *Mad1* in *M. robertsii* (Barelli *et al.*, 2011). If *adsA* played a significant role in these pathways the formation of hyphal coils would vary to that of wild-type, that is hyperconidiation or no formation of the coils. Expression of *adsA* in a non-adherent strain of yeast resulted in the adherence of yeast cells to onion epidermal tissue. This result is distinguishable from the yeast adhesion assay with *M. robertsii Mad1*, where expression of *Mad1* did not confer adherence to onion epidermal tissue (Wang & St Leger, 2007). Although the level of attachment is highly variable based on the nature of the experiment the attachment due to the expression of *adsA* is statistically significant. To improve the accuracy of the degree of attachment seen in the yeast adhesion assay more biological and experimental replicates would need to be carried out. However, in regards to the specific mode of attachment of *E. festucae adsA* it will be different to that observed in the yeast adhesion assay as the component of the cellular surfaces the hyphae are possibly attaching to within the host plant (pectin) are very different to the onion epidermal cells (cutin).

The presence of no significant phenotype differences for *adsB* in culture compared to wild-type, suggests that *adsB* does not play a role in the establishment of the hyphal network of the colony or in development of conidia. A mild plant phenotype of reduced tiller length and root stunting indicated that

adsB has a role in the symbiotic association. Investigation of the growth of Δ*adsB* in pseudostem tissue by confocal microscopy, showed that hyphae were growing parallel to the vascular bundles and were evenly dispersed in the tissue between vascular bundles. However, light microscopy of transverse sections of pseudostem tissue showed that the *adsB* mutant colonises the large vascular bundles of both sheath and emerging leaf blades. The degree of colonisation seen is comparable to that seen in *sakA* mutants (Eaton *et al.*, 2010). Increased colonisation of the sclerenchyma tissue and hyphae present in the phloem tissue of the large vascular tissue was seen for *adsB* mutants this is not a common phenotype seen in wild-type associations. In comparision to artificial associations (Christensen *et al.*, 1997; Christensen *et al.*, 2001) and severe symbiotic mutants such as *noxA* (Takemoto *et al.*, 2007), extensive vascular colonisation is seen in the large vascular bundles. This difference to *noxA* accounts for the minimal whole plant phenotype for *adsB* mutants. Hyphal growth between vascular bundles of these two symbiotic mutants is not restrictive like that of *adsB*. Both *sakA* and *noxA* mutants exhibit prolific uncontrolled growth within the intercellular spaces of tissue between vascular bundles (Takemoto *et al.*, 2007; Eaton *et al.*, 2010). The lack of uncontrolled growth between the vascular bundles in *adsB* mutant associations accounts for the minimal whole plant phenotype. The controlled growth of *adsB* is supported by confocal and light microscopy where the hyphae in tissue between vascular bundles is firmly attached to host cells, evenly dispersed and growing parallel to the vascular bundles, a phenotype seen in wild-type associations. Lack of colonisation of the small vascular bundles indicates that *adsB* mutants are possibly entering the large vascular bundles at the growth apex of the developing tiller and continuing up the bundle by intercalary extension due to being attached to the host cells. Timing of colonisation can be determined because of the colonisation of the large vascular bundles in the emerging leaf in *adsB* mutants. In the emerging leaf small vascular bundles develop when space becomes available in the rapidly growing tissue (Soper & Mitchell, 1956).

Mad2 in *M. roberstii* has been hypothesised to play a role in nutrient stress response due to the presence of a stress responsive element (STRE) and a post-diauxic shift (PDS) element in the promoter region about 100 bp upstream from

the gene (Wyrebek & Bidochka, 2013). When the specific nucleotides for both STRE and PDS that were identified by Wyrebek and Bidochka (2013) were searched for in the *adsB* sequence no corresponding elements were identified in the promoter region. As seen with *Mad2* in *M. robertsii*, *adsB* does confer attachment to onion epidermal tissue. Again, high variation in regards to level of attachment is seen, similar to *adsA*, with the same drawbacks in regards to the experimental design, but the attachment seen is statistically significant. Given the phenotypic results gained to date the specific role *adsB* play in attachment to the host tissue cannot be determined. However, based on the ability of *adsB* mutants to colonise the large vascular tissue of the host plant in all tissue layers suggest that in a wild-type association *adsB* may play a role in the initial association when the new leaf blades are developing. Removal of the *adsB* gene may decrease the overall physical attachment to the host tissue allowing the hyphae to enter the young large vascular bundles at the growth apex. Although, in older sheath tissue hyphae are firmly attached to mesophyll cells that have begun to degenerate a phenotype also seen in wild-type associations. Based on the physical attachment seen in the sheath tissue in *adsB* mutants it can be determined that the genes responsible for the physical attachment of hyphae to the host cells are redundant. That is, more than one gene is responsible for conferring attachment to the host.

Previous research identified that filamentous fungi produce hydrophobins, small secreted proteins, that confer hydrophobicity to the mycelium (Wosten, 2001). Hydrophobins have been identified in many filamentous fungi, including *M. robertsii* and *B. bassiana* in which a homologue for *adsB* is present (Zhang *et al.*, 2011). This research identified two genes identified as hydrophobins, and deletions of these genes reduced the level of conidia adherence (Zhang *et al.*, 2011). Homologues of the *B. bassiana* hydrophobins, *hyd*1 and *hyd*2, were not present in *E. festucae* Fl1 when a BLAST search was carried out against the genome. However, when hydrophobin sequences from *Claviceps fusiformis* (De Vries *et al.*, 1999) were used to BLAST against the *E. festucae* genome two potential hydrophobins were identified. These protein sequences had a high number of BLAST hits in various filamentous fungi, suggesting these particular genes are frequently found in filamentous fungi.

4.1. Conclusion

While distinct and separate functions were identified for *Mad1* and *Mad2* in *M. robertsii* the same cannot be said for *adsA* and *adsB* requiring further experiments to be carried out. In conclusion, based on the phenotypes seen for deletion mutants of *E. festucae* adhesins, *adsA* and *adsB*, and expression of these genes in non-adherent yeast cells both *adsA* and *adsB* play a role in the symbiotic association. The culture and *in planta* phenotypes seen for *adsA* indicates that it does not play a detectable role in the establishment for the colony or *in planta* growth but the attachment of yeast cells expressing *adsA* to onion epidermal tissue indicates that it may play a role in attachment to host tissue. This difference seen for *adsA* compared to *Mad1* is possibly due to gene redundancy in *E. festucae* for physical attachment to host cells.

Based on the colonisation of *L. perenne* large vascular bundles it can be concluded that *adsB* does play a role in the symbiotic association. Based on literature about the development of *L. perenne* vascular bundle development, (Soper & Mitchell, 1956), *adsB* mutants colonise the large vascular bundle at the growth apex of the developing tiller. This is determined by the lack of colonisation of the small vascular bundles, which develop later than the large vascular bundles due to restriction of space for development. The reason why the *adsB* mutant hyphae are able to enter the large vascular bundles is unknown. *adsB* may play a role in the nutrient stress response as seen in *Metarhizium* species (Wyrebek & Bidochka, 2013) as they share high sequence identity within the gene. However, the lack of a stress response element or post-diauxic shift elements in the promoter there is no supporting evidence for this currently. Due to high sequence identity within species for adhesins and their importance in physical attachment to the host it can be assumed that the co-evolution with the host influences the promoter elements present for the genes conferring physical attachment, that is elements relating to nutrient stress are species specific. Based on the results to date the specific function *adsB* plays in the symbiotic association cannot be determined.

Finally, as both *E. festucae adsA* and *adsB* confer plant adherence and the deletion mutants still firmly attach to the host tissue, the true nature of attachment of *E. festucae* hyphae *in planta* is not currently known. As both *adsA* and *adsB* confer adherence to onion epidermal tissue and deletion mutants in *E. festucae* of each gene not abolishing physical attachment to the host cells suggests gene redundancy for this physical attachment seen in wild-type associations. A double deletion of both *E. festucae adsA* and *adsB* might shed light on redundancy of physical attachment in the association.

5. Bibliography

Barelli, L., Padilla-Guerrero, I. E., & Bidochka, M. J. (2011). Differential expression of insect and plant specific adhesin genes, Mad1 and Mad2, in *Metarhizium robertsii*. *Fungal Biology,* **115**, 1174-1185.

Breslow, N. E. & Clayton, D. G. (1993). Approximate inference in generalized linear mixed models. *Journal of the American Statistical Association,* **88**, 9-25.

Byrd, A. D., Schardl, C. L., Songlin, P. J., Mogen, K. L., & Siegel, M. R. (1990). The beta-tubulin gene of *Epichloë typhina* from Perennial Ryegrass (*Lolium perenne*). *Current Genetics,* **18**, 347-354.

Christensen, M. J., Ball, O. J. P., Bennett, R. J., & Schardl, C. L. (1997). Fungal and host genotype effects on compatibility and vascular colonization by Epichloe festucae. *Mycological Research,* **101**, 493-501.

Christensen, M. J., Bennett, R. J., Ansari, H. A., Koga, H., Johnson, R. D., Bryan, G. T., Simpson, W. R., Koolaard, J. P., Nickless, E. M., & Voisey, C. R. (2008). Epichloë endophytes grow by intercalary hyphal extension in elongating grass leaves. *Fungal Genetics and Biology,* **45**, 84-93.

Christensen, M. J., Bennett, R. J., Ansari, H. A., Koga, H., Johnson, R. D., Bryan, G. T., Simpson, W. R., Koolaard, J. P., Nickless, E. M., & Voisey, C. R. (2008). Epichloë endophytes grow by intercalary hyphal extension in elongating grass leaves. *Fungal Genet Biol,* **45**, 84-93.

Christensen, M. J., Bennett, R. J., & Schmid, J. (2001). Vascular bundle colonisation by Neotyphodium endophytes in natural and novel associations with grasses. *Mycological Research,* **105**, 1239-1245.

Christensen, M. J., Bennett, R. J., & Schmid, J. (2002). Growth of *Epichloë/Neotyphodium* and p-endophytes in leaves of *Lolium* and *Festuca* grasses. *Mycol Res,* **106**, 93-106.

Christensen, M. J., Bennett, R. J., & Schmid, J. (2002). Growth of Epichloë/Neotyphodium and p-endophytes in leaves of Lolium and Festuca grasses. *Mycological Research,* **106**, 93-106.

Christianson, T. W., Sikorski, R. S., Dante, M., Shero, J. H., & Hieter, P. (1992). Multifunctional yeast high-copy-number shuttle vectors. *Gene,* **110**, 119-122.

Clay, K. & Schardl, C. (2002). Evolutionary origins and ecological consequences of endophyte symbiosis with grasses. *American Naturalist,* **160**, S99-S127.

De Vries, O. M., Moore, S., Arntz, C., Wessels, J. G., & Tudzynski, P. (1999). Identification and characterization of a tri-partite hydrophobin from *Claviceps fusiformis*. A novel type of class II hydrophobin. *Eur J Biochem,* **262**, 377-385.

Dower, W. J., Miller, J. F., & Ragsdale, C. W. (1988). High-efficiency transformation of *Escherichia coli* by high-voltage electroporation. *Nucleic Acids Research,* **16**, 6127-6145.

Dranginis, A. M., Rauceo, J. M., Coronado, J. E., & Lipke, P. N. (2007). A biochemical guide to yeast adhesins: Glycoproteins for social and antisocial occasions. *Microbiol Mol Biol R,* **71**, 282-294.

Eaton, C. J., Cox, M. P., Ambrose, B., Becker, M., Hesse, U., Schardl, C. L., & Scott, B. (2010). Disruption of Signaling in a Fungal-Grass Symbiosis Leads to Pathogenesis. *Plant Physiology,* **153**, 1780-1794.

Eaton, C. J., Cox, M. P., Ambrose, B., Becker, M., Hesse, U., Schardl, C. L., & Scott, B. (2010). Disruption of signaling in a fungal-grass symbiosis leads to pathogenesis. *Plant Physiol,* **153**, 1780-1794.

Eisenhaber, B., Schneider, G., Wildpaner, M., & Eisenhaber, F. (2004). A sensitive predictor for potential GPI lipid modification sites in fungal protein sequences and its application to genome-wide studies for *Aspergillus nidulans*, *Candida albicans*, *Neurospora crassa*, *Saccharomyces cerevisiae* and *Schizosaccharomyces pombe*. *Journal of Molecular Biology,* **337**, 243-253.

Gwinn, K. D., Collinsshepard, M. H., & Reddick, B. B. (1991). Tissue print-immunoblot, an accurate method for the detection of Acremonium coenophialium in tall fescue. *Phytopathology,* **81**, 747-748.

Itoh, Y., Johnson, R., & Scott, B. (1994). Integrative transformation of the mycotoxin-producing fungus, *Penicillium paxilli*. *Current Genetics,* **25**, 508-513.

Jones, P., Binns, D., Chang, H.-Y., Fraser, M., Li, W., McAnulla, C., McWilliam, H., Maslen, J., Mitchell, A., Nuka, G., Pesseat, S., Quinn, A. F., Sangrador-Vegas, A., Scheremetjew, M., Yong, S.-Y., Lopez, R., & Hunter, S. (2014). InterProScan 5: genome-scale protein function classification. *Bioinformatics,* **30**, 1236-1240.

Latch, G. C. M. & Christensen, M. J. (1985). Artificial infection of grasses with endophytes. *Annals of Applied Biology,* **107**, 17-24.

Leuchtmann, A., Bacon, C. W., Schardl, C. L., White, J. F., Jr., & Tadych, M. (2014). Nomenclatural realignment of *Neotyphodium* species with genus Epicholë. *Mycologia,* **106**, 202-215.

Leuchtmann, A., Schardl, C. L., & Siegel, M. R. (1994). Sexual compatibility and taxonomy of a new species of *Epichloë* symbiotic with fine fescue grasses. *Mycologia,* **86**, 802-812.

Miller, C. W. & Anderson, N. A. (1962). Proliferation of conidiophores and Intrahyphal hyphae in Aspergillus niger. *Mycologia,* **53 (1961)**, 433-436.

Parniske, M. (2008). Arbuscular mycorrhiza: the mother of plant root endosymbioses. *Nature Reviews in Microbiology,* **6**, 763-775.

Petersen, T. N., Brunak, S., von Heijne, G., & Nielsen, H. (2011). SignalP 4.0: discriminating signal peptides from transmembrane regions. *Nature Methods,* **8**, 785-786.

Saikkonen, K., Faeth, S. H., Helander, M., & Sullivan, T. J. (1998). Fungal endophytes: A continuum of interactions with host plants. *Annual Review of Ecology and Systematics,* **29**, 319-343.

Sasan, R. K. & Bidochka, M. J. (2012). The insect-pathogenic fungus *Metarhizium robertsii* (Clavicipitaceae) is also an endophyte that stimulates plant root development. *American Journal of Botany,* **99**, 101-107.

Schardl, C. L. (2001). *Epichloë festucae* and related mutualistic symbionts of grasses. *Fungal Genetics and Biology,* **33**, 69-82.

Schardl, C. L., Leuchtmann, A., & Spiering, M. J. (2004). Symbioses of grasses with seedborne fungal endophytes. *Annual Reviews in Plant Biology,* **55**, 315-340.

Schardl, C. L., Leuchtmann, A., Tsai, H. F., Collett, M. A., Watt, D. M., & Scott, D. B. (1994). Origin of a fungal symbiont of perennial ryegrass by interspecific hybridization of a mutualist with the ryegrass choke pathogen, *Epichloë typhina*. *Genetics,* **136**, 1307-1317.

Schardl, C. L., Young, C. A., Hesse, U., Amyotte, S. G., Andreeva, K., Calie, P. J., Fleetwood, D. J., Haws, D. C., Moore, N., Oeser, B., Panaccione, D. G., Schweri, K. K., Voisey, C. R., Farman, M. L., Jaromczyk, J. W., Roe, B. A., O'Sullivan, D. M., Scott, B., Tudzynski, P., An, Z., Arnaoudova, E. G., Bullock, C. T., Charlton, N. D., Chen, L., Cox, M., Dinkins, R. D., Florea, S., Glenn, A. E., Gordon, A., Gueldener, U., Harris, D. R., Hollin, W., Jaromczyk, J., Johnson, R. D., Khan, A.

K., Leistner, E., Leuchtmann, A., Li, C., Liu, J., Liu, J., Liu, M., Mace, W., Machado, C., Nagabhyru, P., Pan, J., Schmid, J., Sugawara, K., Steiner, U., Takach, J. E., Tanaka, E., Webb, J. S., Wilson, E. V., Wiseman, J. L., Yoshida, R., & Zeng, Z. (2013). Plant-symbiotic fungi as chemical engineers: Multi-genome analysis of the Clavicipitaceae reveals dynamics of alkaloid loci. *Plos Genetics,* **9**, e1003323.

Schmid, J., Spiering, M. J., & Christensen, M. J. (2000). Metabolic activity, distribution, and propagation of grass endophytes in planta: Investigations using the GUS reporter gene system. In C. W. Bacon & J. White (Eds.), *Microbial Endophytes* (295-322).

Scott, B. & Schardl, C. (1993). Fungal symbionts of grasses: evolutionary insights and agricultural potential. *Trends in Microbiology,* **1**, 196-200.

Scott, B., Takemoto, D., Tanaka, A., Young, C. A., Bryant, M. K., & May, K. J. (2007). *Functional analysis of the Epichloë festucae-perennial ryegrass symbiosis.* Paper presented at the International Symposium on Fungal Endophytes of Grasses. Grassland Research and Practice series No. 13 Grassland Association, Dunedin, New Zealand.

Soper, K. & Mitchell, K. J. (1956). The developmental anatomy of perennial ryegrass (*Lolium perenne* L.). *New Zealand Journal of Science and Technology,* **37**, 484-504.

Southern, E. M. (1975). Detection of specific sequences among DNA fragments separated by gel-electrophoresis. *Journal of Molecular Biology,* **98**, 503-&.

Spiers, A. G. & Hopcroft, D. H. (1993). Black canker and leaf-spot of salix in New Zealand caused by *Glomerella miyabeana* (*Colletotrichum gloeosporioides*). *European Journal of Forest Pathology,* **23**, 92-102.

Takemoto, D., Tanaka, A., & Scott, B. (2007). NADPH oxidases in fungi: Diverse roles of reactive oxygen species in fungal cellular differentiation. *Fungal Genetics and Biology,* **44**, 1065-1076.

Tanaka, A., Christensen, M. J., Takemoto, D., Park, P., & Scott, B. (2006). Reactive oxygen species play a role in regulating a fungus-perennial ryegrass mutualistic interaction. *Plant Cell,* **18**, 1052-1066.

Verstrepen, K. J. & Klis, F. M. (2006). Flocculation, adhesion and biofilm formation in yeasts. *Molecular Microbiology,* **60**, 5-15.

Wang, C. S. & St Leger, R. J. (2007). The MAD1 adhesin of *Metarhizium anisopliae* links adhesion with blastospore production and virulence to insects, and the MAD2 adhesin enables attachment to plants. *Eukaryotic Cell,* **6**, 808-816.

Winston, F., Dollard, C., & Ricuperohovasse, S. L. (1995). Construction of a set of convenient *Saccharomyces cerevisiae* strains that are isogenic to S288C. *Yeast,* **11**, 53-55.

Wosten, H. A. B. (2001). Hydrophobins: Multipurpose proteins. *Annual Review of Microbiology,* **55**, 625-646.

Wyrebek, M. & Bidochka, M. J. (2013). Variability in the insect and plant adhesins, Mad1 and Mad2, within the fungal genus Metarhizium suggest plant adaptation as an evolutionary force. *PLoS ONE,* **8**, e59357.

Xiao, G. H., Ying, S. H., Zheng, P., Wang, Z. L., Zhang, S. W., Xie, X. Q., Shang, Y. F., St Leger, R. J., Zhao, G. P., Wang, C. S., & Feng, M. G. (2012). Genomic perspectives on the evolution of fungal entomopathogenicity in *Beauveria bassiana*. *Scientific Reports,* **2**.

Young, C. A., Bryant, M. K., Christensen, M. J., Tapper, B. A., Bryan, G. T., & Scott, B. (2005). Molecular cloning and genetic analysis of a symbiosis-expressed gene cluster for lolitrem biosynthesis from a mutualistic endophyte of perennial ryegrass. *Molecular Genetics and Genomics,* **274**, 13-29.

Zhang, S. Z., Xia, Y. X., Kim, B., & Keyhani, N. O. (2011). Two hydrophobins are involved in fungal spore coat rodlet layer assembly and each play distinct roles in surface interactions, development and pathogenesis in the entomopathogenic fungus, *Beauveria bassiana*. *Molecular Microbiology,* **80**, 811-826.

6. Appendices

6.1. Supplementary Figures

Figure 6.1 pCE55 *adsA* replacement construct

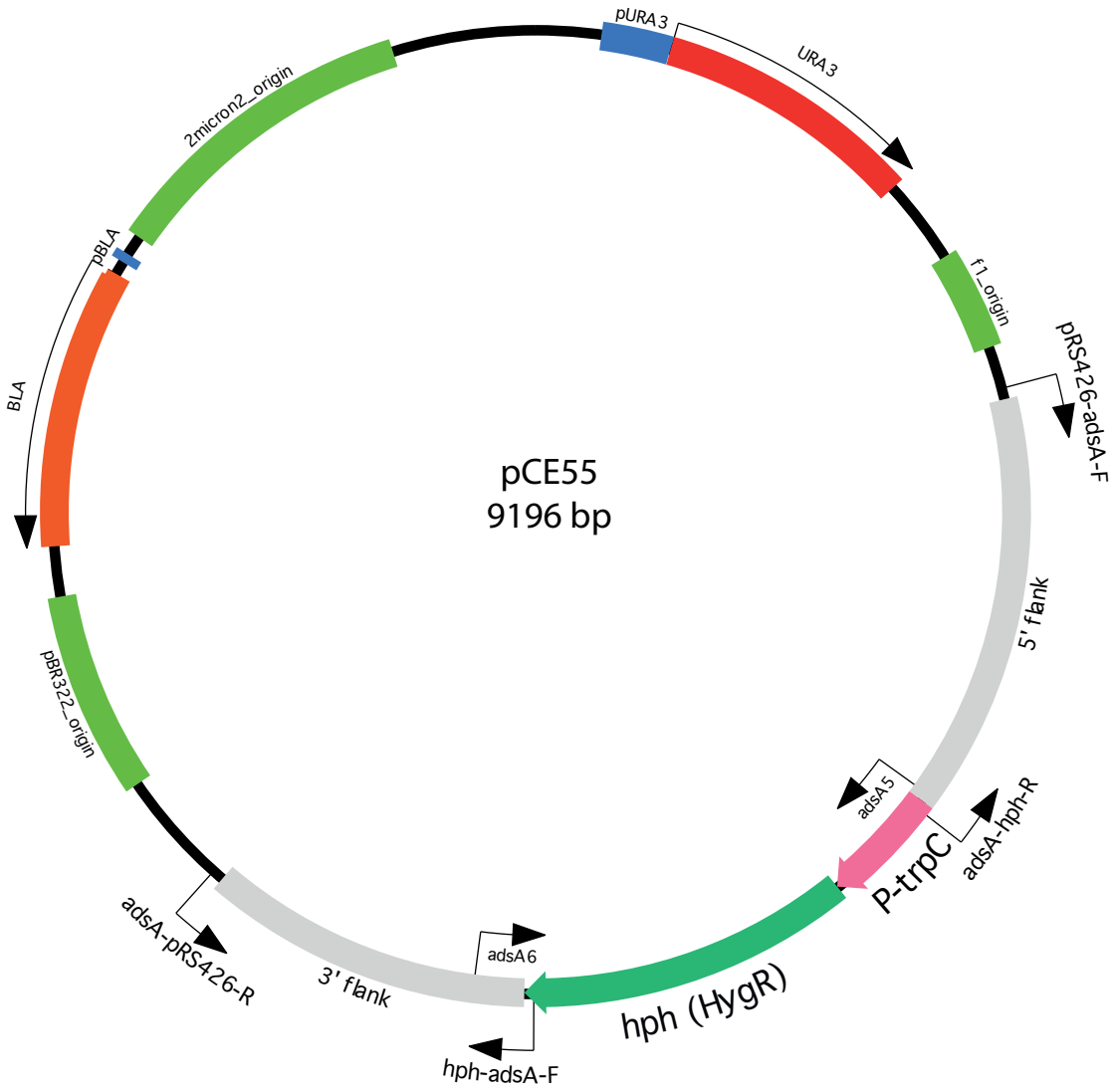

Figure 6.2 pCE53 *adsB* replacement construct

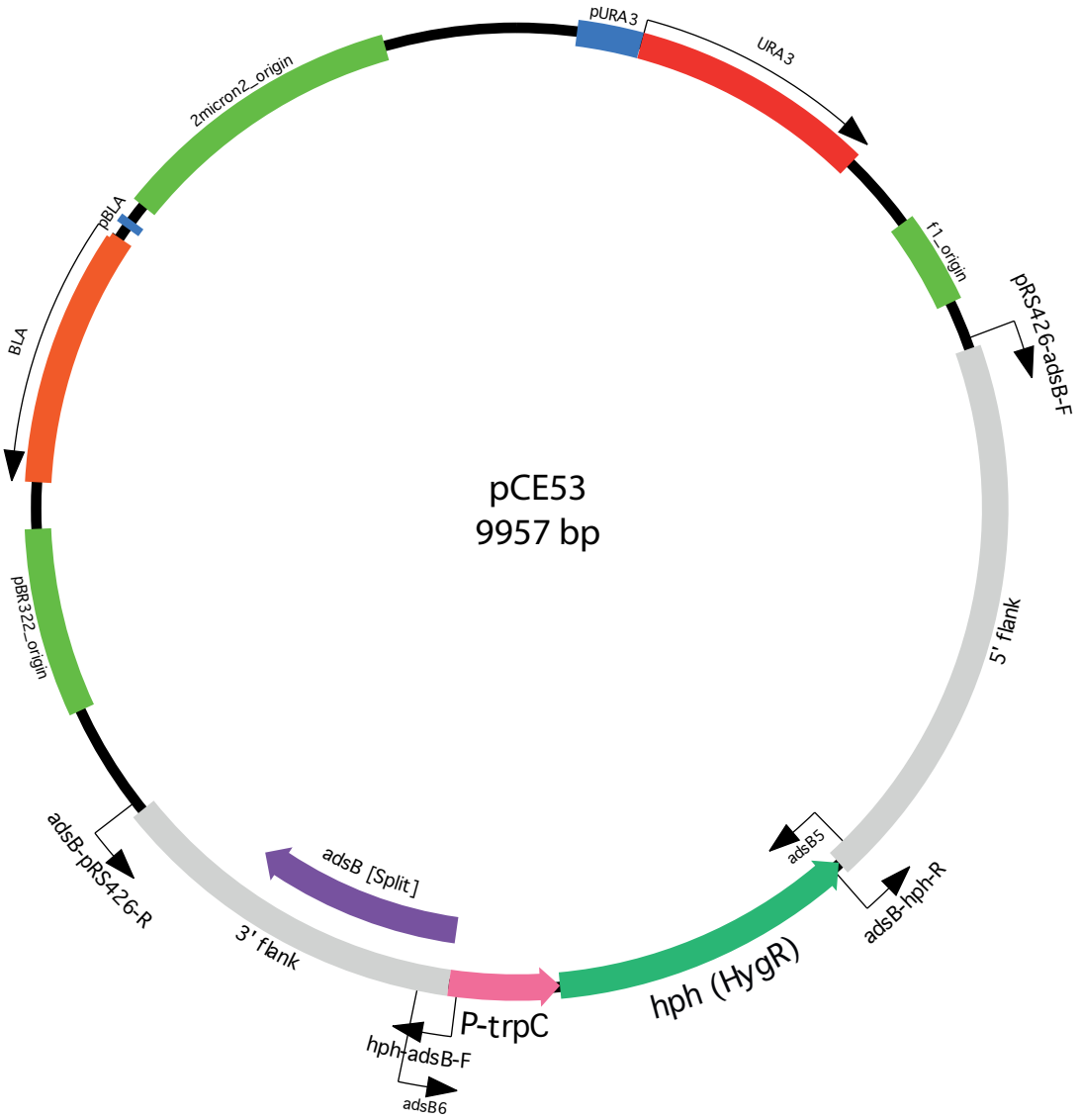

Figure 6.3 pRS426

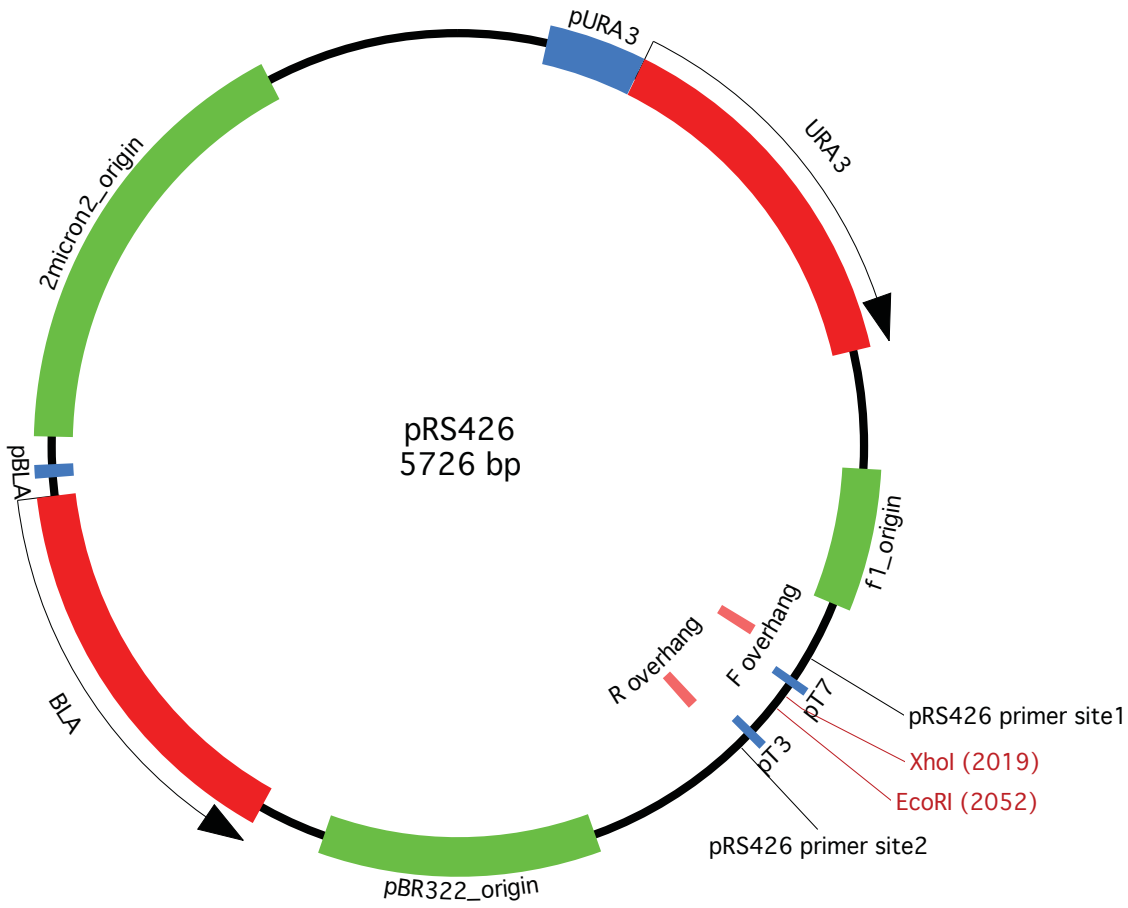

Figure 6.4 pPC2 *adsB* complementation construct

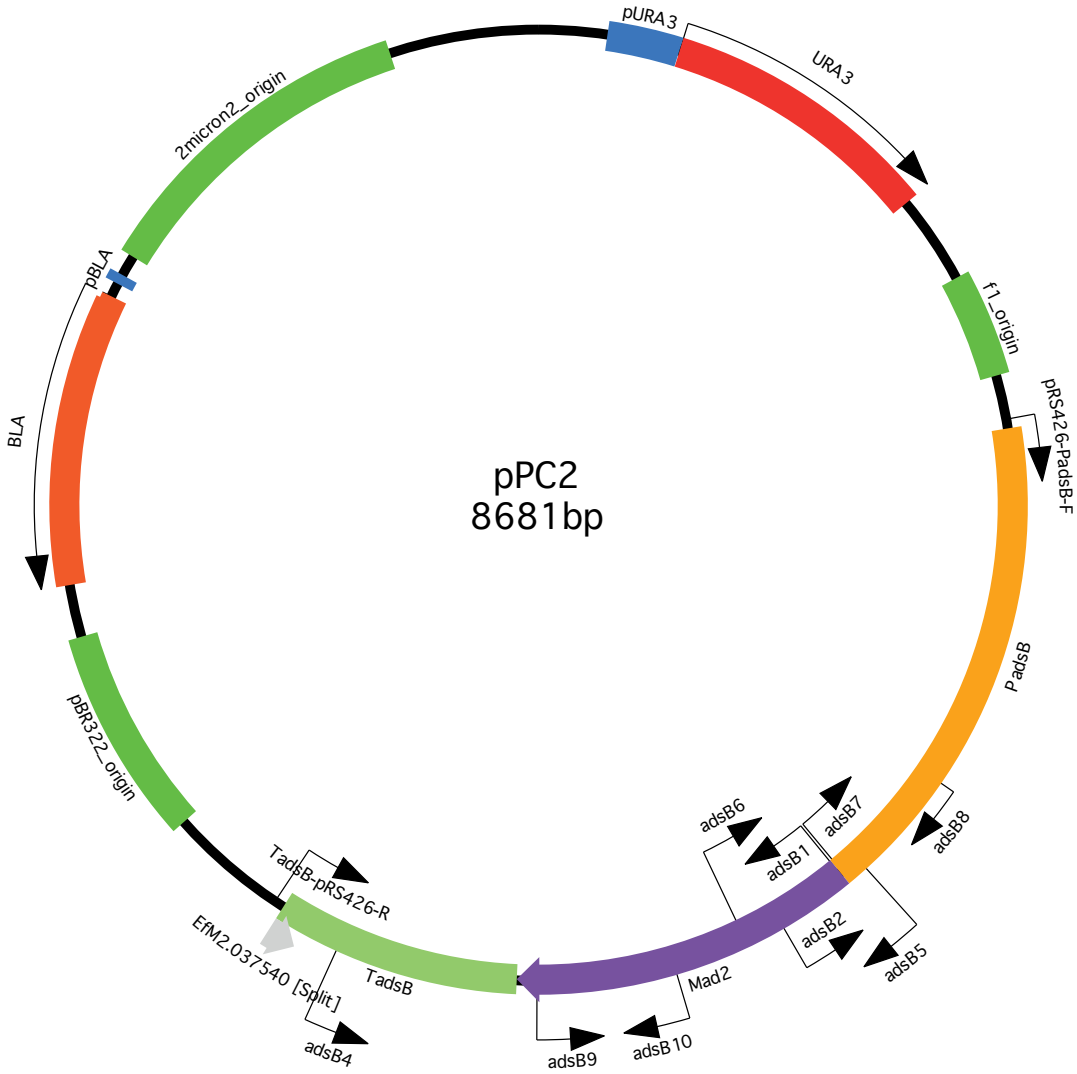

Figure 6.5 pII99

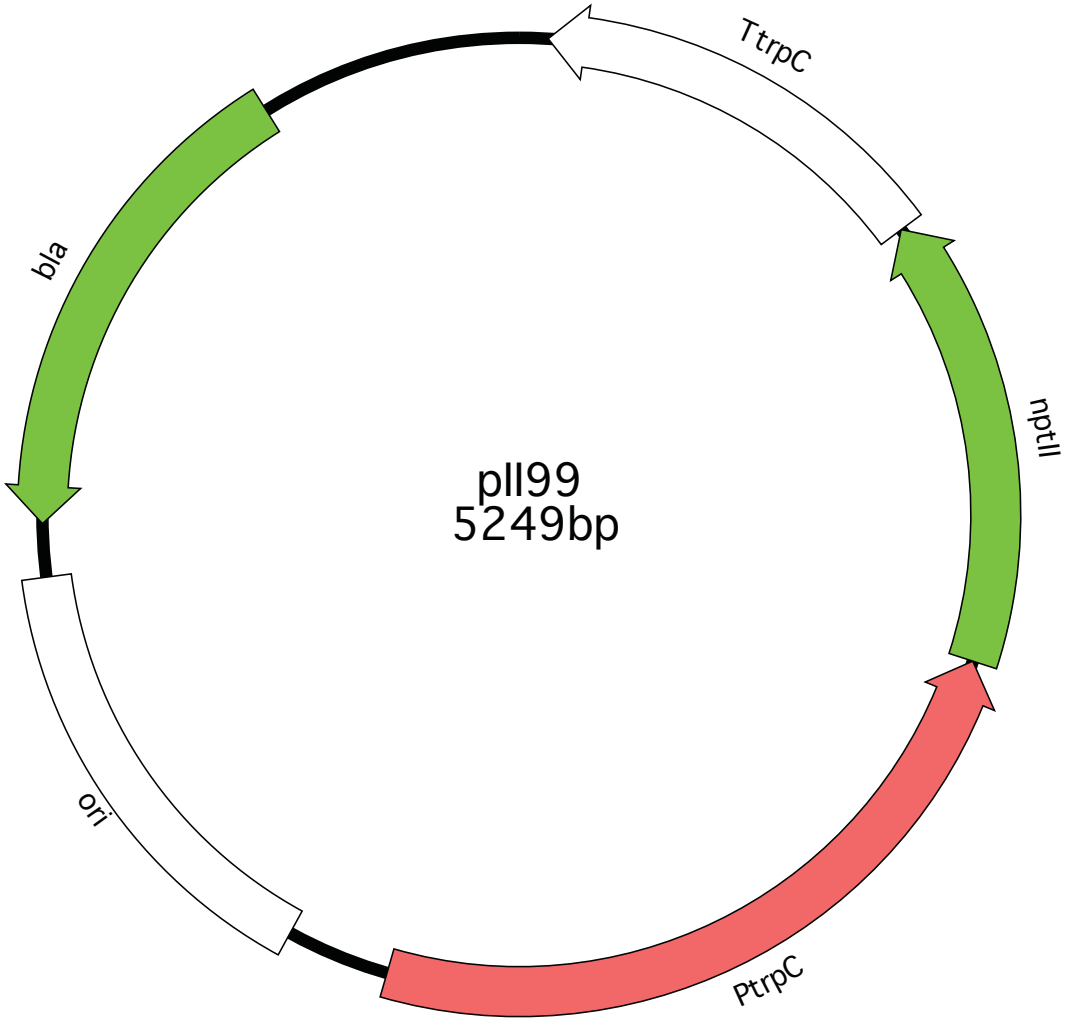

Figure 6.6 pYES2

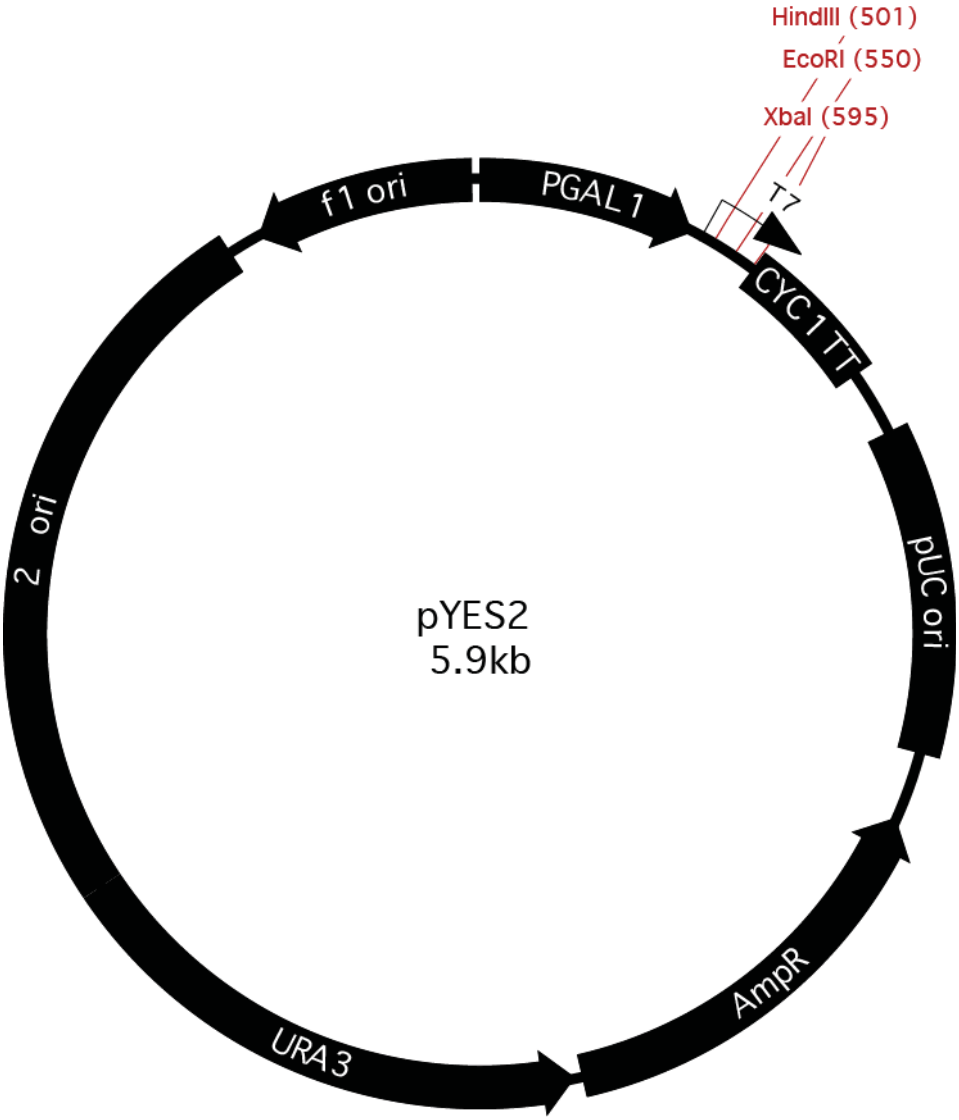

Figure 6.7 pCE87 pYES2/*adsA* construct

Figure 6.8 pCE88 pYES2/*adsB* construct

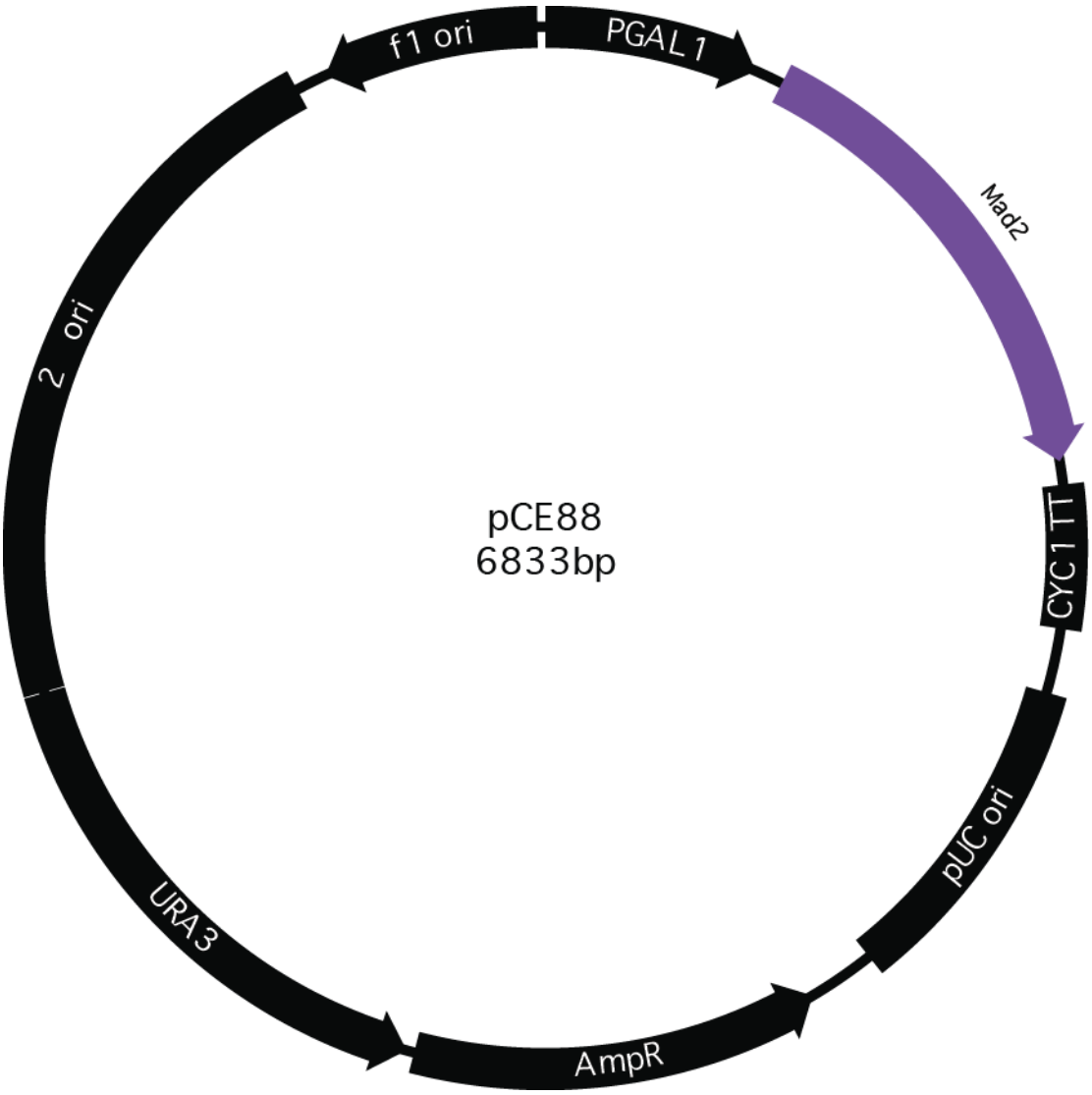

Figure 6.9 Multiple sequence alignment of AdsA and AdsB

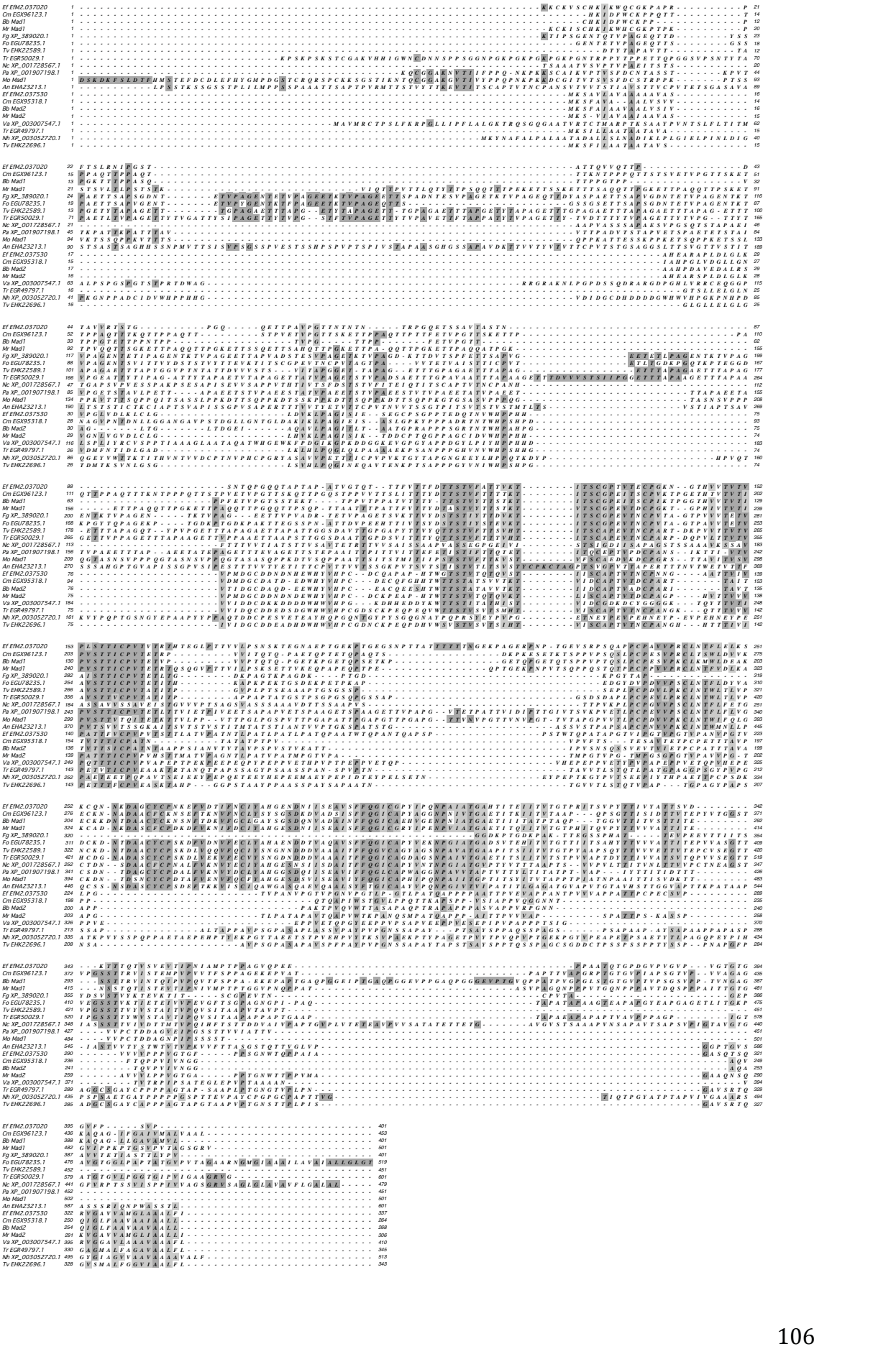

6.2. Supplementary Table

Table 6.1 Raw count data of adhesion assay

	Total Number of GFP yeast cells per Image taken									
	adsA1		adsA2		adsB3		adsB4		pYES2	
Date Taken	Induced	Non-Induced	Induced	Non-Induced	Induced	Non-Induced	Induced	Non-Induced	Induced	Non-Induced
7/03/14	0		0		17		5	4	0	0
	10		73		7		26	0	2	0
	0		32		3		0			
	13									
17/03/14	0	0	0	0					0	0
	0	0	0	0					0	0
	4	1	0	0					0	0
	4	0	0							
	3									
18/03/14					6	1	2	2	0	0
					4	0	0	1	0	0
					0	3	2	0	0	0
					0	0	0	0	0	3
					0		0			
							0			
19/03/14	0	0	17	0					0	0
	12	0	0	0					0	0
	7	0	1	0					0	0
	0		0						0	0
20/03/14					1	0	0	0	0	0
					1	0	2	0	1	0
					0	0	0	0	0	0
					0	0				0
17/02/14	0	0	0	0	18	6	36	0	0	0
	0	0	0	0	0	2	54	0	0	0

6.3. RStudio code used for Generalised Mixed Effects Model (Poisson data) analysis

```
myData <- read.csv(file.choose(), header=T)
#install.packages("lme4",repos=c("http://lme4.r-forge.r-
project.org/repos",getOption("repos")[["CRAN"]]))
myData$Day <- as.factor(myData$Day)
head(myData)

X11()
plot(myData)

# change baseline level
myData <- within(myData, Treatment <- relevel(Treatment,
ref = "Non_induced"))
myData <- within(myData, Gene <- relevel(Gene, ref =
"pYES2"))
library(lme4)
mod <- glmer(Count ~ Treatment + Gene + (1|Day),
family=poisson, data=myData)
summary(mod)
fit_mod <- fitted(mod) # expected counts for each data
point
resid_mod <- resid(mod)# deviance residuals for each data
point
resid_mod_pearson <- (myData$Count-fit_mod)/sqrt(fit_mod)#
Pearson residual
which(resid_mod_pearson==max(resid_mod_pearson))
which(resid_mod==max(resid_mod))
X11()
plot(mod, main="stuff", xlab="Fitted", ylab="Pearson
Residuals")
data.frame(myData,fitted=fitted(mod),resid=residuals(mod))#
deviance residuals
```